TAMPEREEN TEKNILLINEN YLIOPISTO
TAMPERE UNIVERSITY OF TECHNOLOGY

Miika Paloniitty

Novel Water Hydraulic On/Off Valves and Tracking Control Method for Equal Coded Valve System

Julkaisu 1577 • Publication 1577

Tampere 2018

Tampereen teknillinen yliopisto. Julkaisu 1577
Tampere University of Technology. Publication 1577

Miika Paloniitty

Novel Water Hydraulic On/Off Valves and Tracking Control Method for Equal Coded Valve System

Thesis for the degree of Doctor of Science in Technology to be presented with due permission for public examination and criticism in Festia Building, Auditorium Pieni Sali 1, at Tampere University of Technology, on the 2nd of November 2018, at 12 noon.

Tampereen teknillinen yliopisto - Tampere University of Technology
Tampere 2018

Doctoral candidate: Miika Paloniitty
Laboratory of Automation and Hydraulics Engineering
Faculty of Engineering Sciences
Tampere University of Technology
Finland

Supervisor: Adj. Prof. Matti Linjama
Laboratory of Automation and Hydraulics Engineering
Faculty of Engineering Sciences
Tampere University of Technology
Finland

Instructor: Prof. Matti Vilenius
Tamlink Oy
Finland

Pre-examiners: Prof. Kazuhisa Ito
Department of Machinery and Control Systems
College of Systems Engineering and Science
Shibaura Institute of Technology
Japan

Associate Prof. Michael M. Bech
Department of Energy Technology
Aalborg University
Denmark

Opponents: Prof. Torben Andersen
Department of Energy Technology
Aalborg University
Denmark

Prof. Kazuhisa Ito
Department of Machinery and Control Systems
College of Systems Engineering and Science
Shibaura Institute of Technology
Japan

ISBN 978-952-15-4207-7 (printed)
ISBN 978-952-15-4239-8 (PDF)
ISSN 1459-2045

Abstract

Water hydraulics is an interesting alternative to oil hydraulics since it uses a clean, environment friendly, and non-inflammable pressure medium. However, the availability of good control valves, which are essential components in many hydraulic systems, is limited in water hydraulics owing to the challenging characteristics of water. This, in turn, considerably limits the application of water hydraulics. In this thesis, a new digital hydraulic valve technology is investigated in order to promote the applicability of this clean technology; the method using equal-size on/off valves is preferred.

This equal coding method suffers from a lack of suitable valves. Thus, a fast-acting and low-power-consuming miniature valve is developed. The valve development is based on previous experience with oil hydraulic miniature valves and is carried out mainly with heuristic methods, by using simplified electromagnetic equations and scaling. However, the prototypes show good properties for the intended purpose. As another challenge, a high number of these valves are needed in order to achieve sufficient resolution for demanding control. To decrease this requirement, the circulating switching control method is proposed, which can increase the effective flow resolution of the valve system using the existing valves. The method divides the switching duty equally among the valves and can diminish the drawbacks that exist in typical non-circulating switching control.

As the main goal, a water hydraulic servo axis was implemented using the developed miniature valves and the control method. The control system comprises a simple model based valve controller as the lower level part and a filtered P-controller as the upper level motion controller. Excellent tracking and positioning accuracy was achieved with a valve system having 16 miniature valves in total and using this relatively simple controller structure. This verifies that high-performance water hydraulic motion control can be realized with a reasonable effort using on/off seat valves. This gives hope for increasing the applicability of water hydraulics.

Preface

This work was carried out at the Tampere University of Technology (TUT) during 2014-2018, starting at the Department of Intelligent Hydraulics and Automation (IHA) and ending, after the change in the organization, at the Laboratory of Automation and Hydraulics Engineering (AUT). The work was funded by the Doctoral School of Industry Innovations, Tamlink Oy being the partner and co-funder in this project.

I am greatly thankful for my academic supervisor Adj. prof. Matti Linjama (TUT) who has kindly guided me through the long process, giving valuable feedback and advice any time when asked. Great thanks belong also to Prof. Matti Vilenius (Tamlink Oy) for giving the interesting research topic and for his encouraging support and belief in my work. I would also like to thank the head of laboratory Kalevi Huhtala for the great working conditions and atmosphere that the laboratory has provided.

I also want to thank all my colleagues and ex-colleagues at TUT for many fruitful discussions with them and help they have provided me during this process. Great colleagues are the key factor for successful work.

I would like to thank my lovely wife Elisa for her love and support. Thanks to my children Leo, Natalia and Daniel, you are the best children in the world.

Tampere, August 2018

Miika Paloniitty

Contents

Abbreviations

DFCU	digital flow control unit
DOF	degree of freedom
DVS	digital valve system
F4E	Fusion for Energy
PFM	pulse frequency modulation
PNM	pulse number modulation
PWM	pulse width modulation
MVPFM	multi-valve-pulse-frequency-modulation
MVPWM	multi-valve-pulse-width-modulation
WHV1-3	water hydraulic valve 1-3

Nomenclature

β_1	Correction coefficient for area [-]
β_2	Correction coefficient for magnetomotive force [-]
λ	Pulse width of PFM control [s]
μ	Permeability [H/m]
μ_0	Vacuum permeability [H/m]
μ_r	Relative permeability [-]
ω_h	Hydraulic natural angular frequency [rad/s]
ω_c	Closed loop natural angular frequency [rad/s]
Φ	Magnetic flux [Wb]
ρ_1	Performance index [s]
ρ_2	Performance index [-]
τ	Time constant [s]
τ_p	Time constant of pressure filters [s]
ξ_h	Damping factor [-]
ξ_c	Closed loop damping factor [-]
A_A	Piston area in A chamber [m^2]
A_B	Piston area in B chamber [m^2]
$A_\mathrm{c,appr}$	Calculated plunger area [m^2]
$A_\mathrm{c,meas}$	Measured plunger area [m^2]
A_c	Cross sectional area of magnetic core [m^2]
A_m	Cross sectional area of magnetic circuit part [m^2]
A_r	Area sealed by plunger [m^2]
A_x	Cross-sectional area of coil [m^2]
B	Magnetic flux density [T]

B_s Saturation flux density [T]

C Capacitance [F]

E Switching energy [J]

e_max Maximum position error [m]

F Force [N]

f Frequency [Hz]

f_c Compensated pulse frequency [Hz]

f_i Desired pulse frequency with ideal valve [s]

$F_\mathrm{m,appr}$ Calculated magnetomotive force [A]

$F_\mathrm{m,des}$ Desired magnetomotive force [A]

$F_\mathrm{m,meas}$ Measured magnetomotive force [A]

F_m Magnetomotive force [A]

g Air gap distance [m]

H Magnetic field strength [A/m]

I Current [A]

J Current density [$\mathrm{A/m^2}$]

$K_\mathrm{v,AT}$ Mean flow coefficient of valve in AT DFCU [$\mathrm{m^3/(s\sqrt{Pa})}$]

$K_\mathrm{v,PA}$ Mean flow coefficient of valve in PA DFCU [$\mathrm{m^3/(s\sqrt{Pa})}$]

K_v Flow coefficient of an average valve [$\mathrm{m^3/(s\sqrt{Pa})}$]

N Number of valves in DFCU [-]

n_sam Period length of MVPFM in samples [-]

N_w Number of turns in coil [-]

p Pressure [Pa]

p_A A-chamber pressure [Pa]

p_in Input pressure of DFCU [Pa]

p_out Output pressure of DFCU [Pa]

p_S Supply pressure [Pa]

P_hold Holding power [W]

Q_model Flow rate estimate [$\mathrm{m^3/s}$]

R_m Reluctance [1/H]

s	Laplace operator [-]
s_{m}	Length of magnetic circuit part [m]
t_0	Time of opening command [s]
t_{c}	Pulse width error [s]
T_{fast}	Sample time of pulse generators [s]
T_{slow}	Principal sample time of switching controller [s]
t_r	Response time [s]
U	Charging voltage of capacitor [V]
$u_{\mathrm{int,f}}$	Integer control signal from MVPFM [-]
$u_{\mathrm{int,w}}$	Integer control signal from MVPWM [-]
v_{e}	Velocity error [m/s]
$v_{\mathrm{ref,c}}$	Velocity reference of valve controller [m/s]
v_{max}	Maximum velocity [m/s]
w_{c}	Compensated virtual pulse width [s]
w_{des}	Desired pulse width [s]
$w_{\mathrm{pause,min}}$	Minimum pause width [s]
w_{pause}	Pause width [s]
x	Piston position [m]
x_{ref}	Reference position [m]

1 Introduction

Hydraulic actuation is widely used in industrial and mobile applications where high power-to-weight ratio is required. Hydraulic technology is very scalable and has applications over a wide power range. Easy overload protection and convenient heat transferring by the pressure medium are also regarded as the advantages of hydraulic technology. Some applications are primarily power transmission, e.g., hydraulic press or hydrostatic drive train, and some are primarily motion control, e.g., aeroplane control surfaces. The common aspect is that the power is transferred by a fluid, and the motion is controlled by controlling the fluid flow. Hydraulic actuation also has potential for high accuracy motion control.

Hydraulic systems can utilize different fluids; water and oil represent the base types, while mixtures of them and other special fluids are also used. Mineral oil is the most common fluid in hydraulics, because of its superior properties, such as great lubrication. For the environment, however, the use of mineral oil is harmful because of accidents and leakages, which cannot be completely avoided.

The difference between water hydraulics and oil hydraulics is technically just the pressure medium. However, this is not the whole truth when looking at practical applications. For oil hydraulics, a huge variety of components are available from many manufacturers. The component variety includes high-performance actively controllable components such as variable displacement pumps and servo valves. The available components enable the wide utilization of the oil hydraulics for power transmission and motion control for various applications in the industry and in mobile machinery.

Water hydraulics has the same potential in theory, but in practice, this is not seen. The main reason is the lack of components. Although water was the first pressure medium in hydraulic systems, the availability of components and the number of manufacturers are limited. Therefore, water hydraulics is currently used mainly in special applications where the properties of water are vital for the system. Such systems are e.g. press devices that process hot metal in steel industry and ceiling support in mining industry. These applications benefit greatly from the fire resistance of a water based system. If the challenges of using water as pressure medium were ignored, most applications would use water instead of oil. The advantages of water as the pressure medium include easy availability, low cost, environment friendliness, and non-inflammability. However, water is not an easy pressure medium in terms of components. In fact, the properties of water make the design of water hydraulic components difficult. This is the main reason for the limited availability of these components.

Nevertheless, basic systems can be built with existing components. There is a good availability of fixed displacement pumps and motors, cylinders, fittings, hoses, tubes, filters, and even basic valves such as pressure relief valves and on/off directional valves.

This is not the case for proportional and servo valves, as well as variable displacement pumps. These components are needed when designing hydraulic systems for accurate motion control purpose. The control valve, which can adjust the flow rate accurately and rapidly, is the key component in many advanced hydraulic systems. Therefore, the lack of this component in water hydraulics is one of the greatest factor limiting the utilization of the technology. This thesis has the goal to shorten the gap between oil and water hydraulics by developing water hydraulic control valve technology.

1.1 Water as fluid in control valves

As the first requirement, water hydraulic components need corrosion resistance of the materials that are in contact with water. This decreases the variety of suitable materials and increases the price of the components. In control valves, this might become a real problem, since there is another strict requirement for solenoid driven valves, i.e., ferromagnetism. All stainless steel grades do not show ferromagnetic properties, but some of them do. Another generally regarded disadvantage of using water as pressure medium is cavitation. Water has quite high vaporizing pressure, which causes it to cavitate easily. Cavitation can affect serious wearing if that is not taken into account in the design.

Use of low viscosity water requires narrow clearances in spool valves in order to prevent them from excessive leakage, which might become the energy consumption issue in addition to a control challenge. However, the narrow spool clearance increases the risk for contamination originated faults, thus decreasing the reliability. In addition, water is a poor lubricant for steel, thus causing friction issues. There have been attempts to use hydrostatic bearings in the spool in order to decrease the friction, but these have only been prototypes [1, 2].

The seat valves do not require the use of such ultra small clearances as the spool valves, yet they can be leak tight because of the seat type sealing. Thus, seat valves are easier to apply in water hydraulics. This seems to be also true in the markets where water hydraulic seat valves can be easily found. Some companies also offer proportional seat valves; however, they are criticized for their non-linearity and slow response [3]. Thus, something else is needed in order to get closer to oil hydraulics in terms of the control performance.

1.2 Digital hydraulic valve control

To fill this gap, analog control valves were proposed to be replaced with a digital hydraulic flow control unit (DFCU) or units. The DFCU is composed of parallel connected on/off (seat) valves and can control the flow rate in a stepwise manner. [4, 5] Despite quantized output, this method has many advantages, including fast response without overshoot. Further, the discrete states can be modeled accurately, enabling effective model based control, and the on/off valves are robust and parallel connection is redundant. Digital hydraulics has now become a whole branch of hydraulic technology utilizing discrete valued components (not only valves) and intelligent control algorithms. In fact, the technology is mainly adopted in oil hydraulics, even though analog control valve technology does not have the same fundamental challenges in oil hydraulics. The digital hydraulic valves also have industrial applications [6, 7].

A typical DFCU is binary coded, meaning that the relative flow capacities of the parallel connected valves are adjusted according to a binary series, i.e., $[1\,2\,4\,8...2^{N-1}]$, as shown in

Fig. 1.1 a). With the binary coded DFCU, the flow rate is controlled by using combinations. If N is the number of valves in a DFCU, an ideal binary series can realize 2^N different combinations, all of which have a different flow rate. In addition, the flow rate levels are evenly distributed between zero and full flow, and thus, the resolution can be calculated as $2^N - 1$. Binary coding minimizes the required number of valves with a given resolution. Typical implementation uses an array of high flow capacity valves and additional orifices in a serial connection to adjust the flow capacities as designed (see Fig. 1.1 b)). This is a very suitable implementation using commercial valves. However, the full flow capacity of the installed valves is not exploited because of the orifices. This increases the physical size of the system and reduces the flow density, which represents the flow capacity in relation to physical size.

Binary coding has some drawbacks also from the control point of view. To pursue model-based control, each valve–orifice combination should be accurately modeled. This requires considerable effort in the system commissioning stage. In addition, high flow capacity valves tend to have a slower response time as compared to smaller valves. Slow responses make high performance control difficult. Uneven response times are also a challenge with binary coding, resulting in uncertainty to the valve state during the state transitions. This supports the method using one valve model and serial orifices, since it provides good probability to similar responses with direct acting valves.

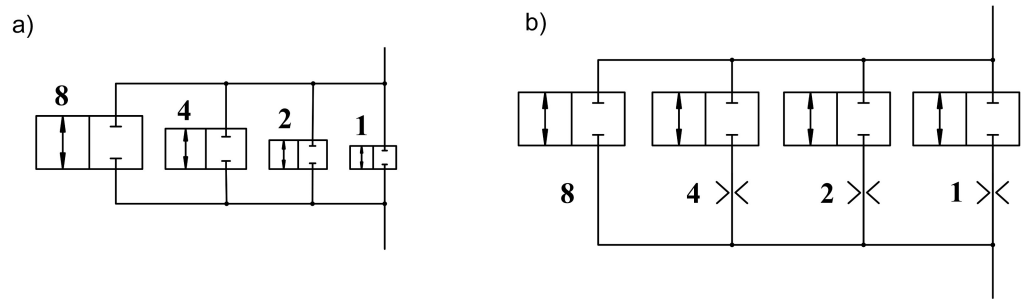

Figure 1.1: a) principle of binary coded DFCU b) typical implementation of binary coded DFCU

1.3 Equal coded DFCU

To solve the challenges of binary coded DFCU, Linjama and Vilenius [8] proposed a DFCU having all the valves equal in size, as presented in Fig. 1.2. Such a DFCU has $N+1$ different flow rates, and the resolution is same as the number of valves. Linjama and Vilenius listed the following main advantages of equal coded over binary coded DFCU:

- Step size uncertainty is small,
- transient uncertainty does not exist,
- there is no need for different size valves,
- and fault tolerance is excellent.

To make it comparable with binary coded DFCU, equal coded DFCU should have much higher number of valves, and they should be small in flow capacity. Linjama [9] analyzed

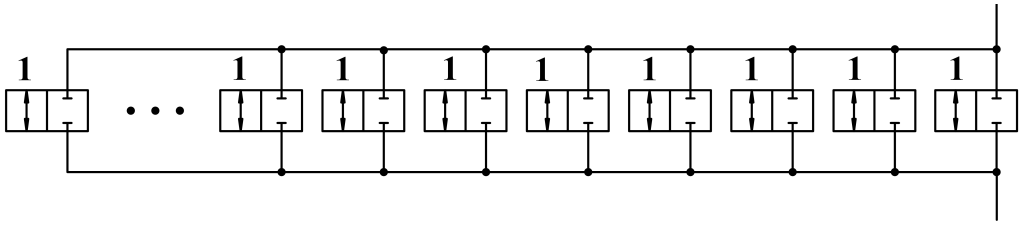

Figure 1.2: Principle of equal coded DFCU

the effect of this on the characteristics of the DFCU, i.e., the situation where one big valve is replaced with multiple smaller valves. He concluded that

- the flow density remains the same,
- the total volume may be smaller because all the installed flow capacity is in use,
- the response is faster,
- and the total switching energy is smaller.

Despite the many advantages, a high number of valves can give rise to some concerns; the modeling effort, for example, might become large. To cope with this, Paloniitty et al. studied the sensitivity of equal coded DFCU against modeling errors and investigated the possibility of using an average model in order to reduce the modeling effort [10]. They found that equal coding is more robust, and the average model is a great for reducing the modeling effort, and only has a small effect on the performance.

The equal coding method has been put into practice in oil hydraulics by developing miniature valves [11 – 13], manifold [14] and control electronics [15]. Promising experimental results are also reported in [16].

1.4 Research questions

As shown in previous sections, the equal coded DFCU seems to be a very promising control valve technology. However, the feasibility of the approach in water hydraulics is unknown, mainly because of a new strict material requirement, i.e., corrosion resistance. This considerably reduces the variety of suitable materials. The alloying elements that increase the corrosion resistance tend to reduce the soft magnetic properties of steel, which is vital for the functionality of solenoid actuated miniature valves. Therefore, reduced performance of the corrosion resistant miniature valve is expected.

A high number of valves is the other challenge within this technology. The high number of valves gives rise to concerns about the total price of the valve system. Thus, it is relevant to search for a method to reduce the number of required valves within equal coding. These challenges lead us to the main research questions in the thesis. These can be written as follows:

- *Is it possible to make a water hydraulic valve, which is suitable to equal coded DFCU?*

- *Is it possible to decrease the number of needed valves in equal coded DFCU by intelligent switching control techniques?*

1.5 Methods and restrictions

The first research question is investigated by designing water hydraulic miniature valves and measuring the achieved properties. The properties that make the valve suitable for the equal coded valve system include fast response, low leakage, high flow density, and low electric power consumption. Also, the durability against switching cycles should be adequate. As a restriction, the durability is investigated at maximum with 11 million switching cycles, which might not be enough for all applications. The design processes include heuristic methods using simple electromagnetic equations and scaling, and magnetic circuit simulation without systematic optimization.

The second research question, in fact, is mainly the question of resolution. It is investigated from the viewpoint of increasing the resolution without increasing the number of valves. Although a high number of valves has been estimated to improve the valve system characteristics, a compromise seems to be required, which does not indicate poor characteristics. To research this topic, switching control methods are extensively investigated. To answer the actual research question, an equal coded valve system with a reasonable low number of valves is implemented and tested with a heavy-loaded cylinder actuator in a tracking control case. The experimental control performance versus number of valves is then analyzed.

1.6 Contributions

To answer the research questions, the author has made the following main contributions:

- Development of a circular buffered switching control method to reduce the number of valves needed,
- development, assembly, testing and analyzing two versions of water hydraulic miniature valves,
- co-design of third valve version with an industrial partner, testing and analyzing that,
- implementation of the control code to the final test setup,
- conducting measurements with the final test setup, demonstrating high performance water hydraulic control with a 4x4 equal coded valve system.

Some parts of this work are already published with co-authors. However, the author has made a major contribution in those publications. Circular buffered switching control is published in [17]. Some details from the paper are specified in this work. The first water hydraulic miniature valve prototype is also published in [18], and an extensive durability study with that prototype is reported in [19].

2 State of the art

This chapter includes three main objectives. First, through a review, it outlines the current situation of analog control valves in the water hydraulics. The objective of this review is to show the challenges that this technology field faces. Second, this chapter reviews water hydraulic control studies in order to obtain a baseline for the experimental results. They are presented in a table 2.1 at the end of this chapter. The final objective is to study and analyze previously investigated control methods that utilizes on/off valves, including DFCU, switching control methods, and a combination of them. All the published methods are not implemented in water hydraulics; however, this is assumed to be possible.

2.1 Water hydraulic control valves

2.1.1 Spool valves

Solenoid actuated spool valves are common in oil hydraulics, and thus, they have been also proposed for water hydraulics. However, there are challenges when implementing those in water hydraulics, because of the characteristics of water. Researchers have found four main challenges: leakage, flow forces, cavitation, and friction. These challenges have led to many research activities within water hydraulic control valves. A basic solution to avoid leakage is to use a very small clearance between the spool and the sleeve. For example, Majdič et al. utilized the clearance of about 2 µm, being really small clearance [20]. Their prototype survived quite well in a durability test of 2.5 million strokes with the system having 5-µm by-pass filtration. However, the reliability is a real question with such small clearances. A sketch of a spool valve is shown in Fig. 2.1.

Flow forces typically act against the solenoid and therefore increase the force requirement

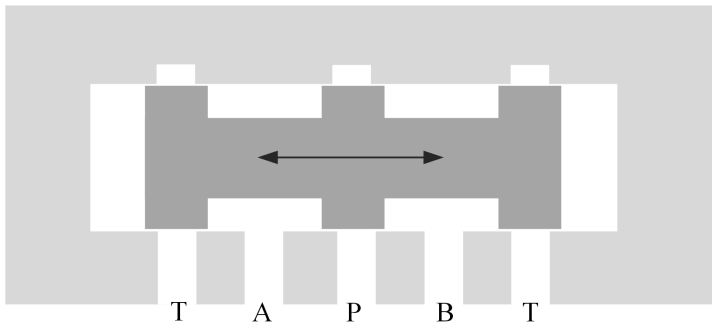

Figure 2.1: Sketch of 4/3 spool valve

and decrease the dynamics. Yang et al. presented an idea to reduce the flow forces. Their method was to shape the spool and the sleeve to increase the efflux angle and thus decrease the flow forces. Results showed that the method was effective to reduce the flow forces, and also to decrease the influence of cavitation. [21] However, they performed a simulation study, and the presented geometries might be difficult to actually produce. The influence of cavitation has also been reduced by using industrial ceramic, which is a stronger material against cavitation erosion [22]. Alumina, as an example of industrial ceramic, has also been reported to have lower friction [23].

Friction between the spool and the sleeve seems to significantly increase the non-linearity of water hydraulic spool valves. To cope with this, two main approaches have been utilized: hydrostatic bearings and spool position feedback. Urata et al., pioneers in water hydraulic control valve technology, developed hydrostatic bearings for spool [1]. Takahashi et al. from Ebara company developed a proportional spool valve using both hydrostatic bearings and spool position feedback [24]. They concluded that the developed valve had moderate leakage flow despite hydrostatic bearings (0.7 l/min @ 7 MPa) and that the valve satisfied the requirements of a basic control valve. However, the power of that leakage is 80 W, which cannot be neglected in all cases. Also, the response time of about 100 ms is slow for demanding control systems. The hydrostatic bearings are also considered in [2, 25]. The vitality of the spool position feedback was recognized also in [3, 26, 27].

The servo valve with a flapper-nozzle pilot stage is a common control valve type in oil hydraulic applications that require high control bandwidth. This valve type has also been developed for water hydraulic usage [22, 28]. Both prototypes also utilized the hydrostatic bearings and the spool position feedback. The spool support with the hydrostatic bearings as well as do the flapper-nozzle pilot stage requires some flow. To avoid leakage loss in the prototypes, the flow from the bearings was partially lead to the nozzles, and thus, the total leakage was reduced. These prototypes achieved about 40 Hz bandwidth with 3 dB gain drop.

Commercial servo valves, which were not originally developed for water hydraulics but were manufactured from stainless steel, have also been tested with water [29]. The investigated valves included one prototype, Moog 26-332, which was designed for water hydraulics (even for use in sea water). The other stainless steel models were Moog E671, Moog D633, and Ultra 465. Results of the study showed that the Moog sea water servo valve and the Ultra servo valve could be used in water hydraulic servo systems but the two other valves are not recommended. [29]

Within spool valves, there have been also propositions to drive the spool with a servo motor and ball screw mechanism [30, 31]. The best result with this mechanism yielded a frequency limit of 40 Hz with 90 degree phase lag. An even more special approach involving the use of positive cam mechanism to drive the spool was proposed in [32], which achieved a response time of 25 ms.

2.1.2 Ball seat valves

The seat valve is another type of valve. The main advantage of the seat valve over the spool type valve is its ability to be leak tight. It is therefore more commonly used in water hydraulics. A sketch of a ball seat valve is shown in Fig 2.2. Although seat type valves are most typically on/off valves, they can be also proportional type valves. The

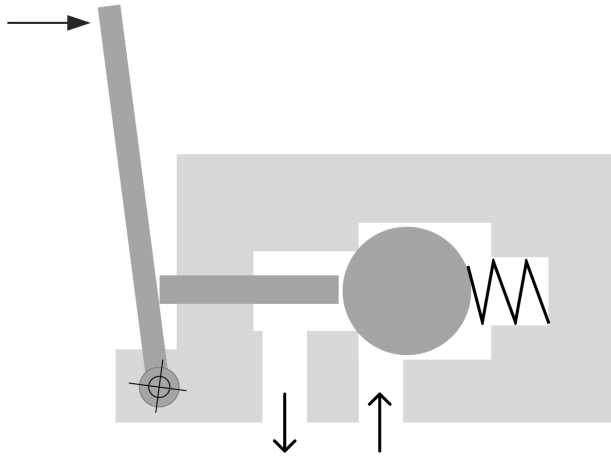

Figure 2.2: Sketch of typical ball seat type water hydraulic 2/2 valve

most common water hydraulic proportional valve is the ball seat type in 2/2 configuration. Other water hydraulic proportional valves are difficult to find.

One disadvantage of the seat structure is that the pressure force holding the valve at the closed position might become large. Therefore, these valves typically have a lever mechanism in order to multiply the solenoid force. Koskinen et al. stated that the advantages of these valves include low leakage, reliable operation, and easy manufacturing. They claim that high non-linearity of the ball poppet is the main disadvantage of this valve structure. These valves also tend to have relatively large moving masses and therefore have response times of around 60-80 ms, which is quite slow, compared with servo valves [3].

2.2 Water hydraulic motion control

2.2.1 On/off control technology

On/off-valves have been used to realize position and velocity control of water hydraulic actuators. This topic started to be extensively studied in the 21st century. First studies searched suitable on/off valves and presented simple on/off position control methods for a water hydraulic cylinder. [33, 34] Subsequently, a method to improve on/off position control was presented. The system utilized serial connected on/off valves and a capacitance between them. A stepper-like motion control was thus implemented to fine-tune the piston position. The achieved positioning accuracy was 0.1 mm. [35]

2.2.2 Parallel connected technology

The concept of a digital flow control unit (DFCU) is an old invention that enables proportional-like control using on/off valves, but it was hardly used before the age of computers. The concept was adopted in water hydraulics in the beginning of 21st century. Linjama et al. presented a control study with a water hydraulic cylinder [4], and Laamanen et al. did the same with a water hydraulic motor [5]. The first position tracking study included two five-bit DFCUs, a directional switching valve, and a 32/16 horizontally assembled cylider with a load mass of 100 kg. The reported natural angular frequency of

the system was 105 rad/s. The system used a fifth order polynomial as a test trajectory for the piston position. [36] In order to develop the tracking accuracy, especially at low speeds, Linjama et al. presented an improved control method using the same cylinder and load as in the previous study. The main concept was to control the cylinder with four DFCUs, and enabled the use of all DFCUs simultaneously. [37]

The technology utilizing multiple parallel connected on/off valves was termed digital hydraulics. The research on this topic continued intensively in oil hydraulics. However, only a few papers have been published on digital water hydraulics after [37]. One from TUT [38] was related to a rock drilling application. The digital hydraulic solution was used to control the amount of water used for binding dust. The valves used in that study were FloControl Q2R-B. Zhang et al. published two papers on the design of a digital water hydraulic valve [39, 40]. Unfortunately, these papers brought little new scientific content over the early published papers by Linjama and Laamanen. Park et al. also developed a high speed on/off valve for water hydraulics [41]. It was a two stage valve with about 2 ms response time. PWM velocity control for a hydraulic motor was successfully implemented with the prototype valve. Later, this prototype was developed for proportional control by adding an internal position feedback for the poppet [42, 43].

2.2.3 Switching technology

The flow rate can be controlled with a single on/off valve utilizing continuous switching techniques, e.g. pulse width modulation (PWM). With this technique, the flow rate can be controlled as an average over the PWM period by varying the ratio of times the valve is in the closed and opened positions. Most studies on switching control are performed with oil hydraulics or pneumatic systems. However, principles of this technique are independent of the used fluid. Therefore, this section introduces the most relevant studies on switching control although water was not utilized in these studies.

Some early studies in this field are reported in [44] and [45]. PWM control has fundamental drawbacks with non-ideal valves, having switching delay and finite movement speed. This causes non-linearity to the average opening. Solenoid valves, which are the most common valves to implement PWM control, have been thought to have five operating modes when driving with PWM. They occur in the following order when the duty cycle is increased from zero to one [46]:

1. Off
2. Ballistic
3. Normal
4. Inverse ballistic
5. On

First the valve stays constantly off, because the control pulse is shorter than the delay time of the valve. Second, the operation mode, where the valve begins to respond but does not reach the full open position, is called ballistic mode. When the control pulse and pause between the pulses are long enough, the valve acts in the normal mode where the full open and full closed positions are alternated. In the inverse ballistic mode, the valve begins to close, but the pause time is too short for the valve to reach the full closed

position. Finally, the valve stays constantly in open position because of the pause time too short for any response.

An ideal valve with no delay and infinitely fast state transitions would have only the normal mode, and the relationship between the average opening and duty cycle would be linear. However, with real valves, the other operation modes come into picture and brings non-linearity to the relationship. One fact is that the portion of normal mode reduces with the increasing frequency [46]. Thus, most linear modulation requires low switching frequency. This, however, would reduce the quick response of the system and might result in discontinuing movements. Therefore, other methods have been used in order to deal with the non-linearity. In early studies, simple compensation was used in order to linearize the output. The remaining drawback, however, is that the other modes are sensitive to parameter changes, and therefore, the linearization is effective only in constant conditions.

Muto et al. developed a differential pulse width modulation method that eliminates most of the non-linearities of PWM control. They used a symmetric cylinder and two 3/2-valves, one connected to both of the cylinder chambers. Zero velocity was realized by using identical 0.5 duty cycles for both valves, resulting in high, but equal, pressure alternation in both cylinder chambers. When the duty cycles are different, one chamber is connected for longer to the high pressure, which results in a movement of the piston. [47] The core idea seems to be the transition of the zero velocity point into the most linear area, i.e., the middle of the duty cycle span. Thus, the nonlinearities occur mostly in the extreme regions of the control area, and the most critical area, around zero, is most linear. This method, however, requires a symmetric cylinder and loses the ability for separate metering.

Varseveld and Bone used an asymmetric pneumatic cylinder and two 3/2-valves, connected as reported in [47], and analyzed four different PWM schemes [48]. The most advanced scheme used 0.5 duty cycles for both valves to keep the cylinder stationary, as reported in [47]. In addition, they used non-linear control of the duty cycles and took the minimum feasible duty cycle into account to linearize the output. As a result, they achieved quite a linear output, but the maximum velocity was dropped below 40 % of the original maximum velocity. Furthermore, the differential PWM method consumes a significant amount of energy even at zero velocity when applied in pneumatics.

Belforte et al. developed a dynamic response of PWM control. They presented a solution to manage with the conflict of fast response and good controllability in a pneumatic application. They proposed the use of two parallel connected PWM valves and used them in different PWM frequencies. The one with the higher frequency can respond faster but has a narrow usable duty cycle range. The one with the lower PWM frequency has wider controllable duty cycle range but responds slower. By using these together, they achieved better controllability than that possible with one valve. [49]

Schepers et al. developed a model based optimal control method for a hydraulic switching valve. They performed extensive analysis on different switching methods, including PWM, PFM, inverse PFM and even DFM, in which the duty cycle is kept constant and the frequency is varied. They concluded that their new method is most close to inverse PFM but has better controllability at small control values. Another conclusion was that PFM or DFM cannot be used for control tasks in combination with a single on/off valve. [50] However, the optimal control method largely utilizes the ballistic modes, which are sensitive to parameter alteration. Therefore, an accurate valve model and stable

conditions are required. The method might not be suitable with seat valves without a pressure balanced plunger, because of the pressure-dependent response times.

2.2.4 Combination

Some digital hydraulic studies are presented in which both parallel connection and switching techniques are exploited. Huova and Plöckinger built a four-way valve system in which each of the four control edges comprised four parallel connected valves, for which sizing was near the binary coding. The two smallest valves were fast switching valves that were driven with PWM when profitable. They used the system to control the movement of a horizontally assembled 63/45 cylinder with 500 kg load mass. They presented a ratio between the minimum and maximum velocity to increase from 50 to 350 when utilizing switching control. They also discussed that the provided increase in resolution might not be needed in high velocities.

Ferraresi performed a study with a pneumatic valve system having nine parallel connected on/off valves. They studied different methods for valve system control. Their analysis included different sizing schemes, some of them in combination with PWM control. They stated that the best configuration was the method where all the valves were in the original size, without additional orifices (equal coding); one of the valves was driven with PWM and all other were used to bias the flow rate level. They achieved quite a linear response from zero to full flow. [51] However, a dedicated PWM valve requires high frequency switching and will naturally wear faster due to high number of switching. In addition, the nonlinearity of PWM control remains, although the effect is on a smaller magnitude.

Kogler and Scheidl utilized the parallel connection of multiple switching converters in order to increase the effective output frequency. They set a certain phase shift to each converter and obtained the effective output frequency to be multiplied by the number of converters. [52]

Paloniitty et al. studied the advantages of using PFM control with an equal coded valve system controlling a vertically assembled 32/18 hydraulic cylinder. The valve system had two DFCUs with eight equal valves and controlled the inflow and outflow of chamber A. Chamber B was directly connected to supply pressure. They compared the PNM method with a combination of PNM and PFM in trajectory tracking control. Significant improvement in the tracking accuracy was achieved in small velocity trajectory when the PFM method was utilized. In addition, the positioning accuracy was improved from 300µm to 17µm. [53]

2.2.5 Water hydraulic servo control

Mäkinen and Virvalo studied motion control of a 63/36 cylinder with an inertia load having a natural angular frequency of 90 rad/s. They used a servo valve with a state controller and a feedforward controller. [54] Cho et al. implemented a sliding mode tracking controller in a water hydraulic system having a horizontally assembled 32/16 cylinder and 200 kg inertia load. The natural angular frequency of the system was not given, but it can be estimated based on similar studies. [55] Sairiala et al. utilized a commercial proportional directional control valve with a proportional controller and a feedforward controller to perform tracking control of a 32/16 cylinder with 200 kg inertia load. They used non-linearity compensation of the valve [56]. Sairiala et al. also performed motion control with 2-DOF manipulator using two 4/3 proportional valves,

which were developed in [24]. They utilized simple proportional control and concluded that better controllers are needed. [57]

Virvalo and Mattila studied the accuracy of a see-saw type water hydraulic test bench. They studied the bench in the unloaded condition with a 32/25 cylinder and reported the natural angular frequency of the system to be 15 rad/s. The controller was a feedback state controller. [58] Linjama et al. compared a servo valve and a digital valve system in the same see-saw test bench as in the previous study. This time, the cylinder was larger, 125/80, and a load mass of 500 kg was attached on the boom, resulting in a natural angular frequency of 44 rad/s. They achieved the same accuracy with both of the valve solution. [59]

Zhai et al. performed a series of studies aiming to develop a water hydraulic motion control for ITER remote maintenance system. Two of them reported tracking results. The first one was performed again with the same test bench as in previous two studies cited above. The loading conditions and cylinder size were not reported. However, the natural angular frequency was extensively studied, giving a minimum value of 50 rad/s. They utilized a filtered proportional controller, where the error signal is filtered with a first order low pass filter. [60] The second one was a study with 4-DOF mock-up of the ITER cassette manipulator. Each axis was studied separately. The studied axes were named as lift, tilt, CRO, and HRO. Lift and tilt actuators had both high static and inertia load and the natural angular frequency of 31 rad/s while CRO and HRO had inertia load only and much lower natural angular frequency having value of 6 rad/s. From lift and tilt, better results were achieved with lift axis using filtered proportional and feedforward controllers. From CRO and HRO, better results were achieved with CRO utilizing state controller.

Furthermore, Mäkinen and Virvalo compensated the non-linearity of a servo valve and improved the positioning accuracy [61]. Sairiala et al. modified a pneumatic 4/3 proportional valve for water hydraulic use and compensated for its non-linearity. Their study included steady state accuracy measurements with a 32/16 cylinder having a 200 kg inertia load. [62] Wu et al. developed a parallel water hydraulic weld/cut robot having 5 DOF and reported maximum position errors in actuator space [63]. Ito et al. studied a simple adaptive controller with servo cylinder having a piston diameter of 30 mm. [64]

2.3 Summary

Many types of water hydraulic control valves have been developed. The flapper nozzle servo valve is the only type that has achieved response time below 10 ms. Attempts to avoid flapper nozzle mechanism due to its disadvantages with water have lead to slow response. However, there are currently no commercially available flapper nozzle type servo valves designed for pure water. Some stainless steel valves exist, but the reliability and life time in water usage are questionable. Most commercially available water hydraulic control valves are proportional ball seat valves in the 2/2 configuration. However, they have drawbacks of non-linearity and slow response. The availability of on/off valves is also limited, especially of on/off valves that have good properties for digital hydraulics. The demanded properties include compact size, fast response, low energy consumption, and moderate price. The commercial on/off valves that were utilized in the digital hydraulic studies can be made acceptable fast, using proper power electronics, but the maximum pressure is rather low for general use. In addition, their size and power consumption are hardly acceptable in digital hydraulic use.

Table 2.1: Control results in reference studies

Reference	Valve type	ρ_1 [ms]	ρ_2 [-]	SS error
Linjama & Vilenius 2005 [37]	digital	5	500	170 µm
Sairiala et al. 2003 [56]	analog	9	*900	50 µm
Mäkinen et al. 2001 [54]	analog	10	594	
Linjama et al. 2003 [36]	digital	10	1050	
Linjama et al. 2008 [59]	analog	13	550	
Linjama et al. 2008 [59]	digital	13	550	
Cho et al. 2002 [55]	analog	31	*3100	
Zhai et al. 2009 [60]	analog	67	3366	
Sairiala et al. 2005 [57]	analog	80	*3517	0.05 deg
Zhai et al. 2010 [66] CRO	analog	83	521	0.015 deg
Virvalo & Mattila 2007 [58]	analog	120	1800	
Zhai et al. 2010 [66] lift	analog	333	10456	0.01 deg
Sairiala et al. 2003 [62]	analog			200 µm
Wu et al. 2005 [63]	analog			10 µm
Ito et al. 2012 [64]	analog			10 µm
Mäkinen & Virvalo 2000 [61]	analog			50 µm

* Natural frequency is estimated

Most servo control studies are carried out with a cylinder and they can be divided into two categories: positioning control and trajectory tracking control. Positioning control is typically evaluated with the final position error, and trajectory tracking control with the maximum position error during the trajectory. However, the system scale directly affects the error values, and it should therefore somehow be taken into account. One method, presented by [65], is to scale the maximum position error during trajectory $e_{\max}$ with the maximum velocity $v_{\max}$ as follows:

$$\rho_1 = \frac{e_{\max}}{v_{\max}}, \tag{2.1}$$

However, this does not take the natural angular frequency of a system into account. Thus, a new performance index is proposed:

$$\rho_2 = \rho_1 \omega_{\mathrm{h}}, \tag{2.2}$$

where ω_{h} is the hydraulic natural angular frequency of the system.

Water hydraulic motion control and positioning studies have been carried out with servo valves, digital valves, and proportional valves. The studies with proportional valves used spool type valves, which were either prototypes or commercial valves that are no longer available. Some studies used servo valves but did not specify the valve model. Digital hydraulic control systems within water hydraulics have been built using commercial on/off valves. The maximum pressure in the studies has been 7 MPa. One study directly compared the tracking accuracy when using a servo valve and a digital valve. The results show similar tracking performance with both valve systems. In addition, the best tracking result of all the analysed studies was achieved with the digital hydraulic valve system. All the results, emphasizing tracking control, are presented in Table 2.1. The studies are sorted by the performance index ρ_1.

Potential digital hydraulic methods that have not been utilized in water hydraulics are also analyzed. They include switching control and a combination of parallel connection and switching control. The non-linearity of the PWM control has been widely recognized. Many attempts have been made to address this. However, single valve switching control has serious disadvantages when considering high-performance water hydraulic servo control: low durability, sensitivity to modeling errors and parameter variations, and non-linearity. The most promising technique is the combination of parallel connection and switching control. It seems to be effective to reduce the disadvantages of the single valve switching control.

3 Miniature Solenoid Valve Design

As shown in the previous section, only some water hydraulic valves exist that are suitable for digital hydraulic control. The existing valves are far from optimal for use in an equal coded valve system. Therefore, a new valve prototype is required in order to answer the research questions of this thesis. In oil hydraulics, the miniature valves for the equal coded valve system started to be developed in 2010 with an ideology of having as simple valve as possible in order to enable cheap mass production and further miniaturization [11]. The same idea is followed in this thesis and the basic valve structure is not changed. Thus, the valve to be developed is a solenoid actuated, spring returned, unidirectional seat valve. Even with this fixed structure, the optimization is a difficult multi-objective problem. Therefore, systematic optimization methods were not utilized. Instead, heuristic methods such as basic equations, scaling and assumptions were used. This chapter introduces the theory that is utilized in the design process.

3.1 Introduction

A solenoid actuator is widely used in electrohydraulic valves. It has a set of good properties for usage in hydraulic valves: moderate high forces, moderate long stroke, moderate speed, and low price. A simple solenoid can generate force in one direction. The return movement is usually carried out with a spring. Figure 3.1 presents a schematic structure of miniature valves considered in this study.

The design objectives for the solenoid of a miniature valve are small size, low electric power consumption, and fast response. The last objective is the most important from the control point of view; however, it requires little attention, because miniature valves seems to be fast [11, 13, 67]. Electric power consumption is influenced by many design parameters that might conflict with the small size. However, based on the experience with oil hydraulic miniature valves, the power consumption will probably not be a problem. Thus, the small size is the main design objective. The objective of low power consumption is taken into account by avoiding undersizing of the magnetic circuit, which may lead to inefficient force generation. In addition, the opening and holding stages are considered separately because of very different conditions.

3.2 Ferromagnetic materials

Proper operation of solenoid requires ferromagnetic materials. Ferromagnetism is a known phenomenon where the material amplifies an external magnetic field. The most important magnetic property is permeability, which is generally represented as μ. The permeability

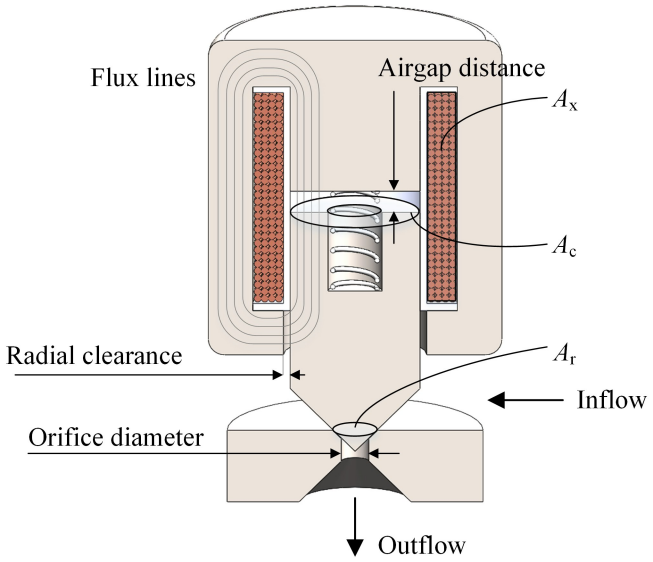

Figure 3.1: A schematic structure of a miniature valve

determines the magnetic induction in the material with a basic expression

$$B = \mu H, \tag{3.1}$$

where B is the magnetic flux density and H is the external magnetic field strength. Permeability is usually divided into vacuum permeability μ_0 and relative permeability μ_r, thus giving the relation $\mu = \mu_0\mu_r$. In ferromagnetic materials, permeability is not constant and it varies with H. The nonlinear relationship between the external magnetic field H and induced flux density B is usually presented with a material specific B-H curve. Figure 3.2 presents a schematic example of the B-H curve shape. At the beginning of the curve, the relative permeability can be on the order of thousands, but with increasing the external field, it decreases. After a certain point, the slope of the curve equals the vacuum permeability. This means that the material is saturated, and a further increase in the external magnetic field increases the flux density only because of vacuum permeability. The flux density at this point is designated as saturation flux density B_s. That is the most important magnetic property of a material for miniature valves because the available force is a function of flux density. Therefore, the saturation flux density is a justified value to be used as B in the valve dimensioning.

Selection of core materials for water hydraulic valve excludes typical high saturation flux density materials such as pure iron and permendur (50% Fe 50% Co) because of their poor corrosion resistance. Pure iron has a saturation flux density of 2.15 T and permendur as high as 2.45 T [68]. Stainless steels, by definition, contains a minimum of 10.5 % of chromium by weight [69], but unfortunately, the chromium content decreases the saturation flux density [70, 71]. Thus, there is a conflict between the high saturation flux density and corrosion resistance. Based on the approximation of the chromium content effect on the saturation flux density (presented in [71]) and the minimum percentage of chromium, it can be stated that the maximum saturation flux density value of stainless steel is about 1.75 T. In addition, all stainless steel types are not ferromagnetic. However,

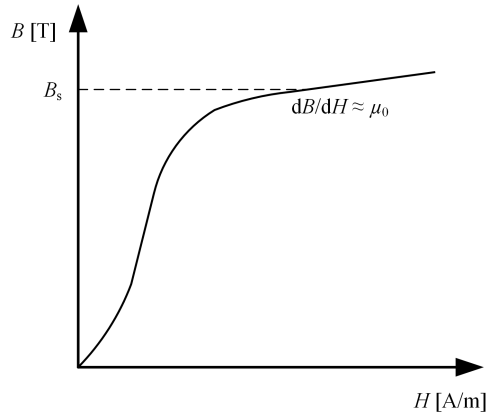

Figure 3.2: Schematic B-H curve of ferromagnetic material with an occurrence of saturation.

ferritic and martensitic grades can have good magnetic properties including high saturation flux density and high permeability [70].

One big difference between ferritic and martensitic grades is that martensitic grades can be hardened by heat treatment. A hard surface in the plunger tip is required within the design of the miniature valve. However, the quenching negatively affects the magnetic properties [72]. Therefore, the magnetic circuit parts should not be quenched fully, but partial hardening of the plunger tip is possible.

3.3 Design procedure

The simplified design procedure is presented in Fig. 3.3. The process includes two steps where the objective is to minimize a quantity related to the physical size of the solenoid. In the first step, two conflicting properties are good corrosion resistance and high saturation flux density. In the second step, increasing energy consumption and heat load limits the miniaturization of the coil.

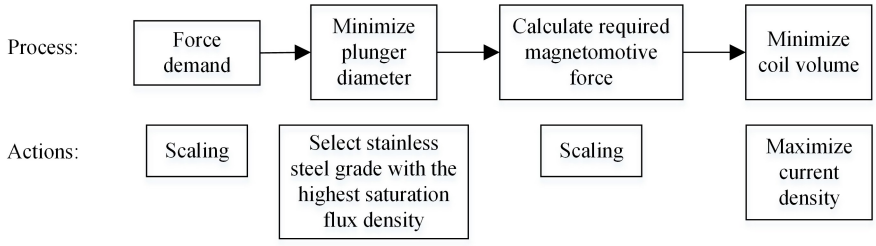

Figure 3.3: The simplified design procedure with the main design actions

It is good to start solenoid design from the force requirement. The force of a solenoid can be estimated with the well-known approximate equations of magnetic force [73]:

$$F = \frac{B^2 A_c}{2\mu_0}, \tag{3.2}$$

where B is the magnetic flux density, A_c is the cross-section area of the magnetic core near the air gap, and μ_0 is the vacuum permeability. Thus, there are two main parameters that affect the available force: B and A_c. As stated previously, the saturation flux density of the core material is a justified value for B. The required core area can then be calculated to satisfy the force demand. By assuming that the pressure force is the only counteracting force of the plunger, the core area can be expressed as:

$$A_c = \frac{p\, A_r 2\mu_0}{{B_s}^2}, \tag{3.3}$$

where p is the design pressure and A_r is the area sealed by the plunger (outer diameter of the orifice bevel).

Next, the magnetomotive force is designed. It can be done with the reluctance method, by utilizing a simple equation that is analoguous to the well-known Ohm's law: [73]

$$F_m = R_m\, \Phi, \tag{3.4}$$

where F_m is the magnetomotive force, R_m is the magnetic reluctance, and Φ is the magnetic flux. Thus, the required magnetomotive force can be calculated if the reluctance and magnetic flux are known. The magnetic flux can be written as:

$$\Phi = B_s\, A_c, \tag{3.5}$$

and therefore is known, but the accurate reluctance of the magnetic circuit is more complicated. The reluctance of a magnetic circuit part can be written as:

$$R_m = \frac{s_m}{\mu_r\, \mu_0\, A_m}, \tag{3.6}$$

where s_m is the length and A_m is the cross sectional area of the circuit part. Owing to the changing permeability, accurate reluctance calculation requires the B-H curve of the material to be known and may need iterations. However, in the simplest approximation, ferromagnetic parts can be neglected, because their permeability is much higher that of the airgaps. It can be assumed that the main airgap is the only remarkable reluctance in the magnetic circuit. Now, assuming that air permeability equals the vacuum permeability and substituting Eq.(3.6) and Eq.(3.5) into Eg.(3.4) yield the expression for the desired magnetomotive force:

$$F_{m,des} = B_s \frac{g}{\mu_0}, \tag{3.7}$$

where g is the air gap distance.

Once the desired magnetomotive force is known, the coil can be designed. The expression for the magnetomotive force, generated by the coil, can be written as:

$$F_m = N_w\, I, \tag{3.8}$$

where N_w is the number of turns in the coil, and I is the current through the coil. Thus, the coil can be designed to have less turns and to be driven with higher current or vice versa. The ratio between those affects the operating voltage of the solenoid. In fact, Eq.(3.8) tells nothing about the actual size of the solenoid. To design the actual dimensions, one new parameter should be considered, i.e., the current density, which can be written as:

$$J = \frac{N_w\, I}{A_x}, \tag{3.9}$$

where A_x depicts the cross-sectional area of the coil. It can be seen that the current density defines the cross-sectional area of the coil since the magnetomotive force is known already. The higher the current density, the smaller the coil and vice versa. As a drawback, a small coil causes higher resistive loss. However, a smaller coil makes the magnetic circuit shorter, which might be beneficial. In order to design miniature valves, the current density should be maximized.

The remaining design feature is the cross-sectional shape of the coil. The same cross-sectional area can be achieved with different shaped coils. Thus, the final geometry remains as a design parameter. The wire selection also affects the geometry, because the dimensions can be only multiple of that. If both coil wires should end at the same side of the coil, the thickness should be a multiple of two wire diameters.

3.3.1 Maximizing current density

The easiest way to use a solenoid is by constant DC voltage. It means that the coil should bear full time the current, which is needed for the pull. Most of the solenoids are designed for that, being super simple to use: connect voltage source to open and disconnect to close. However, that design method does not fit well in the miniature valves because the operation conditions of the pulling stage and holding stage differ so much and because the current density should be maximized. The pulling stage begins in the situation, where the air gap and pressure force are maximum. In contrast, in the holding stage, the main air gap is closed and the pressure force is minimum. The closed airgap implies easier force generation because of smaller reluctance. The spring force, however, is at maximum at the holding stage but it is typically much smaller than the pressure force. Thus, the holding stage might need only a fraction of the current that is needed in the pulling stage. This is also shown by experimental studies with oil miniature valves [11, 13].

Thus, the current density can be increased in the pulling stage, if the maximum value is used only for a short time to open the valve. After that, the current can be significantly lowered. With this method, the current density in the pulling stage can be increased without increasing the average heat dissipation, which is the limiting quality when increasing the current density.

The proposed approach is to use the above described method to design the pulling stage, and to use the maximum current (giving the designed J) for as short time as possible. The reasonable time value is slightly longer than the maximum response time of the valve. This method generates a constant amount of heat on each switch, and therefore, the average dissipation is a function of switching frequency. Thus, the designed current density affects the maximum switching frequency of the valve.

Figure 3.4 depicts the difference in the electric power feed of a typical valve and a miniature valve. The voltage and current axes are normalized to have unity values at the holding stage. As shown in the figure, the typical valve can be driven either with constant DC voltage or by using voltage peak to increase the current faster and, consequently, shorten the response of the valve. However, the feed of a miniature valves differs from both these methods, having a peak also in the current, as discussed earlier.

3.3.2 Design by scaling

The above presented design method includes many assumptions and simplifications. The calculation of A_c with Eq.(3.3) does not take all the counteracting forces into account and

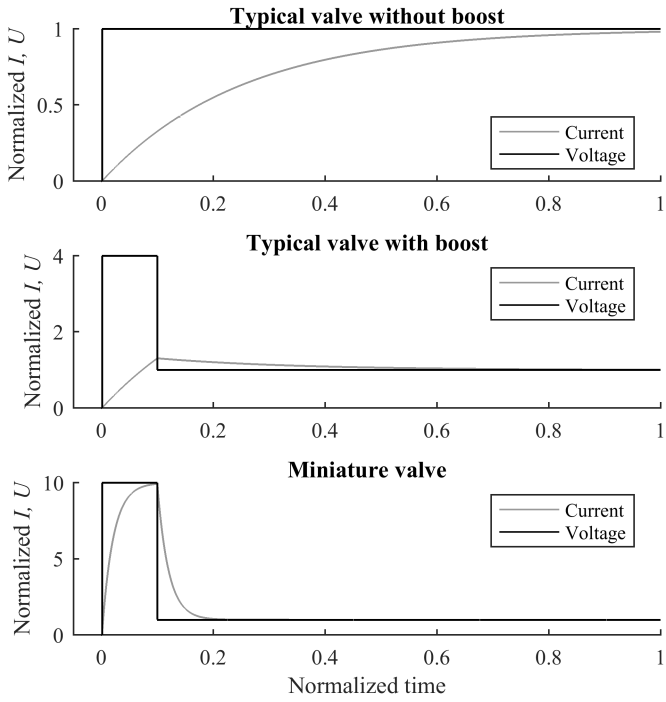

Figure 3.4: Electric power feed of miniature valve differs considerably from that of a typical valve: a) constant DC usage of typical valve b) peak and hold strategy with typical valve c) peak and hold strategy with miniature valve

therefore may lead to undersizing. Similarly, the calculation of $F_{\mathrm{m,des}}$ with Eq.(3.7) does not take all the reluctances into account and may also lead to a value that is too small. Therefore, direct use of the method likely leads to shortcomings in the performance.

Scaling can be used to increase the accuracy of the design method. It requires a similar type reference valve where the real values and theoretical values of design parameters can be inspected. Then, for the similar type of valve, it can be assumed that the relationship of those remain constant. Thus, one can calculate the correction coefficients for the design parameters by using a reference valve as follows:

$$\beta_1 = \frac{A_{\mathrm{c,meas}}}{A_{\mathrm{c,appr}}}, \qquad \beta_2 = \frac{F_{\mathrm{m,meas}}}{F_{\mathrm{m,appr}}}, \tag{3.10}$$

where $A_{\mathrm{c,meas}}$ and $F_{\mathrm{m,meas}}$ are measured values from the reference valve and $A_{\mathrm{c,appr}}$ and $F_{\mathrm{m,appr}}$ are estimated values from the reference valve. Then, multiplying the calculated A_{c} of the new valve with β_1 and $F_{\mathrm{m,des}}$ with β_2, we get the corrected values for the new valve.

4 Novel Switching Method

The possibilities of combining an equal coded DFCU and switching control were investigated with an aim to increase the output resolution of a DFCU, retaining it as an individual control edge. This enables the unit to be used as a part of an independent metering valve system. The proposed method enables the control of an equal coded DFCU with a proportional value. However, the method is best to be used in combination with a flow rate model, when it becomes a pressure compensated flow metering edge. In this Chapter, the developed switching method is described and analyzed.

4.1 Overview of the method

The main idea is to create a control edge that can be controlled with a proportional value. In this case, the reasonable scaling of the control value is $0...N$, because then the value refers to the number of open valves and fit well together with a flow rate model of an average valve. The value can be divided into an integer part and a decimal part. Ferraresi used a similar scaling and realized the integer part of the control value with static open valves and the decimal part with a single PWM valve [51]. Conveniently, the decimal part was used directly as the duty cycle of the PWM valve. The output is then a sum of the static open valves and pulses of the PWM valve. In the ideal case, the output of the proposed method looks the same; however, the pulses are created in a different way.

One idea behind the novel switching method is to divide the switching duty among all the valves in a DFCU, thus keeping the switching frequency of a single valve as low as possible. The output frequency can be maintained high since many parallel switching valves carry out the switching control. The low switching frequency of a single valve is beneficial to the control linearity. Scheidl and Kogler used many parallel connected switching converters to increase the effective output frequency [52]. However, their method could not respond at the high output frequency; instead, the lower frequency of a single converter determined the control interval. Therefore, their method does not fulfill the requirements of this study.

Figure 4.1 shows the implementation of a control value of 2.1 with Ferraresi's method, having four equal valves and one of them as a dedicated switching valve performing the decimal part of the control value, as reported in [51]. Figure 4.2, in turn, shows the same control value implemented with the proposed method where all valves take part in switching control. The sum of the control signals of all the valves are equal between the methods; however, the control signal of single valves differs considerably.

Depending on the valve dynamics and the used switching frequency, the switching valve of the first case may ignore the control pulses, which makes the effective output to be 2.0. The proposed method, however, probably can realize the switching sequence owing to the

lower frequency and longer pulses of a single valve. In addition, the proposed method divides the total number of switches equally to all valves and thus extends the lifetime of the system compared to the first solution.

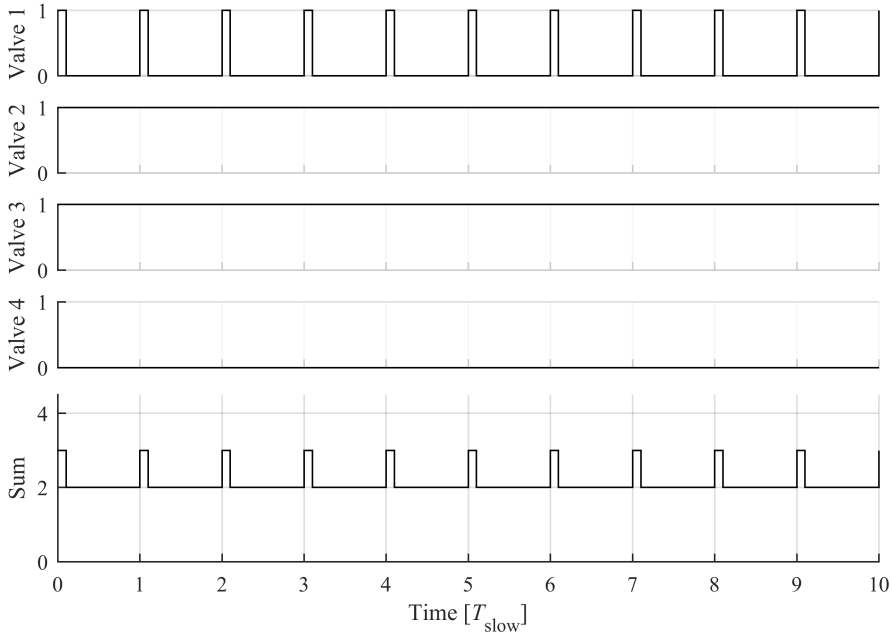

Figure 4.1: Control value of 2.1 implemented with a DFCU and dedicated switching valve

One important aspect within switching control is the linearity of the response. As discussed in Chapter 2, high switching frequency decreases the linearity of the valve output. By using the proposed switching method, the linearity remains on the level corresponding to low frequency response, yet with the high output frequency and ability to respond quickly. The situation is illustrated in Fig. 4.3. The response curves are approximations based on the measurement with WHV2 shown in Fig. 4.5.

In order to linearize the remaining non-linearity at the beginning of the control span, pulse frequency modulation was used. The idea is to prevent the valve from too short pulses, controlling the effective opening by changing the frequency. In other words, when the pulse width modulation would lead to pulses that are too short and to a mode other than normal mode, the frequency is decreased instead of the pulse width. The block diagram of the method is presented in Fig. 4.4. Both parts of the method, the orifice model and the dynamic valve model, are modeling the average behavior of the valves in a DFCU.

There are three principal parameters in the method: T_{slow}, T_{fast}, and λ. T_{slow} depicts the principal sample time of the switching controller. The average output with MVPWM can be changed at that sampling rate. It is also used as the period length for the MVPWM control and thus determines the carrier frequency for MVPWM control as $f = \frac{1}{T_{\text{slow}}}$. T_{fast} depicts the sample time of the pulse generation part. The faster sample time is required for the timing of pulses in switching modulation. The last principal parameter, λ, is the

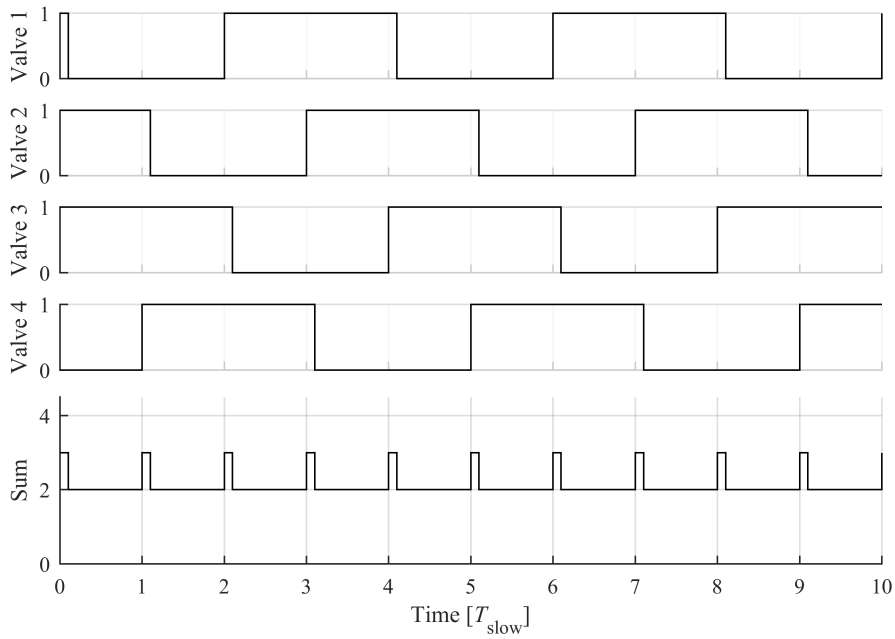

Figure 4.2: Control value of 2.1 implemented with the proposed switching method

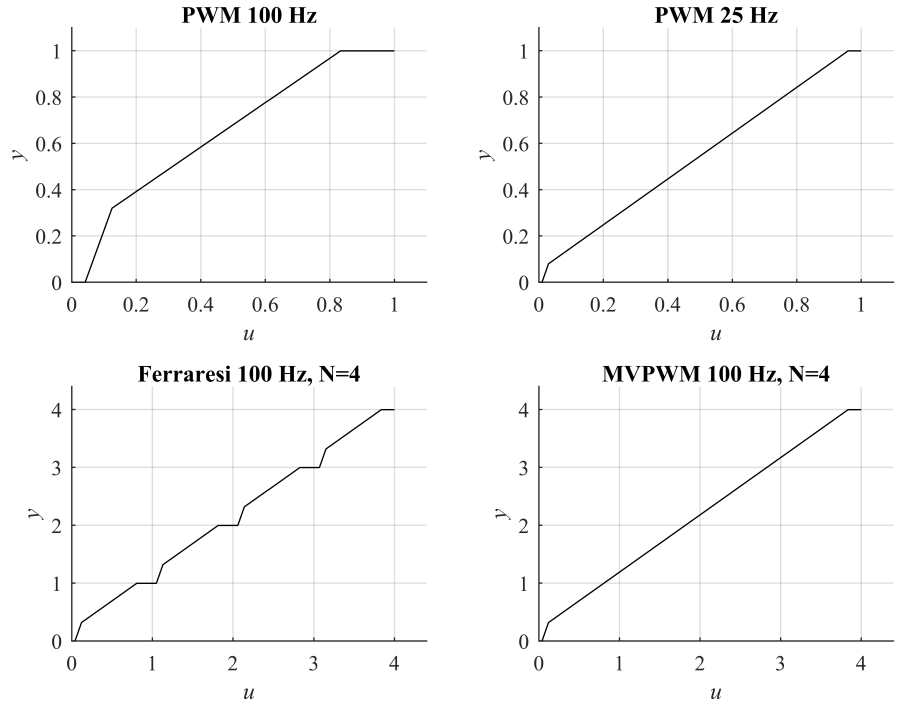

Figure 4.3: Principal comparison of response of different switching methods

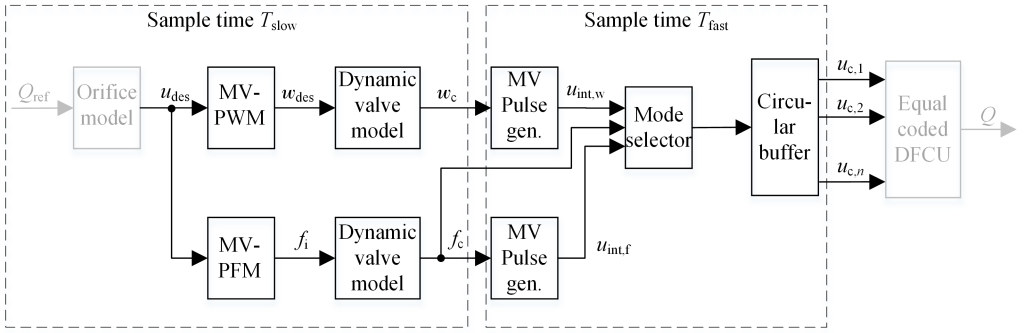

Figure 4.4: Block diagram of the novel switching method. Black lined blocks represent the core of the method and grey blocks are to be used with the method.

pulse width of MVPFM control. It is selected according to a valve dynamics, as will be discussed later.

4.2 Multi-valve-pulse-width-modulation

Multi-valve-pulse-width-modulation (MVPWM) is used when compensated pulse frequency f_c is above f. MVPWM outputs *the virtual pulse width* that represents the required pulse width in order to realize u_{des} on average over the PWM period. In contrast to the basic pulse width modulation, the pulse width might be longer than the PWM period; therefore, it is called *virtual pulse width*. To realize this, multiple valves are needed. The equation for the MVPWM can be written as:

$$w_{des}(u_{des}) = \frac{u_{des}}{f}, \tag{4.1}$$

where f is the PWM carrier frequency, and u_{des} is the floating point control value, which can have values from zero to N, i.e., the number of valves in the DFCU.

4.3 Multi-valve-pulse-frequency-modulation

Multi-valve-pulse-frequency-modulation is used when f_c is below f. Thus, small control values that would lead to short virtual pulse width, are realized with MVPFM control, by decreasing the pulsing frequency rather than decreasing the virtual pulse width. This way, no minimum value exists for the average opening. However, as a drawback the period length, over which the output averages, could be long, resulting in jerky output. Nevertheless, very small velocities are often related to the actuator positioning task, where small steps towards the final position might not be a problem.

The MVPFM block outputs an ideal pulse frequency f_i, representing the desired pulse frequency with ideal valve. It uses the minimum allowed virtual pulse width λ as the pulse width in the calculation. Thus, the block can be expressed as:

$$f_i(u_{des}) = \frac{u_{des}}{\lambda} \tag{4.2}$$

4.4 Single parameter dynamic model

Within the method, at least one opening and one closing event are conducted within each period. By opening a valve and closing it, we produce an opening pulse. However, by opening a valve and closing another, we produce another opening pulse. If all the valves are identical in dynamic behavior, and if the pulse is long enough to be produced with a single valve, the output pulses would be identical in both cases. In the method, all valves are assumed to be identical, and therefore, the dynamic model of a single valve is assumed to be accurate enough.

The output of a switching controlled solenoid valve is strongly non-linear due to delays and finite moving speed in state transitions between the open and close positions. To overcome this issue, some dynamic models are developed. Currently, the most sophisticated dynamic model for solenoid valves is presented in [74]. This model involves six parameters and can represent not only the dead bands of a valve response but also the ballistic modes. However, the novel switching method does not use the pulse widths that yield the valves to ballistic modes or other strongly non-linear areas because of the sensitivity of these areas against modeling errors and parameter alteration. The valves are used only in the area where they show more linear behavior. Therefore, a simpler model can be utilized.

Figure 4.5 represents a typical output of a PWM-driven miniature valve as a function of pulse width. The curve was measured with WHV2 at 25 Hz carrier frequency and 5 MPa supply pressure. The outflow volume per pulse was calculated from longer measurement by dividing the outflow volume by the number of pulses. The total outflow was measured with a precision scales. At the beginning of the curve, where the pulse length is short, the measured period was 4.0 s corresponding a hundred pulses. While the passed volume per pulse increased, the number of measured pulses was decreased in two steps, ending with 25 pulses after the pulse length of 7 ms. Also the measurements were taken in shorter intervals near the end points of the curve and with longer intervals in the middle region, being 0.1 ms at minimum and 2 ms at maximum. The actual measuring setup was the same as presented in Chapter 6.2. The figure presents also the output of an ideal valve, which would be linear. It can be seen from the figure that there is a region where the difference between curves seems to be approximately constant. The dynamic behavior in that region can be modeled with a single parameter that represents the difference between these curves. In fact, that parameter represents the difference between the opening and closing delays. When they are different, a constant error can be seen in the realized pulse width.

Thus, the dynamic behavior of the valve is modeled simply with a single parameter t_c, representing the pulse width error. The error value is positive when the valve performs longer pulse than controlled (closing is delayed more that opening) and negative in the opposite situation. However, the first situation is more typical. In the case of MVPWM, the pulse error can be simply subtracted from the virtual pulse width, as follows:

$$w_\mathrm{c}(w_\mathrm{des}) = w_\mathrm{des} - t_\mathrm{c}, \tag{4.3}$$

and thus obtaining the compensated virtual pulse width w_c.

Conversely, in the case of MVPFM, the expression for the compensated pulse frequency f_c can be written as:

$$f_\mathrm{c}(f_\mathrm{i}) = \frac{f_\mathrm{i}\,\lambda}{\lambda + t_\mathrm{c}}, \tag{4.4}$$

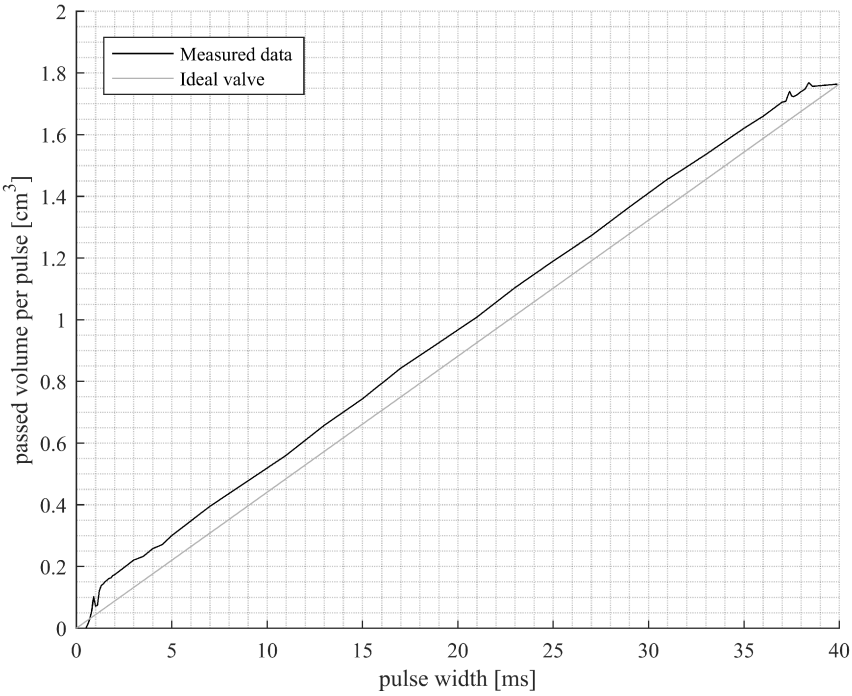

Figure 4.5: PWM response of WHV2 at 25 Hz carrier frequency and 5 MPa supply pressure

4.5 Multi-valve pulse generation

The process of the pulse generation for MWPWM control is presented with a block diagram in Fig. 4.6. The output $u_{\mathrm{int,w}}$ is composed of the PWM signal, which is responsible for the partial openings, and a number of valves that should be open for the whole PWM period. The input w_{c} is allowed to change with a sample time of T_{slow}, whereas the output can change with the sample time of T_{fast}. In fact, the resolution of the PWM control is defined as $\frac{T_{\mathrm{slow}}}{T_{\mathrm{fast}}}$.

The pulse generation process of the MVPFM has two steps. First, the period length in samples n_{sam} is calculated as follows:

$$n_{\mathrm{sam}} = \mathrm{round}(\frac{1}{f_{\mathrm{c}}\, T_{\mathrm{fast}}}), \tag{4.5}$$

where T_{fast} is the sample time of the pulse generation. Second, Algorithm 1 is used to generate the binary control signal $u_{\mathrm{int,f}}$. Note that the sample time of signal f_{c} is T_{slow}.

In the algorithm, the lines 5 – 8 are responsible to begin the opening pulse when the period length (up-counter) reaches the value of n_{sam} and to reset the period length calculation. The lines 9 – 12 are responsible to perform the rest of the opening pulse and to continue the period length calculation. While the period length is not reached and the previous pulse is finished, the lines 14 – 15 are executed, thus continuing the period length calculation and outputting zero. This implementation of the pulse generation cannot yield overlapping pulses, i.e., the previous pulse should be ended before the next one.

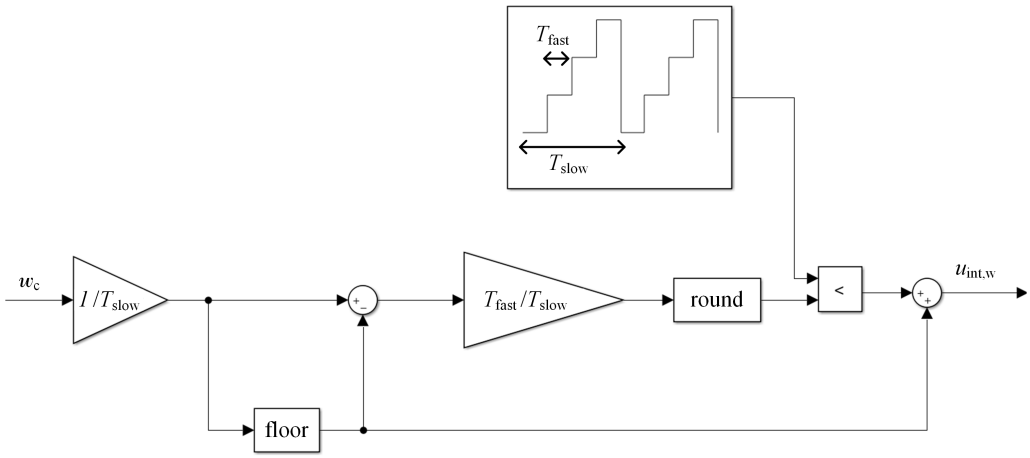

Figure 4.6: Block diagram of the MVPWM algorithm. The block with the symbol < outputs unity when the upper signal is smaller than the lower signal.

In first round
Initialize *upcounter* to 1
Initialize *downcounter* to 1
while Running **do**
  if $n_{sam} \leq upcounter$ **then**
    $u_{int,f} = 1$
    $upcounter = 1$
    $downcounter = \lambda$
  else if $downcounter > 1$ **then**
    $u_{int,f} = 1$
    $downcounter = downcounter - 1$
    $upcounter = upcounter + 1$
  else
    $u_{int,f} = 0$
    $upcounter = upcounter + 1$
  end if
  Wait until next sampling instant
end while

Algorithm 1: Pulse generation for MVPFM

This would be possible with multiple valves in the DFCU, but in the implementation in this thesis, that is not necessary.

4.6 Circular buffer

A circular buffer acts as the core of the proposed method. It is responsible to deliver the opening and closing commands to proper valves. The use of the circular buffer equalizes the switching cycles of each valve. It also makes it possible to conduct short pulses, which are not possible with a single PWM driven valve. An idea of circular buffering an equal

coded DFCU is previously presented in [9] with an aim to equalize the duty of valves.

The implementation of the circular buffer is demonstrated in Fig. 4.7. As shown in the figure, the valve array is considered to form a circle by connecting the last valve back to the first valve. When more valves are needed to be open, the head index i_h is moved clockwise; and similarly, when less valves are needed, the tail index i_t is moved clockwise. The buffer is implemented in a way that i_h indicates the valve that is last opened and i_t the valve that is last closed. Thus, all the valves between the indices and the valve pointed by the head index are kept open.

u_int	3	5	3	7	6	4
i_h	3	5	5	1	1	1
i_t	8	8	2	2	3	5

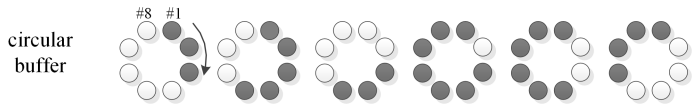

Figure 4.7: An imaginary sequence with the circular buffer. Gray color indicates an opened valve.

4.7 Analysis of Novel Switching Method

There are limitations for the control signal that the proposed switching scheme can follow. They come from the valve dynamics and from the decision to use the valves in the normal mode only. That ensures the most linear behavior of the system. There are own limitations for the MVPWM- and MVPFM-modes. One fact from the MVPFM-mode is that the smaller the control value, the longer the period and therefore the slower the response. Thus, the control bandwidth decreases with the decreasing control value.

For static situations, the maximum control value is limited, i.e., the MVPWM mode has the maximum control value u_max, which is smaller than N. In contrast, there is no limit for the minimum control value because of the unlimited minimum frequency of the MVPFM mode. However, in practice, the upper level controller tends to define the minimum control value, below which the valve controller is deactivated. To determine u_max, we need to analyze the pause time of a single valve when driving the control with a constant u. It can be noted that the *virtual pulse width* determines the real pulse width of each valve if the control signal is kept constant. The same happens for the *virtual pause time*, which can be written as:

$$w_\mathrm{pause} = N\,T_\mathrm{slow} - \frac{u}{f} + t_\mathrm{c}. \tag{4.6}$$

There is a minimum value for w_pause, which keeps the valve in normal mode. Using a shorter pause time would cause the valve to be in inverse ballistic mode. Thus, u_max can be calculated using the minimum pause time, $w_\mathrm{pause,min}$, as follows:

$$u_\mathrm{max} = (N\,T_\mathrm{slow} - w_\mathrm{pause,min} + t_\mathrm{c})f \tag{4.7}$$

The control value where the MVPFM is changed to MVPWM, represented as u_tr, is the minimum control value for the MVPWM, and is therefore a relevant inner parameter. It

Table 4.1: Simulation parameters

N	4
λ	5 ms
T_{slow}	10 ms
T_{fast}	1 ms
f	100 Hz

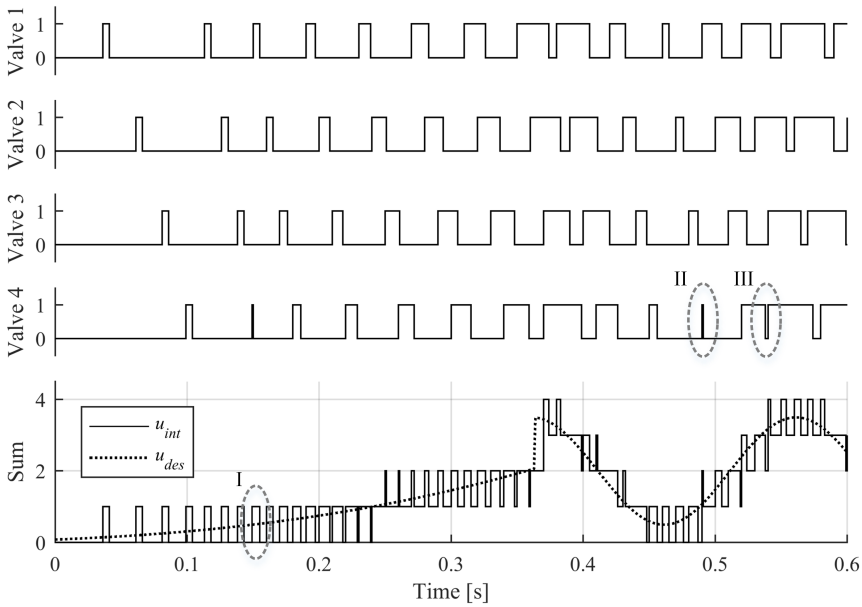

Figure 4.8: Simulated control sequence with the NSC and DFCU having four valves

can be determined using Eq. 4.1 and substituting the minimum pulse length λ to w_{des} yielding:

$$u_{\text{tr}} = (\lambda + t_{\text{c}})\, f. \tag{4.8}$$

The functionality of the novel switching method is simulated with the parameters gathered by Table 4.1. The simulation is performed without the valve model and by using an arbitrary signal as u. The signal starts to increase slowly after which there is a step change into a 5 Hz sine wave. The shape of the signal is selected to show the advantages and flaws of the method. The simulation result in Fig. 4.8 shows both the modulation methods in operation. The lower switching frequency of single valves are also clearly seen. The result show also that the system can sharply respond to an input step at the next sampling instant without extra delay.

There are also some misbehaviors in the simulated sequence. The controlling task begins with the MVPFM mode and transitions into MVPWM mode at about 0.15 s. The first flaw occurs at that time. Since the PFM period can start and end in any sampling instant of T_{fast} and the PWM period starts always at the sampling instant of T_{slow}, a synchronization error might occur. In the simulation, the last pulse of PFM modulation is aborted by the first pulse of PWM modulation. In this case, two pulses are conducted

one after the other, resulting in a too long pulse in sum (instance I in the Fig. 4.8). With the algorithm, the pulses are conducted with different valves, and the aborted pulse may therefore be ignored by the valve, thus reducing the error at the output. However, the error might be one extra pulse at maximum, depending on the timing of the modulation method change. The misbehavior is opposite when the transition from MVPWM mode to MVPFM mode, where the maximum error is a loss of one pulse.

There are dynamic situations where the MVPWM modulation generates a too short pulse or a pause to a single valve. In these situations, the sum signal follows the desired control value as expected, but the method is not able to deliver proper pulses to the single valves. The first too short pulse occurs when the integer control value changes from zero to value 2 and back to value 1 so that the duration at value 2 is a too short opening pulse for a single valve. This cannot be avoided because both valves are just opened and one of them should be closed, unfortunately too early for the valve. The same situation can happen with any too short pulse, which begins from zero. To simplify, it can be said that exceeding the control value 1.0 too fast may result in one too short pulse (instance II in the Fig. 4.8). Similar misbehavior occurs at the high control values if a short pause occurs before the full opening (instance III in the Fig. 4.8). Because of the following full opening, the short pause before that realizes in a single valve and therefore might be neglected by the valve.

These misbehaviors in dynamic situations are related only to certain control sequences, with a rapidly changing control value. Considering also the fact that the maximum error is smaller than the shortest pulse or pause, these misbehaviors are assumed to be negligible.

Another concern within the proposed method is the individual differences between the valves. There might be differences in the dynamic response and in the flow characteristics. The proposed solution is to use average models in the controller. Owing to the circulating switching method, the active valve is changing continuously, and therefore, the average models are assumed to predict the system behavior well enough. For example, with the above presented system, having four valves and 100 Hz PWM frequency, one round takes 40 ms. After each round, the cumulative flow volume should match with the calculated flow volume of an average valve. Deviation of an individual valve (from the average behavior) produces a disturbance to the system at 25 Hz frequency. Depending on the system and the magnitude of the deviation, the disturbance might be negligible.

5 Prototype designs

In this thesis, three versions of a water hydraulic miniature valve were developed. The first water hydraulic valve design (WHV1) exploits an oil hydraulic miniature valve design as a reference. This design was the fourth version in the series of oil hydraulic miniature valve designs that were developed at TUT. Thus, it provides a good base for the further development of water hydraulic miniature valves. WHV1 was made with minimum changes from the reference oil hydraulic design. This yielded two main drawbacks: the valve did not have an outer magnetic circuit and faced a fundamental durability issue. The lack of outer magnetic circuit becomes a problem with the water hydraulic version, since a stainless steel manifold may not be ferromagnetic. Thus, major changes were made to the second water hydraulic valve design (WHV2). The last design, WHV3, was developed in co-operation with an industrial partner. In this valve, the commercial viewpoint was considered more than in WHV1 and WHV2, which were purely university prototypes. Both the university prototypes as well as the reference valve design are described in detail. In contrast, the detailed design of WHV3 is not provided; however, the main design changes are described.

5.1 Oil hydraulic reference valve design

The oil hydraulic reference valve is a direct controlled seat valve that is composed of five machined parts. In addition, two o-ring seals, a return spring, and a coil are involved in the valve assembly. The valve structure and parts are presented in Fig. 5.1. The valve utilizes a cone type seat geometry with an angle of 90 degrees and is assembled fully inside the manifold.

The valve has an unique solution to make it pressure-proof; it exploits a coil to carry the major part of the pressure force. On/off valves typically have a steel tube around the plunger, which is pressure-proof. However, this unique structure decreases the number of parts in the assembly, enables the use of plastic as a sliding surface for the plunger, and improves the magnetic circuit of the solenoid. As a drawback, the coil needs to be reinforced by filling with epoxy resin, in order to achieve adequate stiffness against pressure forces. Another drawback is the need for a glue joint between the stator and coil frame. The reliability of that joint in long-term usage as well as the ease of assembly is low.

The other unique feature in the valve design is that the valve assembly itself does not have a part outside the coil that closes the magnetic circuit. The whole valve is assembled inside the manifold, which in this case forms that part of the circuit. This obviously requires the manifold material to be ferromagnetic, which is not a problem in oil hydraulics because typical manifold materials have sufficient ferromagnetic properties. However, most typical

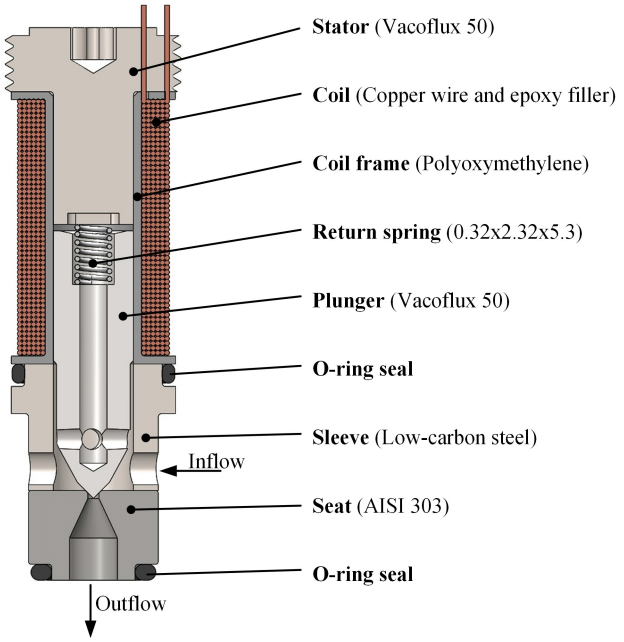

Figure 5.1: Parts and materials of the oil hydraulic miniature valve used as a reference design for WHV1.

Table 5.1: Dimensions and properties of reference valve

Coil outer diameter	10.2 mm	Measured resistance (at 20°C)	2.3 Ω
Coil length	16 mm	Magnetomotive force	1500 A
Total length	34.5 mm	Orifice diameter	0.75 mm
Spring rate	2.57 N/mm	Spring pre-compression	1.6 mm
Number of coil turns	288	Orifice bevel outer diameter	1.0 mm
Coil wire diameter	0.28 mm	Design pressure	21 MPa
Airgap distance	0.38 mm	Core saturation flux density	2.35 T
Plunger diameter	4.9 mm	Open response time	< 2.3 ms
Spring cavity diameter	2.5 mm	Close response time	< 3.4 ms
Design pull voltage	12 V	Flow rate @ 3.5 MPa	1.4 l/min
Current density at pull	45 A/mm^2		

stainless steel grades are not ferromagnetic, and therefore, other grades must be used with this valve structure.

Data from the reference valve is presented in Table 5.1, including dimensions, design values, and some measured properties. Response times were measured using a capacitor-based circuit with 24 V charging voltage [13]. This circuit, with the reference valve, produces a current peak corresponding a magnetomotive force of 1500 A.

5.2 First water hydraulic valve prototype WHV1

Structure and materials of WHV1 are presented in Fig. 5.2. The main difference with the reference valve is larger diameter of the orifice and that of the overall design. The orifice diameter is increased from 0.75 mm to 1.0 mm.

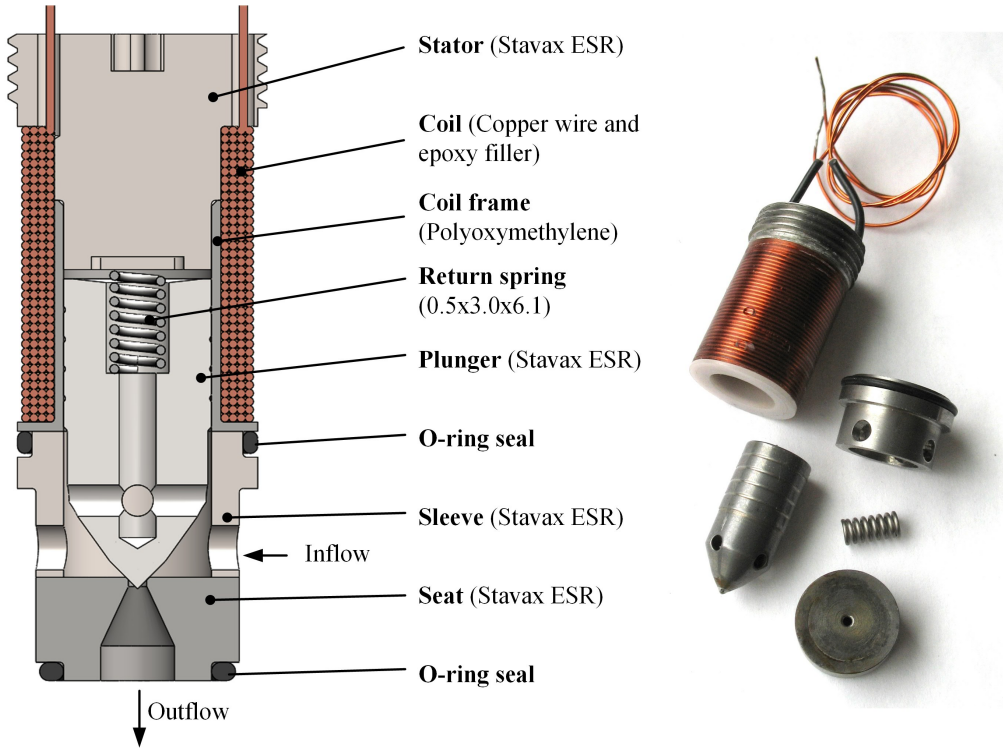

Figure 5.2: Left: Cross-sectional view of WHV1 with part names and materials. Right: Photo of WHV1 parts.

5.2.1 Magnetic circuit design

The selected material for the WHV1 magnetic circuit was martensitic stainless steel within grade of AISI420 (trade name Stavax). It provides relatively high saturation flux density in the soft condition and enables achievement of high hardness through heat treatment. Nevertheless, the high hardness value and good magnetic properties cannot be attained at the same time [72]. Therefore, only the plunger tip is allowed to harden, which is the only region in the plunger that needs to be hard.

Since Eq. 3.3 is approximate, it is used with the scaling method instead of direct usage. Thus, the plunger area of the reference valve was measured, and the theoretical required value was calculated. The correction factor β_1 was then calculated according to Eq. (3.10) to be 1.86. By substituting the necessary design values of WHV1 to Eq. 3.3, we obtained the theoretical core area for WHV1. Multiplying that value with β_1 and taking the spring cavity area into account, we obtained 8.3 mm as the required plunger diameter. However, we made a small compromise with the plunger diameter in order to keep the outer diameter of the valve small. Thus, 8.0 mm was selected as the plunger diameter.

5.2.2 Required magnetomotive force

The approximate required magnetomotive force was calculated using Eq. (3.7). Again, the scaling method was used instead of direct calculation. Thus, the approximate value was calculated also for the reference valve. Then, the correction factor β_2 was calculated according to the Eq. (3.10) to be 2.11. Multiplying the theoretical required magnetomotive force of WHV1 calculated by Eq. (3.7) with the correction factor, we obtained the value of 1469 A. This value is close to the realized value of the reference valve, and thus, the same 1500 A was used as the design value for WHV1.

One thing to note is that the correction factor is quite large. This indicates greater reluctance than that estimated. The main reason for this is the fact that the reluctance of the ignored ferromagnetic parts become significant near the saturation flux density.

5.2.3 Coil design

The next step is to design the coil, which actually generates the magnetomotive force. The case is quite clear owing to the same design value for the magnetomotive force and the aim to make as little changes as possible. However, the new coil diameter is larger due to the increased diameter of the plunger. Therefore, the resistance of the coil increases if the same number of turns with the same diameter of wire are used. The increased resistance would need higher voltage. However, the aim is to keep the operating voltage at the same level, and therefore, a thicker wire was used.

Thus, the cross-sectional area and the shape of the coil are kept unchanged, and the wire diameter is increased. The coil of the reference valve was composed of six layers of wire and filled the coil volume. The same number of layers cannot fit to the given space with the thicker wire. Considering also that the number of layers should be even because the winding needs to start and end to the same side, four layers is the next possible number. Then, the next design problem is that if the given space is not filled completely with the wire, the current density and resistive losses with it would increase. Therefore, the selected wire should fill the space with four layers. The wire diameter of 0.4 mm was found to satisfy these criteria.

The produced coil prototype showed a resistance of 0.72 Ω, while having 135 turns of wire, as presented in Table 5.2. Thus, Eq. (3.8) reveals that we need about 11 A to obtain the design value for F_{m}. Then, the well-known Ohm's law reveals that the operating voltage should be only 8 V in order to reach this current. Thus, the requirement to not increase the operating voltage resulted in a moderate reduction in the voltage.

5.3 Second water hydraulic valve prototype WHV2

5.3.1 Modifications in the design

The WHV2 design is based on the WHV1; however, major design changes were made. Figure 5.3 depicts the cross section of WHV2. The most important design objective of this second prototype was better durability. The following changes were made in order to improve the durability.

The ceramic ball was inserted into the plunger tip, and thus, the valve type changes into the ball-seat valve. This removes the requirement of high wear resistance from the plunger material and enables the choice of the plunger tip material for the best durability. The

Table 5.2: Dimensions and properties of WHV1

Coil outer diameter	13 mm	Spring cavity diameter	3.4 mm
Spring rate	6.18 N/mm	Spring pre-compression	0.5 mm
Coil height	16 mm	Measured resistance (at 20°C)	0.72 Ω
Total length	35.2 mm	Design pull voltage	12 V
Number of coil turns	135	Design F_m	1500 A
Radial clearance	0.2 mm	Orifice diameter	1.0 mm
Coil wire diameter	0.40 mm	Bevel outer diameter	1.33 mm
Airgap distance	0.50 mm	Design pressure	21 MPa
Plunger diameter	8.0 mm	Core saturation flux density	1.75 T
Design current density	47 A/mm^2		

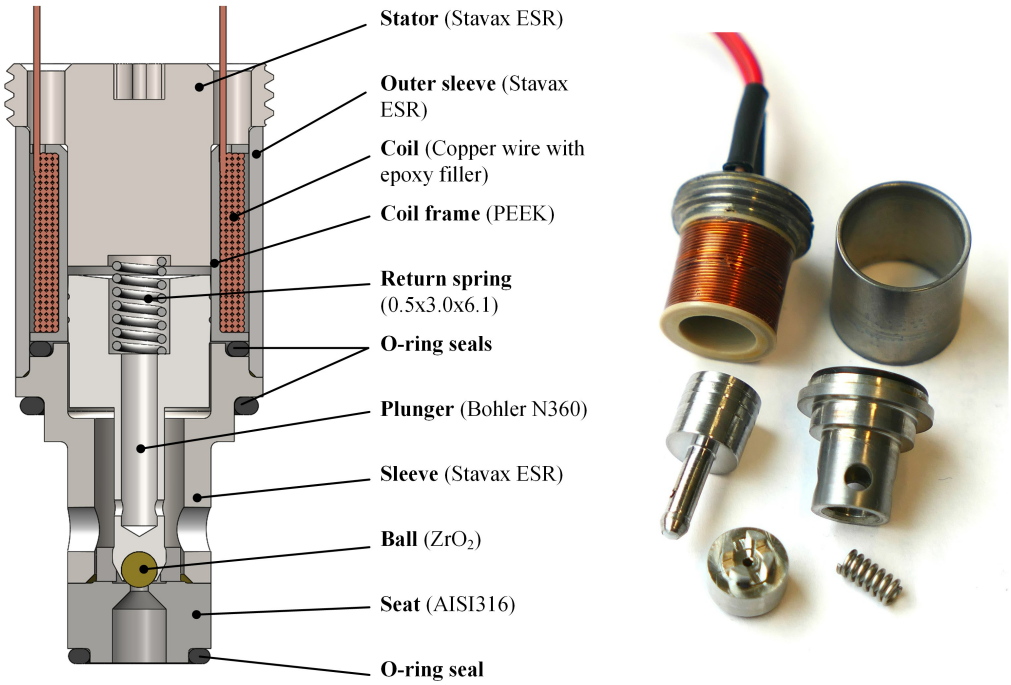

Figure 5.3: Left: Cross-sectional view of WHV2 with part names and materials. Right: Photo of WHV2 parts.

balls produced from industrial ceramic provide a hard, corrosion-resistant, wear-resistant, and smooth surface. They also have good geometric accuracy, which helps the valve to be leak-tight.

In order to improve the alignment of the plunger tip and the seat, guidance is added. The new plunger tip geometry enables the use of sliding guidance near the seat, which limits the misalignment. This is done by adding ribs to the seat part around the orifice.

The plunger weight is reduced significantly with the new design. The air gap position is moved from the middle-coil closer to the seat, thus shortening the part of the plunger

that is inside the coil. In contrast, another side of the plunger is longer; however, all unnecessary material is removed as the plunger tip is designed to be as thin as possible. This also increases the elasticity of the plunger, which may have a positive effect on the durability because of the softer contact.

Inclusion of the outer magnetic circuit in the valve assembly was another significant design change. When the valve assembly includes all the parts needed for the magnetic circuit function, the manifold material does not need to be ferromagnetic. This increases the diameter of the valve but enables the use of most typical stainless steels of austenitic grades as the manifold material. The maximum increase of 1 mm in the valve diameter was allowed.

In addition, one aim was to make the coil shorter owing to the encouraging results of the extensive electromagnetic study on miniature solenoid valves by Lantela et al. [75]. This study showed that coil shortening would be beneficial despite the increase in current density. Owing to major changes in the magnetic circuit and coil, the design was finalized with finite element method simulations. The next section briefly describes that part of the design process.

5.3.2 Electromagnetic simulation

Electromagnetic simulations were carried out with Comsol Multiphysics simulation software. The coil length was decreased from 16 to 10 mm. First simulations were carried out with the same wire diameter as in the case of WHV1 coil, thus resulting in a reduction in the number of turns because of the shorter coil. The allowed maximum increase in diameter was exploited directly by the ferromagnetic sleeve around the coil, thus yielding a thickness of outer magnetic path of 0.5 mm. With these initial design values, the first simulations were carried out. Results showed a significant reduction in the solenoid maximum force as well as the holding stage force compared to WHV1. The force of the solenoid can be increased by using more power and more energy but then the efficiency is decreased. To avoid that, some design changes were studied.

The plunger guidance in the new design prevents the contact between the plunger side and the sleeve, enabling the use of smaller radial clearance and yielding smaller reluctance. The reluctance of the clearance has no significant effect on the pulling stage because the reluctance of the open air gap is many times higher. However, in the holding stage, the main air gap is closed and the radial clearance becomes relatively more significant. Thus, it is assumed that the clearance affects the holding stage to a greater degree. The effect of the clearance to the valve behavior was one of the studied design changes.

The force reduction in the pulling stage was revealed to mainly be due to the thin outer sleeve. Two methods were found to increase the thickness, while maintaining the outer diameter of the valve. First, the coil diameter could be reduced, thus also reducing the plunger diameter. Here the question is the balance of the material in the plunger and in the outer sleeve. Secondly, the coil thickness could be reduced by using a thinner wire in the coil while maintaining the same number of wire layers in the coil. Here it is possible to keep the plunger diameter unchanged and increase the thickness of the outer sleeve as much as the coil thickness is reduced. With this method, the current density increases, but the overall effect may be positive.

These modifications were simulated with the following conclusions. The reduction of the radial clearance and thus its reluctance effectively increases the holding stage force. Therefore, the reluctance was decreased not only by decreasing the clearance, but also

Table 5.3: Main dimensions of WHV2

Number of coil turns	107	Airgap distance	0.50 mm
Coil wire diameter	0.30 mm	Plunger diameter	8.0 mm
Outer sleeve thickness	0.78 mm	Spring cavity diameter	3.4 mm
Spring rate	6.18 N/mm	Spring pre-compression	0.6 mm
Radial clearance	0.1 mm	Measured resistance (at 20°C)	0.90 Ω
Coil outer diameter	12.2 mm	Orifice diameter	1.0 mm
Sleeve outer diameter	13.8 mm	Design pressure	21 MPa
Coil length	10 mm	Core saturation flux density	1.75 T
Total length	33.5 mm	Current density	$\sim$ 80 A/mm^2

by making it longer. In addition, using a thinner wire in the coil was revealed to be the best way to give more space to the outer sleeve. The diameter of the plunger is best kept unchanged. Thus, the dimensions of WHV2 are presented in Table 5.3.

5.4 Third water hydraulic valve prototype WHV3

The design of WHV2 served as a starting point for WHV3 design. However, the commercial and production aspects were taken more carefully into account. The structure of the valve was changed to have a separate coil assembly, which is installed afterwards on the valve cartridge, as can be seen in Fig. 5.4. The cartridge part can carry all the pressure forces alone and does not require glued joints. The reliability of sealing was improved by using thicker o-rings. All these improvements in the practicality and mechanical reliability and involving the electric connector in the valve, resulted in a significant increase in dimensions. The outer diameter of the coil is 20 mm, and the overall length of the valve is 72 mm.

Figure 5.4: WHV3 having screw-in cartridge and separate coil

The hydraulic part of this valve utilized the same ceramic ball concept as WHV2; however, the orifice diameter was decreased from 1.0 to 0.9 mm. A detailed explanation of the design is not given here. However, the measured characteristics are presented hereafter.

6 Prototype results

6.1 Measuring setup and procedure of WHV1

WHV1 was tested in two different versions where the plunger and seat were prepared differently. In the base version (WHV1), both the plunger and the seat were induction hardened to full hardness. In addition, the plunger tip surface was left in the as machined condition. The achieved hardness values were 650 HV for the seat part and 700 HV for the plunger head. In the modified version WHV1.1, the plunger was polished up to Ra value of 0.2 µm and the seat was annealed down to a hardness value of 407 HV. All the specification measurements were carried out with the first version. The aim of the second version was to study the possibilities to improve the durability by a better surface finish or higher hardness difference between the plunger and the seat.

The functionality and characteristics of WHV1 were measured with the valve installed in the manifold produced from Stavax. Measured characteristics include response times, flow curve, leakage flow, minimum switching energy, and minimum holding power. The valve was driven with a prototype power electronic circuit (hereafter AC booster) where the energy for the opening was stored in the boost capacitor in order to perform a sufficient current peak automatically when the capacitor was connected to the coil [13]. The circuit diagram is presented in Fig. 6.1. The use of 24 V charging voltage and 470 µF boost capacitor lead to 14% higher current peak than designed.

The measurements were carried out with a Danfoss Nessie water hydraulic power unit that was filled with tap water. The temperature of water was kept below 30°C during the tests. A diagram of the test setup is presented in Fig. 6.2. For the response measurements, there was a serial orifice assembled near after the valve. The response times were deduced from the pressure between the valve and the serial orifice, as presented in [67]. The valve was assumed to switch state when 90 % of the change in the middle pressure occurred.

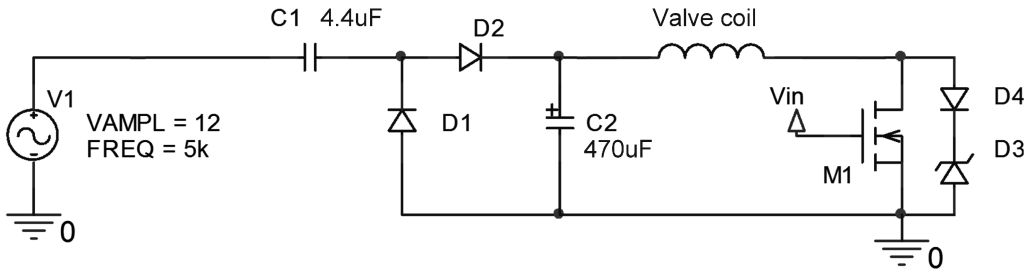

Figure 6.1: Circuit diagram of the AC booster [13]

The serial orifice was removed, except for the response measurements.

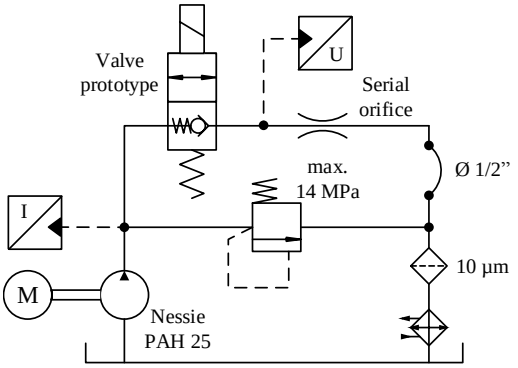

Figure 6.2: Hydraulic diagram of the measuring setup of WHV1 for response measurements

In response measurements, a hundred open and close cycles were performed at each pressure level with a frequency of 5 Hz and a duty cycle of 50 %. Because of the pressure drop in the serial orifice, the closing response could be measured up to 8.2 MPa pressure difference over the valve. In contrast, the opening response could be measured up to the pump maximum pressure of 14 MPa. The holding power was set to 200 mW in the response measurements.

Two electric power consumption related properties were measured: a minimum holding power and a minimum switching energy. They were measured in a function of pressure difference. With each supply pressure, the minimum current value, which can barely hold the valve open, was searched. In these measurements, the boost voltage was kept as 24 V. Once the minimum value for the holding current was found, the valve was switched on for a few seconds several times in order to confirm the proper operation. The minimum holding power was then calculated from the voltage and current measurements as $P_{\text{hold}} = UI$.

The minimum switching energy was searched by switching the valve with different charge voltages of the boost capacitor. The minimum switching energy was then calculated from the minimum charge voltage that was able to switch the valve, as follows:

$$E = \frac{1}{2} C\, U^2, \tag{6.1}$$

where U is the charging voltage, and C is the capacitance of the boost capacitor. The measuring equipment is presented in Table 6.1.

The flow rates were measured by measuring the outflow for a few seconds with a 250 ml measuring glass having a resolution of 2 ml. The time that the valve was kept open was varied with pressure in order to control the outflow volume to fit the measuring glass. The measuring operation seemed to give equal results when repeated. Therefore, the flow measurements were performed only once. Leakage flow, however, changed considerably between measuring events, and was therefore measured 3 times by gathering 5 minutes leakage to a cup at 10 MPa pressure and weighing it.

The durability of the valve against the opening cycles was studied by conducting a million opening cycles with 14 MPa pressure differential and measuring the leakage flow and

Table 6.1: The measuring equipment for the WHV1 measurements

Purpose	Device	Accuracy
Controller board	dSpace DS1102	
Supply pressure transmitter	Trafag NAH 25	±0.3%
Middle pressure transmitter	Kistler RAG25A500BV1H	3-4 kHz ±0.25%
Voltage transducer	LEM LV 25-P	±0.9%
Current clamp	Fluke i30	20 kHz ±1 mA

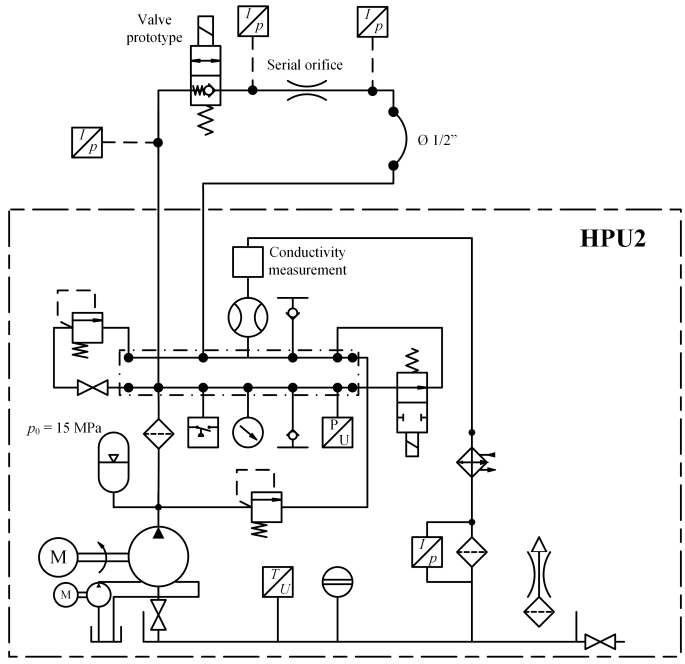

Figure 6.3: Hydraulic circuit diagram of test measurements of WHV2 and WHV3

inspecting the parts after the test. This was done for the both the seat-plunger versions. With WHV1, the cycles were run at a frequency of 25 Hz with a pulse width of 5 ms. During the durability test of WHV1.1, the frequency was increased up to 80 Hz.

6.2 Measuring setup and procedure of WHV2

Measurements of WHV2 were carried out with a pump unit based on CAT 1861 three piston pump. This unit was able to produce a supply pressure of 21 MPa. The main reasons for the change were the higher maximum pressure and problems with the pump of the first unit. A hydraulic circuit diagram of this test system is shown in Fig. 6.3. The pressure medium in this pump unit was de-mineralized water, whose temperature was kept around 20° C.

WHV2 was measured with two different power electronic circuits. It was measured with the same circuit as WHV1 (AC booster) but also with another circuit designed for digital

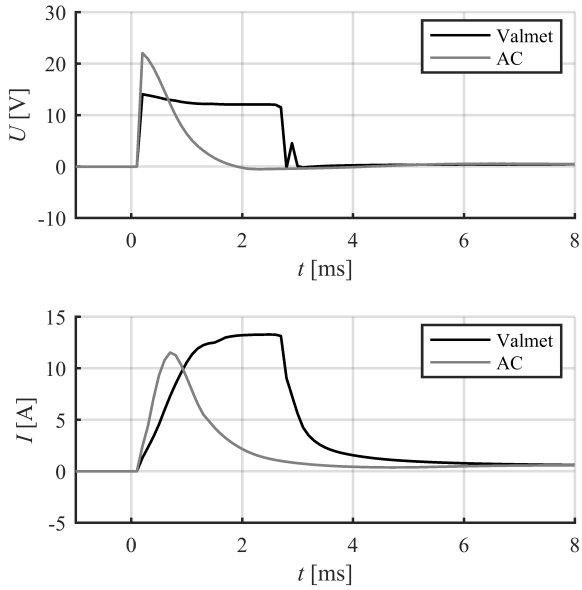

Figure 6.4: Measured currents and voltages with Valmet booster and AC booster with WHV2 at 15 MPa pressure differential. Signals are averaged from 46 openings.

hydraulics from Valmet corporation [6]. This circuit uses two voltage sources: one for the opening stage and the other for the holding stage. The voltage source for the opening stage was connected to the coil for few milliseconds after which the voltage was switched to the lower holding voltage. The holding power was set to 250 mW in the response measurements with both of the circuits. The circuit of Valmet is designed for 48 V opening voltage, while WHV2 is designed for 12 V. We also noted that under these conditions, the circuit was not able to deliver enough current for WHV2. This problem was solved by connecting four channels parallel. The resulting current and voltage curves are presented in Fig. 6.4.

The orifice was left as sharp edged. The ceramic ball is hard enough to form the bevel itself. The advantage of this method is that the bevel build up is just as large as needed. This minimizes the pressure forces. Thus, the running in period of 100 000 opening cycles against 21 MPa was performed before the measurements. The internal leakage flow was measured after the running in period by gathering the leakage of 5 min into a cup and weighing it. Ten opening cycles were performed right before the measurement.

All the characteristics of WHV2 were measured as in the case of WHV1. The minimum opening energy with Valmet booster was measured differently. It were calculated afterwards from the response time measurements, as follows:

$$E = \int_{t_0}^{t_r} U(t) \cdot I(t) dt, \tag{6.2}$$

where t_0 is the time of opening command, and t_r is the respose time. The flow curve measurement was repeated after the durability test. The measuring equipment of WHV2

are presented in Table 6.2.

Table 6.2: The measuring equipment in the WHV2 measurements

Purpose	Device	Accuracy
Controller board	dSpace DS1005	
Analog to digital card	DS2001	16-bit
Digital to analog card	DS2102	16-bit
Supply pressure transmitter	Druck unik 5000 (25 MPa)	3.5 kHz ±0.2%
Middle pressure transmitter	Druck unik 5000 (25 MPa)	3.5 kHz ±0.2%
Tank line pressure transmitter	Trafag NAH 25	±0.3%
Coil voltage	Testec TT-SI9001	25MHz ±2%
Coil current	Fluke i30	20 kHz ±1 mA
Outflow volume	250 ml measuring class	2 ml

A similar one million cycles durability test was conducted with WHV2 as in the case with WHV1. The test was carried out with the opening frequency of 80 Hz and pulse width of 5 ms.

6.3 Measuring setup and procedure of WHV3

WHV3 was measured with the same pump unit and similar installation as WHV2. The coil was designed for 24 V boost voltage, thus being more suitable for the Valmet booster circuit. Therefore, the valve could be driven with a single channel of that circuit. The measuring procedure was similar as that of WHV2 with a few exceptions: response times were measured with only three pressure differentials and using 300 mW holding power, the minimum holding power was not measured, and the durability test was run further. The durability test began with a similar full-pressure million-cycle test but continued with 10 million cycles at 5 MPa supply pressure. The leakage of the valve was measured at the beginning, after the million cycles and after the 10 million cycles.

6.4 Measured characteristics

Measured flow rates of all the valves (Fig. 6.5) fit well to the square root curves, i.e., flow characteristics match well to the basic flow equation of turbulent orifice. The highest flow rate was achieved with WHV1. The flow rate of WHV2 was slightly smaller than that of WHV1, despite the same orifice diameter. The WHV3 showed the smallest flow rate as expected while having a smaller orifice. One unexpected result was the magnitude of change in flow rate of WHV3. Its flow rate was significantly increased during the durability test.

The measured response times are plotted in Fig. 6.6. The upper graph shows the results with the AC booster and the lower graph shows the results with the Valmet booster. All results exhibit fast opening and closing and quite similar pressure dependence of the response times; the closing time decreases when the pressure difference increases and for the opening the other way around. Also the pressure difference, where the opening and closing times are equal, are very close to each other, about 14 MPa in all the cases. However, these valves are typically used at lower pressure differential, yielding asymmetric

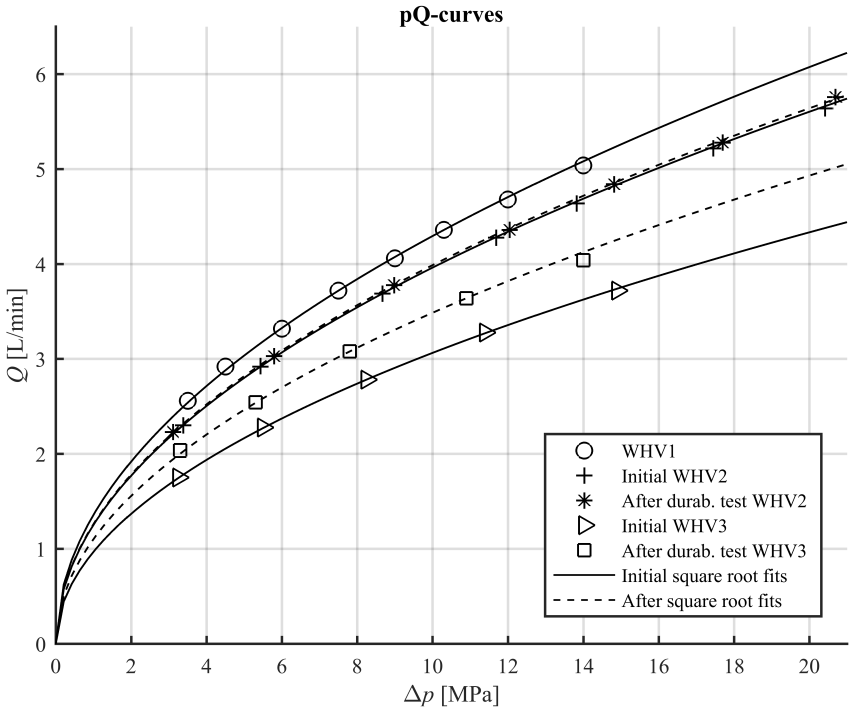

Figure 6.5: Flow curves

opening and closing delays. One clear result is that WHV2 is faster than WHV1 in both, opening and closing. Since the WHV2 was measured with the both boosters, the results show the AC booster is faster, which was expected. The WHV3 is slightly slower than WHV2 to open but faster to close at low pressures. Also, the pressure dependence of the closing response seems to be smaller, resulting the closing to be slower at high pressure.

The measured minimum holding powers with WHV1 and WHV2 are presented in Fig. 6.7. The results of WHV2 show that the pressure dependency is stronger with the Valmet booster. On average, the difference between boosters is quite small. As the main result, the required holding power of the both prototypes are small.

The required minimum opening energies are presented in Fig. 6.8. The difference in the results measured with different boosters seems clear. In contrast, the results of WHV1 and WHV2 with AC booster are very close to each other. The difference of boosters was expected.

The durability of valves was evaluated mainly by inspecting the contact areas with a microscope. Figure 6.9 presents WHV1 and WHV1.1 plunger-seat pairs after a million opening cycles. The left figure pair show clear wearing in the first plunger-seat pair. The size of the bevel in the seat is not increased as much as in the second seat. The second plunger was expected to wear much less because of softer seat and better surface quality. The figure shows the less worn plunger, but there is visible wearing. In addition, the figure shows a much more worn seat. Corrosion is clearly visible in both seats and in the second plunger. The materials are the same but the preparation processes differ since the

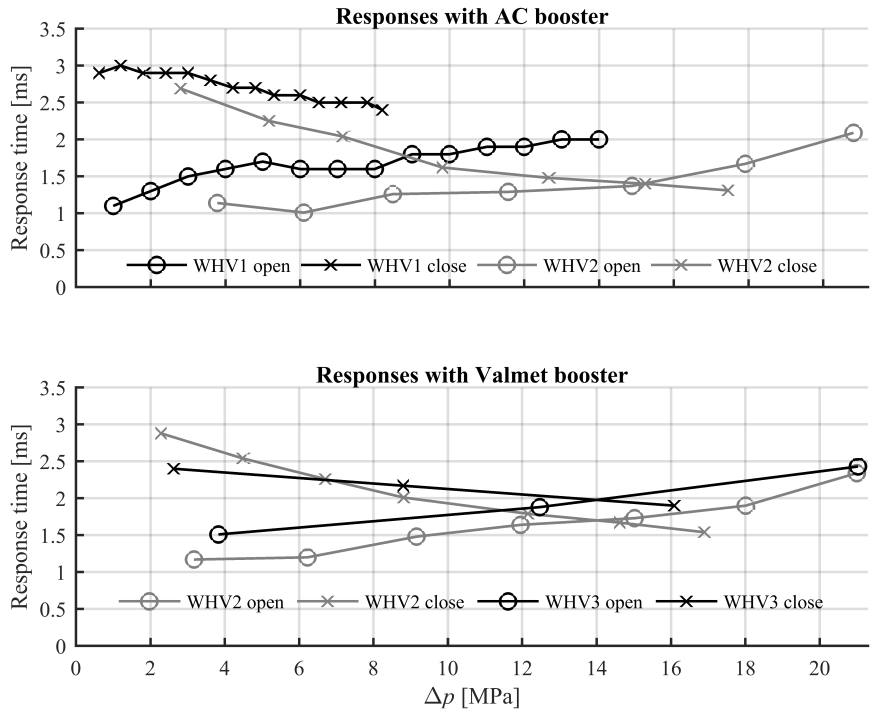

Figure 6.6: Responses

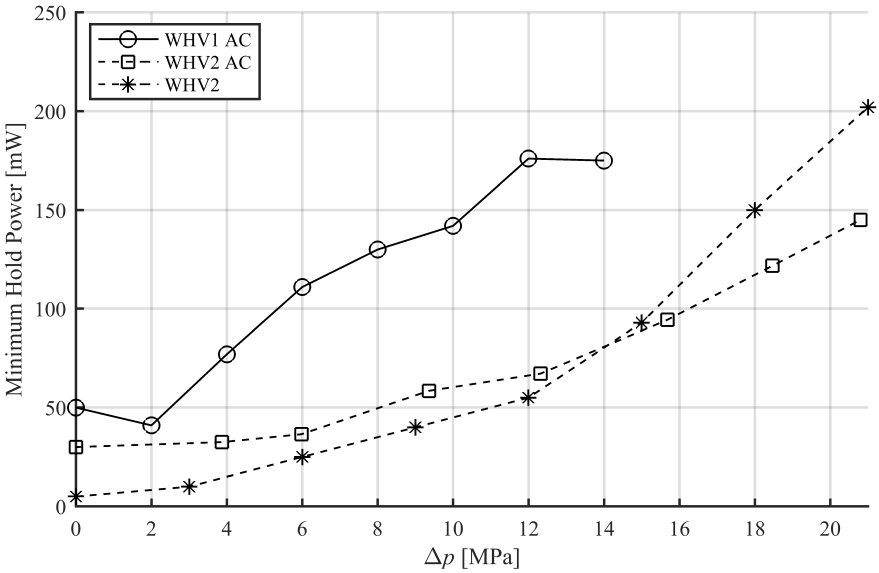

Figure 6.7: Measured minimum holding power

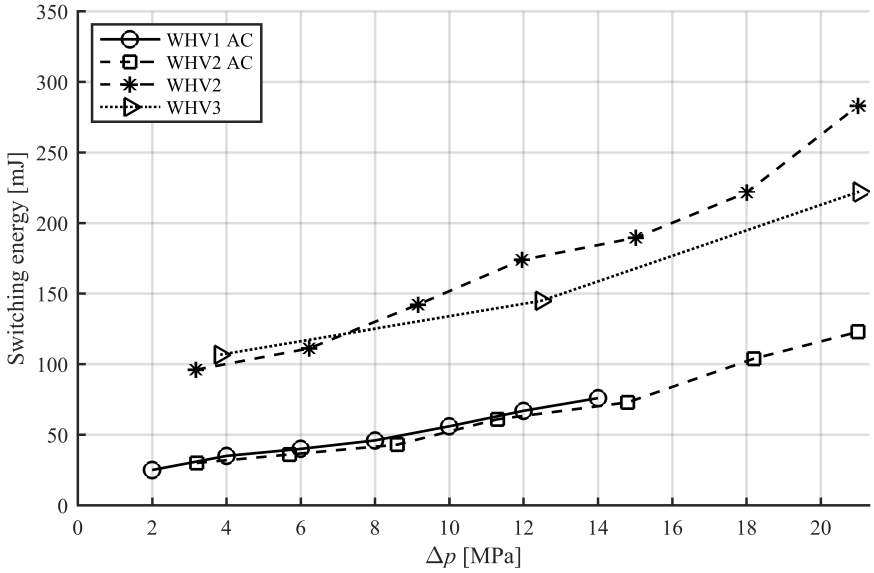

Figure 6.8: Measured switching energies

second plunger is polished and the second seat is annealed.

The microscope figures of WHV2 contact areas are quite different. No wearing can be observed in the plunger tip, which was a ceramic ball in this valve (Fig. 6.10). Also, the seat looks quite different having a very small bevel as the contact area. This seat was left as sharp edged, thus allowing the ceramic ball form the bevel. It was assumed that the ceramic ball is hard enough to hit the sharp edged seat without damage. The bevel is not symmetric.

Measured leakages are shown in Fig. 6.11. WHV1 and WHV2 are compared with leakage flow at 10 MPa pressure differential. WHV2 and WHV3 are, in turn, compared with leakage at 21 MPa. The results show increasing leakage with cycles in all valves. One observation is that WHV2 and WHV3, which have ball seats, are at first virtually leak tight. However, they also begin to leak during the durability test. Nevertheless, the highest leakage is less than 2 ‰ from the flow rate of the valve.

To enable an easier comparison of the experimental results with all the prototypes, the main characteristics are gathered by Table 6.3. Three first properties at the table are values with the pressure differential of 3.5 MPa and two last properties, with the pressure differential of 14 MPa. The first pressure differential, 3.5 MPa, was selected as nominal pressure differential in control valves. The two last property, are more relevant to compare at higher pressure differential because they are power electronic circuit related properties that should be adjusted for the highest pressure differential. However, the WHV1 was measured maximum with 14 MPa pressure differential, and therefore, comparable data is not available at 21 MPa. Thus, 14 MPa was selected as the comparison point. The values in the table (except flowrate values) are interpolated or extrapolated linearly due to lack of measured data at these particular points. The flow rate values are taken from the fitted flow curves before the durability tests.

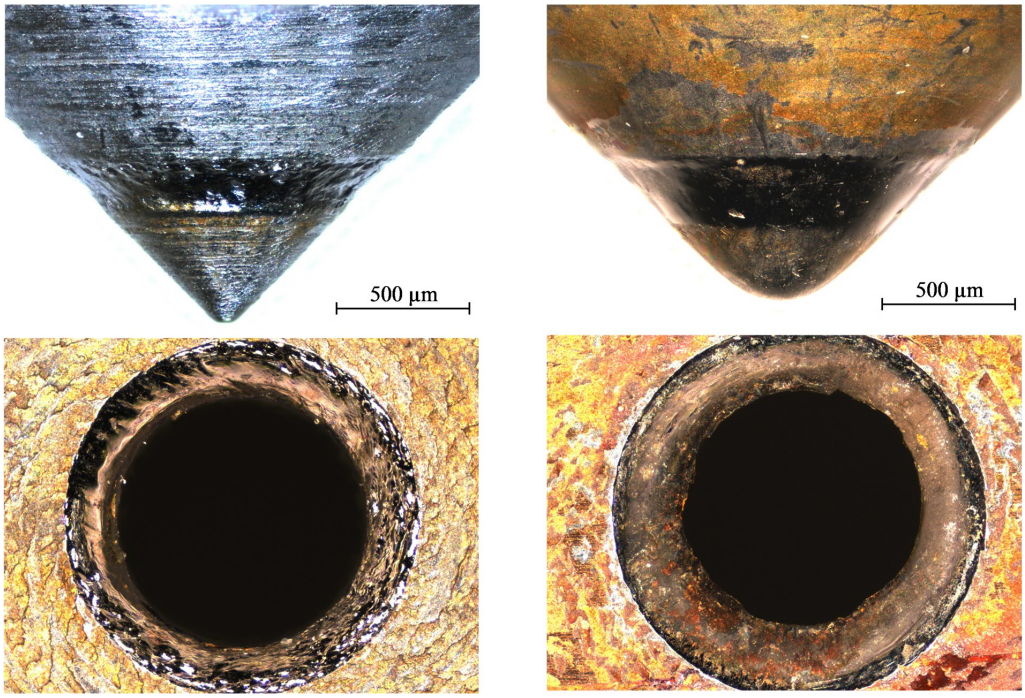

Figure 6.9: WHV1 after a million cycles on left, and WHV1.1 after a million cycles on right

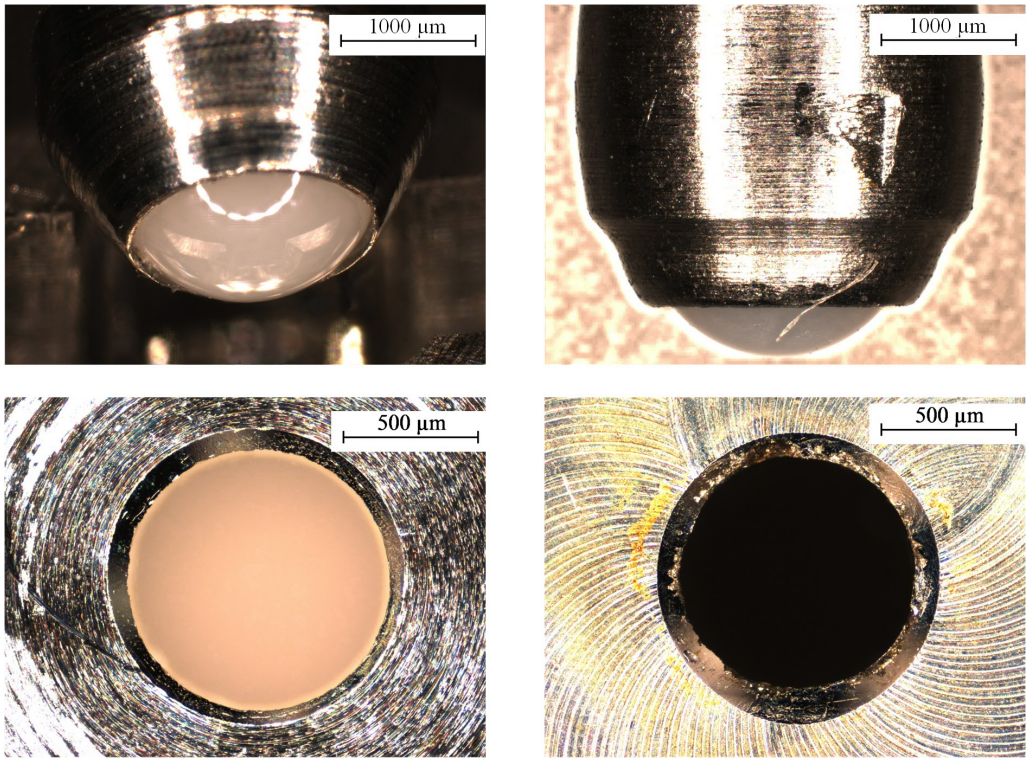

Figure 6.10: WHV2 after a million cycles on left, and WHV3 after 11 million cycles on right

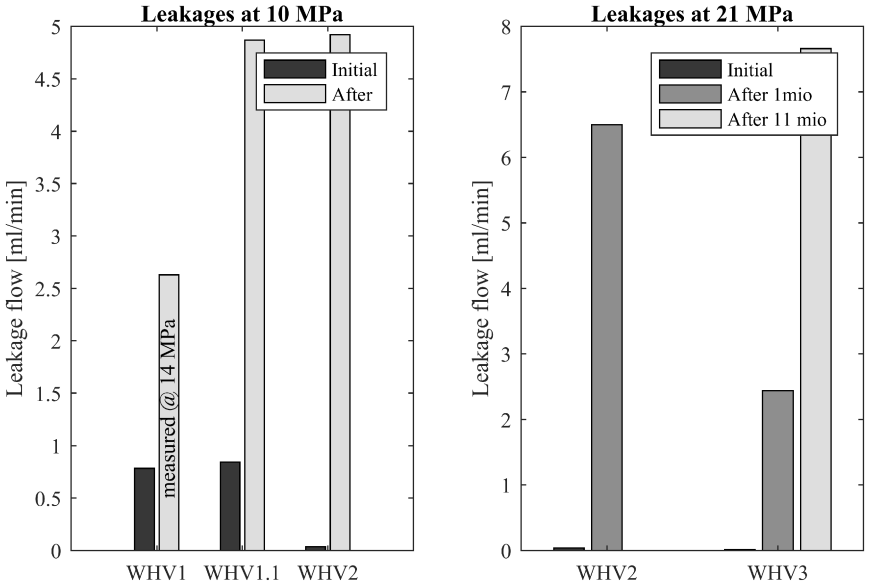

Figure 6.11: Leakages before and after durability tests

Table 6.3: Comparison table of measured characteristics

Prototype	Open [ms] @ 3.5 MPa	Close [ms] @ 3.5 MPa	Q [l/min] @ 3.5 MPa	Open E [mJ] @ 14 MPa	Hold P [mW] @ 14 MPa
WHV1 AC	1.6	2.8	2.5	76	175
WHV2 AC	1.2	2.6	2.3	70	81
WHV2 Valmet	1.2	2.7	2.3	184	80
WHV3 Valmet	1.5	2.4	1.8	159	-

6.5 Conclusion

The measured characteristics of WHV1 showed that a fast and low-power water compliant miniature valve can be produced. However, WHV1 faced a severe durability problem in the seat-plunger contact area. In order to decrease wearing, different preparations of the plunger and seat were tested with new parts. Another plunger was polished in order to decrease the seat wearing, and another seat was annealed to a softer condition to decrease the plunger wearing. This setup, named WHV1.1, resulted in decreased wearing of the plunger, but wearing of the seat was increased. Thus, the wearing problem cannot be solved by using proper hardness values in the parts because it seems that a soft seat still resulted in wearing of the plunger. Next, an extensive study on the durability was performed. However, no satisfactory solution to the problem was found. One finding was that the main source of the wearing seemed to be the misalignment of the plunger tip and the seat [19]. All results for WHV1 yielded motivation to develop a second prototype, WHV2.

The measurements of WHV2 showed successful design improvements. The three main targets were to significantly improve the seat-plunger contact area durability, to include

the outer magnetic circuit to the valve assembly, and to make the coil shorter. Despite these changes in the design, the results showed slightly faster responses and significantly lower minimum hold power. As the main result, the durability was improved. The durability problems of the plunger head were resolved by using a ceramic ball as the sealing element. The durability of the seat part was also significantly improved. One key factor for this might be the ability of the ceramic ball to roll. The seat can withstand high contact force and rolling better than high contact force and sliding. Despite the relatively soft seat material (AISI 316, which cannot even be hardened by heat treatment), the end size of the seat bevel was a fraction of the bevel in WHV1. This clearly shows that a rolling ceramic ball causes much less wearing on the seat.

Despite major changes in the valve design, WHV3 showed quite similar properties with WHV2. At low pressure, it was slightly slower to open but faster to close. Overall, its response is little less dependent on the pressure differential, which is a good feature. WHV3 was the only valve, for which durability was tested up to 11 million cycles; however, the end result does not differ much from the end result of WHV2. Both visual and leakage inspection show quite similar results.

7 Control results

This chapter introduces the experimental proof-of-concept study with the developed valve system and controller. The main goal of this thesis was to develop and implement a high-resolution and high-performance water hydraulic servo axis, which can perform demanding tracking control. The experimental study is conducted with the system that was designed and dimensioned for the Fusion for Energy (F4E) project, and thus, some dimensions, e.g., number of valves, come as given. The system design principle was to make the valve configuration and controller as simple as possible in order to achieve the required tracking performance. The following sections describe the system overview and the experimental study.

7.1 Test setup

The study is conducted with a single degree of freedom test platform, as shown in Fig. 7.1. The device was built for ITER remote maintenance system development [76]. The study case is tracking control with a heavy loaded double acting cylinder. The system has a constant pressure supply of about 12 MPa. Requirements from the F4E project resulted in the valve system having four DFCUs and four WHV3 valves per DFCU connected to the cylinder, as shown in Fig. 7.2.

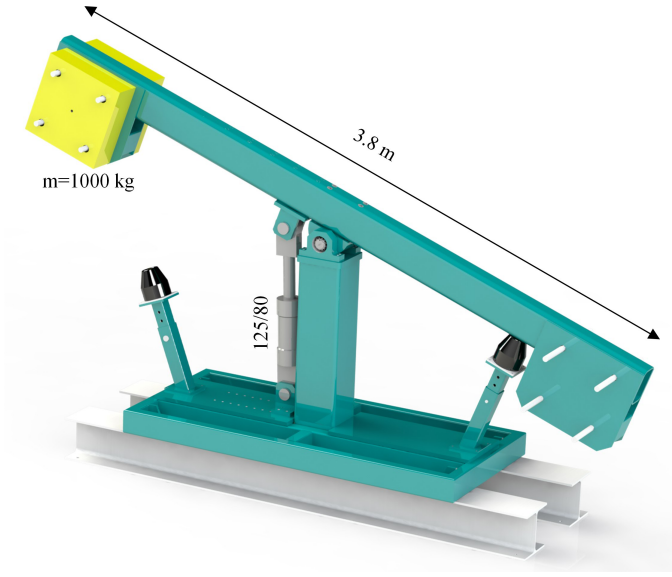

Figure 7.1: The single axis test device

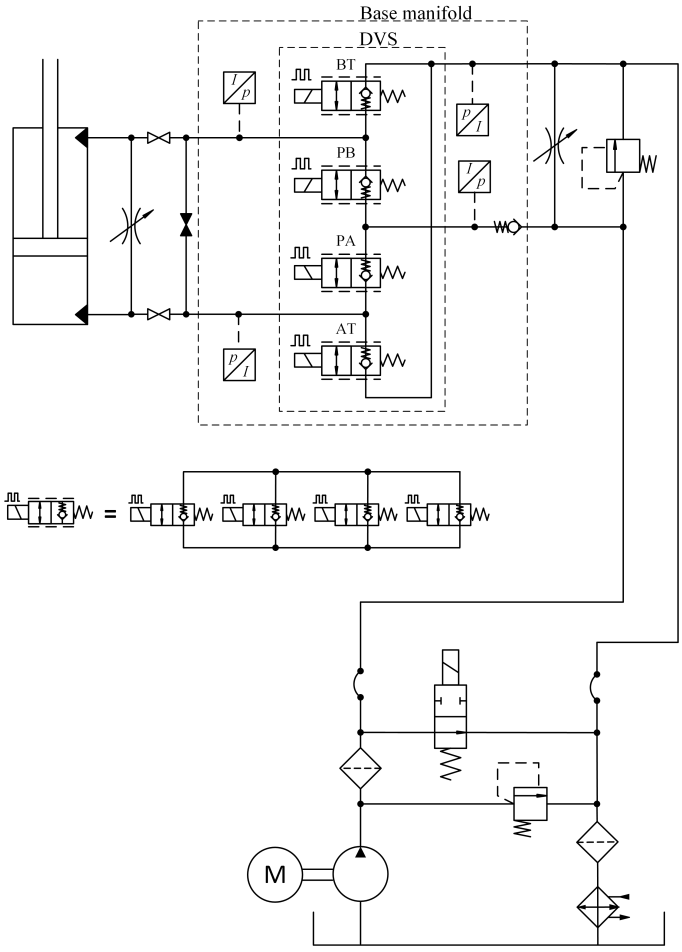

Figure 7.2: Valve configuration in test setup

The valve system was assembled close to the cylinder and connected to it with short tubes. The assembly is shown in Fig. 7.3. The digital valves were installed into a single manifold, having dimensions of 170 x 127 x 50 mm, including the valves. Before the measurements were carried out, the same setup was driven for few months, resulting in certain number of switchings to the valves. After that, they were disassembled, and all the plungers and ten seats were replaced with new ones. The six seat parts that were not replaced were PA1-3 and PB2-4. The number of switchings conducted already with these seats was approximately 2.6 million for PA valves and 0.8 million for PB valves.

The control system is shown in Fig. 7.4. The controller has two levels: the motion controller and the model-based valve controller. The model-based valve controller included four novel switching controllers, one for each DFCU. The motion controller consists of a filtered position feedback P-controller (PT1) and a velocity feed-forward controller. It outputs a controller velocity reference $v_{\mathrm{ref,c}}$, which is fed to the model-based valve controller. The first step there is to calculate the desired flow rates of DFCU PA ($Q_{\mathrm{des,PA}}$) and DFCU

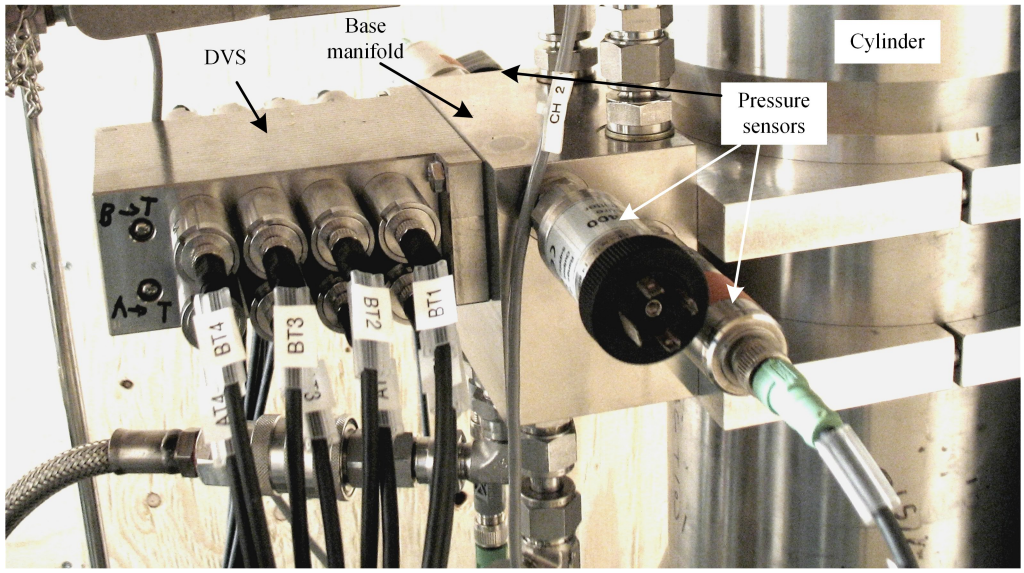

Figure 7.3: Photograph of the assembled valve system

AT ($Q_{\mathrm{des,AT}}$). They are calculated as follows:

$$\begin{cases} Q_{\mathrm{des,PA}} = v_{\mathrm{ref,c}} A_{\mathrm{A}}, & Q_{\mathrm{des,AT}} = 0, & v_{\mathrm{ref,c}} > v_{\mathrm{tol1}} \\ Q_{\mathrm{des,PA}} = 0, & Q_{\mathrm{des,AT}} = -v_{\mathrm{ref,c}} A_{\mathrm{A}}, & v_{\mathrm{ref,c}} < -v_{\mathrm{tol1}} \\ Q_{\mathrm{des,PA}} = 0, & Q_{\mathrm{des,AT}} = 0, & |v_{\mathrm{ref,c}}| \leq v_{\mathrm{tol1}}, \end{cases} \tag{7.1}$$

where A_{A} is the piston area in cylinder chamber A and v_{tol} is a tolerance value of the velocity. In the implementation, there is a hysteresis in the tolerance value in order to prevent the system from excessive mode changing after stopping the movement. Thus, the valve controller is activated when the absolute value of $v_{\mathrm{ref,c}}$ increases above the tolerance value v_{tol1} and deactivated when that fall below the tolerance value v_{tol2}. Theoretical static positioning accuracy can be thus calculated as $e_{\mathrm{ss}} = v_{\mathrm{tol1}}/K_{\mathrm{p}}$.

The real-time control system was implemented with a dSpace controller board. The dSpace communicated to valves via CAN bus. Since the utilized valve driver does not include CAN support, a separate CAN module was placed in between them. The main equipment of the measuring system is presented in Table 7.1.

The valve control was implemented such that the input and output flows of a chamber A, i.e., DFCU PA and DFCU AT, are controlled according to the desired flow rate values, as presented in Fig. 7.4. In contrast, DFCU PB and DFCU BT are opened in relation to DFCU AT and DFCU PA, respectively; the openings are scaled with the area ratio of cylinder chambers. This implementation is simple and cannot control the pressure levels. Thus, all the potential of the valve system is not utilized.

The control values for A side DFCUs were calculated by flow rate models. Both DFCUs were modeled as four equal orifices, even though there might be individual differences between the valves. The flow rate estimate of a single orifice was calculated as follows:

$$Q_{\mathrm{model}} = K_{\mathrm{v}} \sqrt{p_{\mathrm{out}} - p_{\mathrm{in}}}, \tag{7.2}$$

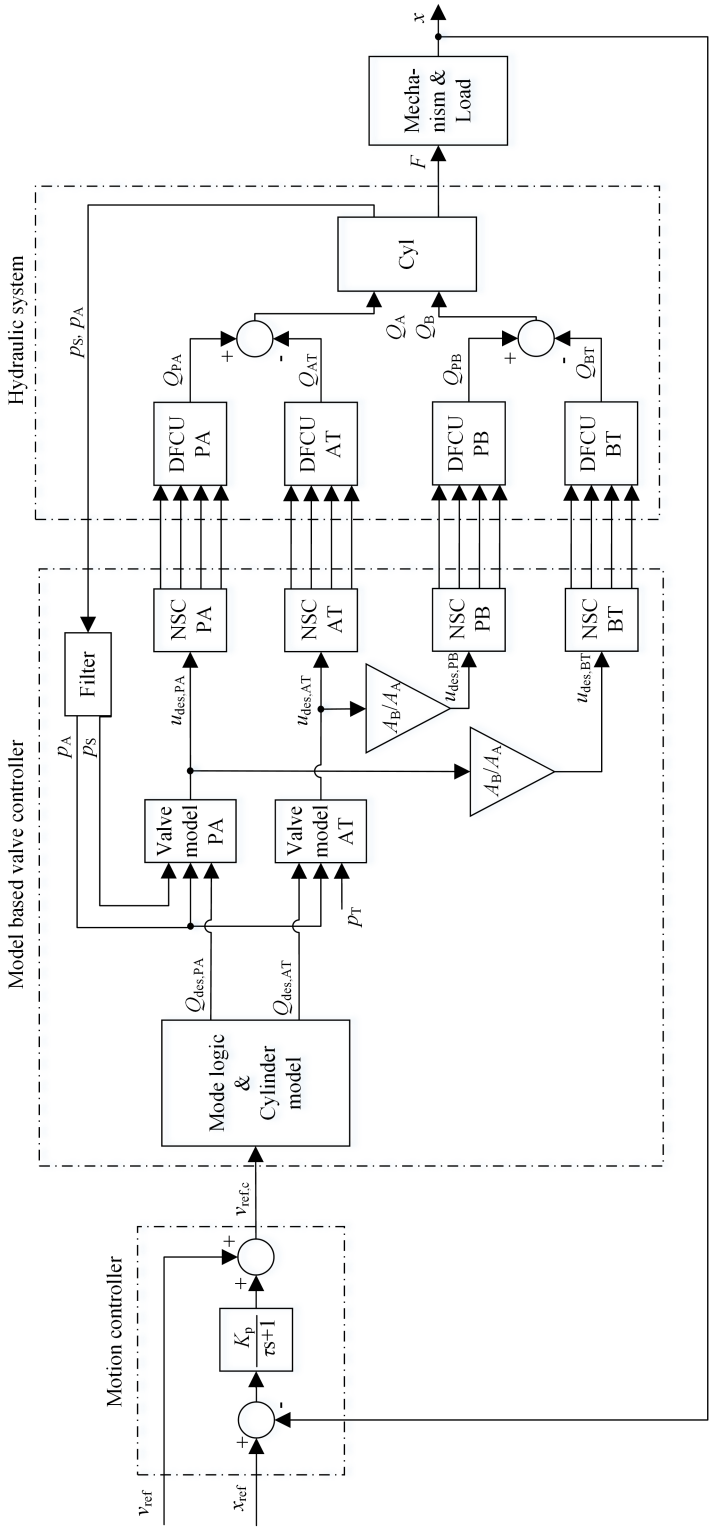

Figure 7.4: Block diagram of the control system

Table 7.1: Test setup equipment

Purpose	Device	Accuracy
Controller board	dSpace DS1103	
Power electronics of valves	Valmet booster	
CAN module	In-house prototype	
Supply pressure transmitter	Druck PTX 1400 (40 MPa)	
Chamber A pressure transmitter	Druck unik 5000 (25 MPa)	3.5 kHz ±0.2%
Chamber B pressure transmitter	Druck unik 5000 (25 MPa)	3.5 kHz ±0.2%
Tank line pressure transmitter	Trafaq NAT2.5A (0.25 MPa)	
Boom angle sensor	Heidenhein pulse sensor	$0.72 \cdot 10^{-3}$ deg
Non-return valve	Tiefenbach CC25	
Pump	CAT 781 (displacement 11 cm^3)	

where p_{in} and p_{out} are the input and output pressures of the DFCU, respectively, and K_{v} is the flow coefficient of an average valve.

7.2 Tuning of motion controller

The PT1 controller tuning is based on linear analysis. At first, the approach assumes that the transfer function from $v_{\text{ref,c}}$ to Q_{A} equals A_{A} in the applied frequency range. Second, the cylinder-load system is regarded as an integrator with second order dynamics [77]. Now, the transfer function from $v_{\text{ref,c}}$ to x can be written as:

$$\frac{x}{v_{ref,c}} = A_{\text{A}} \frac{\frac{1}{A_{\text{A}}}}{s\left(\frac{s^2}{\omega_{\text{h}}^2} + \frac{2\xi_{\text{h}} s}{\omega_{\text{h}}} + 1\right)}, \tag{7.3}$$

where ω_{h} depicts the hydraulic natural angular frequency and ξ_{h} depicts the damping factor. When the time constant of the P-controller filter is selected to be significantly larger than $1/\omega_{\text{h}}$, the dynamics of the cylinder-load system can be neglected. In this case, the open loop transfer function from x_{ref} to x can be written as:

$$\frac{x}{x_{\text{ref}}} = \frac{K_{\text{p}}}{s(\tau s + 1)}, \tag{7.4}$$

where τ is the time constant of the P-controller, K_{p} is the gain of the P-controller, and s is the Laplace operator.

An addition of an ideal feedback (unity gain) results in a second order closed loop transfer function. Now, the closed loop natural angular frequency and damping factor can be written, according to [78], as:

$$\omega_c = \sqrt{K_p/\tau}, \tag{7.5}$$

$$\xi_c = 1/(2\sqrt{K_{\text{p}}\tau}). \tag{7.6}$$

Thus, to keep eq. 7.5 and 7.6 valid, the time constant of the filter is selected as $\tau = 3/\omega_h$, where ω_{h} is the minimum measured natural angular frequency of the system having value

of 37.6 rad/s. Then, the target damping factor ξ_c is selected, after which the gain K_p can be calculated as follows:

$$K_p = \frac{1}{4\,\xi_c^2\,\tau}. \tag{7.7}$$

The parameters of the final tuning of the motion controller are presented in Table 7.2. The discrete implementation of the P-controller filter was done with backward differentiation.

Table 7.2: Motion controller parameters

ξ_c	0.6
K_p	8.71 $\frac{1}{s}$
ω_h	37.6 $\frac{rad}{s}$
τ	0.08 s
T_c	10 ms

7.3 Tuning of model-based valve controller

Flow coefficients for the models were measured with the test setup. The cylinder was manually driven full speed in both directions. First, the extending movement was produced by opening all four valves in both PA and BT DFCUs. The velocity and pressures were measured, and the mean flow coefficient was calculated as follows:

$$K_{v,PA} = \frac{1}{N}\,\frac{|v|A_A}{\sqrt{p_S - p_A}} \tag{7.8}$$

Flow coefficient of AT DFCU was measured similarly by driving the retracting movement with PB and AT DFCUs. $K_{v,AT}$ was then calculated as follows:

$$K_{v,AT} = \frac{1}{N}\,\frac{|v|A_A}{\sqrt{p_A}}. \tag{7.9}$$

The pulse error values were calculated based on the velocity response of the system. The velocity response was measured with a fifth order position trajectory, giving a smooth acceleration and deceleration. The trajectory was selected to give maximum velocity of 10 mm/s for both directions and by exploiting the full stroke, in order to get as slow acceleration and deceleration as possible. The velocity error with openloop control was then plotted as a function of velocity reference, as shown in Fig. 7.5. The data are filtered with a first order Butterworth low-pass filter having a cut off frequency of 3 Hz and utilizing forward backward filtering to avoid phase shift. The cut off frequency is selected low to diminish the effect of natural frequency of the system.

The result in Fig. 7.5 shows approximately constant velocity error after a certain control value if the fluctuation is neglected. This occurs in the MVPWM mode, where the pulse frequency remains constant. Thus, the constant velocity error indicates a constant pulse width error, which can be compensated. Assuming a linear relationship between velocity reference and control value, the pulse error t_c can be estimated as follows:

$$t_c = \frac{u\,v_e}{v_{ref}\,f}, \tag{7.10}$$

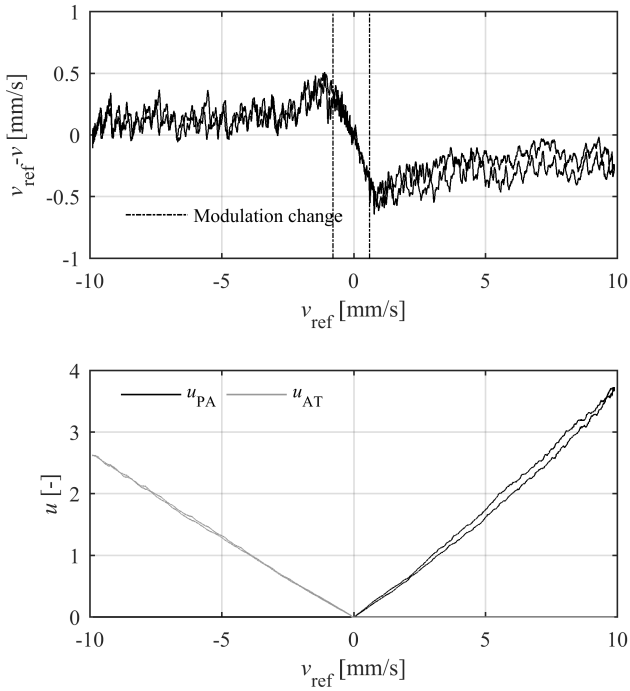

Figure 7.5: Upper graph: openloop velocity response without pulse time correction. Lower graph: control values of A side DFCUs.

where v_e is the velocity error, u is the control value, and v_{ref} is the velocity reference of a selected data point. Applying this equation to data points near full speed, we obtain error values of 0.26 ms for AT and 0.73 ms for PA. These values are used as the time correction values in the dynamic models. Since the piston velocity is controlled with A side DFCUs, the correction values cannot be obtained for the B side DFCUs with this measurement. Accurate values for these values would be necessary with the simultaneous pressure control, but that is excluded in this study. Thus, by giving a sufficiently accurate approximation, the same correction value was used in both B side DFCUs and AT DFCU.

It would also be possible to estimate the pulse error values based on the response time measurements and pressure differentials over the DFCUs. However, this requires laboratory measurements with the utilized valve in similar conditions with the target system. In this case, they are available, but for better accuracy and more general approach, the first explanation was applied.

The valve controller utilized two measured pressures: the supply pressure and chamber A pressure. The tank pressure was assumed to be zero. Both pressure signals were filtered similarly with two serial connected filters. The first of them was a three sample median filter, which involves three sample buffer and outputs the median value of the three samples. Its purpose is to remove individual disturbed samples of the pressure signal. The output of the median filter was fed to a discrete first order low pass filter. Both filters were run in the sampling interval of T_{fast}. The time constant of the low pass filter (τ_p) was tuned experimentally to remove most of the pressure fluctuation without generating

Table 7.3: Valve controller parameters

$K_{\mathrm{v,PA}}$	$2.09{\cdot}10^{-8}$	$\frac{m^3}{\sqrt{\mathrm{Pa}}}$
$K_{\mathrm{v,AT}}$	$1.58{\cdot}10^{-8}$	$\frac{m^3}{\sqrt{\mathrm{Pa}}}$
τ_{p}	0.1	s
v_{tol1}	90	µm/s
v_{tol2}	60	µm/s
λ	2.0	ms
T_{fast}	1.0	ms
T_{slow}	10	ms

too much delay. The cut-off frequency of the filter combination is not affected by the median filter as can be seen in Appendix B. The parameters of the valve controller were gathered by Table 7.3.

7.4 Experimental Results

Before the tracking control experiment, the accuracy of the model-based valve controller and the proper tuning of the motion controller were studied. The accuracy of the model-based valve controller was studied by conducting the velocity response experiment again with the calculated pulse error values. The resulting velocity response is shown in Fig. 7.6. The data are filtered in similar way as in the previous velocity response measurement.

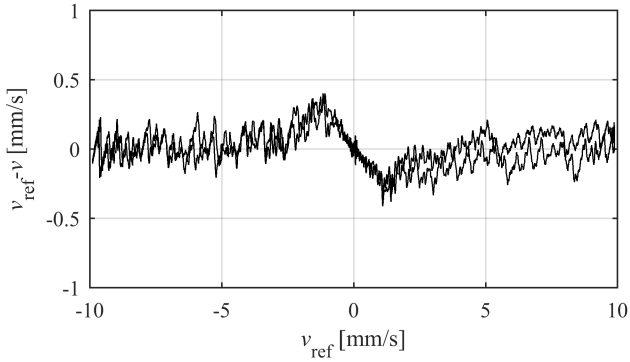

Figure 7.6: Openloop velocity error with using pulse error compensation

The proper tuning of the motion controller was studied with step response measurements with different step sizes. The results are plotted in Fig. 7.7 – 7.10. Results show a larger overshoot than 10 %, which is an expected value with the given damping factor [79]. With most of the responses, the overshoot is very similar for both directions. The step responses show excellent positioning accuracy well below 10 µm, which was the threshold of the controller to stop the activity. The oscillation at the natural frequency is clearly seen in the responses, but after about one second, its amplitude is below 10 µm.

The final test trajectory had three successive extending and retracting movements with different velocities and strokes. All of them are fifth order polynomial trajectories. The

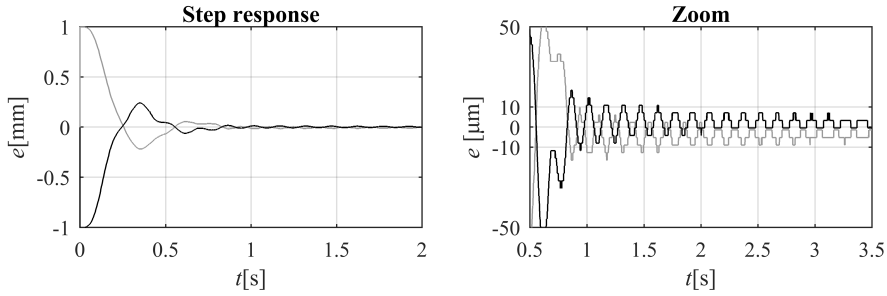

Figure 7.7: Step responses to both directions with a step size of 1.0 mm

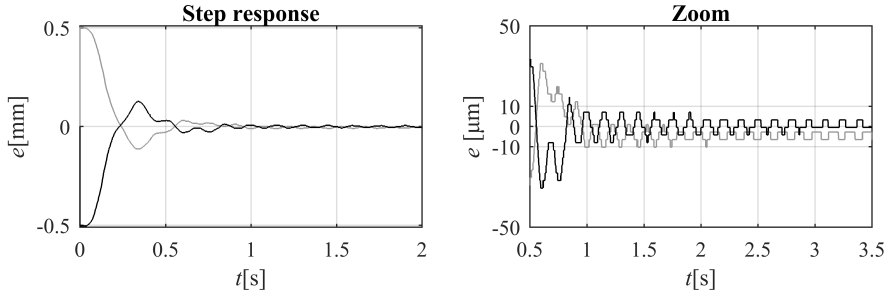

Figure 7.8: Step responses to both directions with a step size of 0.5 mm

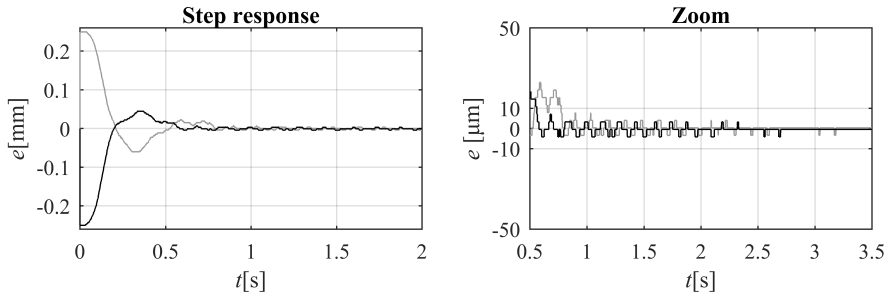

Figure 7.9: Step responses to both directions with a step size of 0.25 mm

measured results are plotted in Fig. 7.11 and Fig. 7.12. Graph a) in Fig. 7.11 presents the piston position reference and the measured position; in the scale of the graph, they overlap. The piston position error is presented separately in the scale of micrometers in graph b) in Fig. 7.11, showing the maximum error to be below 50 µm. Graph c) in Fig. 7.11 shows the reference velocity and the measured velocity, which generally seems to follow the reference quite well, but has a ripple with an amplitude of about 25% of the maximum velocity. Graph d) in Fig. 7.11 shows the measured supply pressure, the filtered supply pressure, and the measured tank pressure. The supply pressure seems to decrease with increasing velocity. The last graph e) in Fig. 7.11 presents the cylinder chamber pressures, both raw data and filtered. The raw data show high pressure ripple in the cylinder. From the pressure signals, the controller utilized only the filtered supply pressure and filtered chamber A pressure. The pressure of chamber B was filtered afterwards to understand

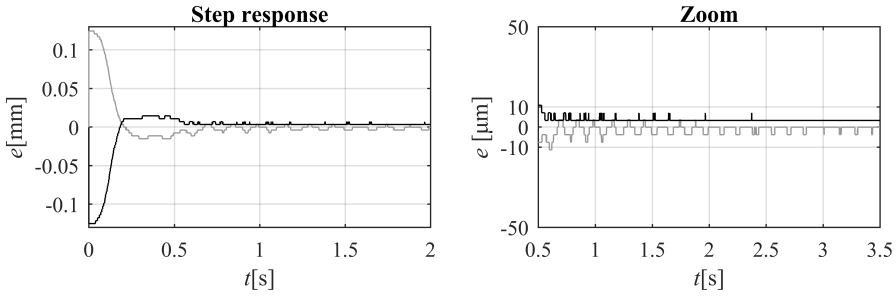

Figure 7.10: Step responses to both directions with a step size of 0.125 mm

the average behavior. All the pressures were measured from the base manifold close to the valve system.

Figure 7.12 depicts the inner controller signals during the trajectory tracking. Three quantities of each DFCU are plotted: desired control values and integer control values in graphs a) and b), and desired switching frequencies in graphs c) and d). Because of high switching frequency and long total plot, the integer control value only shows the number of opened valves that the control value is between.

In order to see the switching controller functionality in more detail, a part of the fastest retracting movement is presented separately in Fig 7.13-7.15. Figure 7.13 shows exactly the same signals as Fig. 7.11. Individual valve control signals of the AT DFCU as well as their sum (integer control signal of AT DFCU) are presented in Fig. 7.14. The graphs clearly show the lower switching frequency of single valves compared to the total summarized output of the DFCU. The last graph of Fig. 7.14 shows the desired frequency of the AT DFCU. The same graphs of the DFCU PB are shown in Fig. 7.15.

The trajectory tracking results show the synchronization error when the modulation method changes between MVPFM and MVPWM, as presented in Chapter 4. As an example, this modulation method change occurs seven times in the PA DFCU. The control pulses at the changing moments are plotted in Fig. 7.16. Since the transition to MVPWM has always a paired transition back to MVPFM, from each occurrence, both transitions are plotted. In the third occurrence, for example, the first MVPWM pulse comes too early, and when changing back to the MVPFM, the first pulse is delayed. One thing to note is that the transition error pairs compensate each other. The effect of single errors cannot be seen in the responses, however, many successive errors during the last, slowest movement, seems to affect the pressure ripple.

To show the accuracy of the model-based control strategy, the final trajectory was also driven with openloop control. Figures 7.17 and 7.18 show the same graphs with the same signals as Fig. 7.11 and 7.12 respectively, but from the openloop experiment. As shown in Fig. 7.17, the maximum position error with openloop control is about 1.1 mm, and the position error at the end of the trajectory is less than 0.3 mm. The water temperature measured from the tank during all the measurements presented in this chapter was between 20° and 27°C.

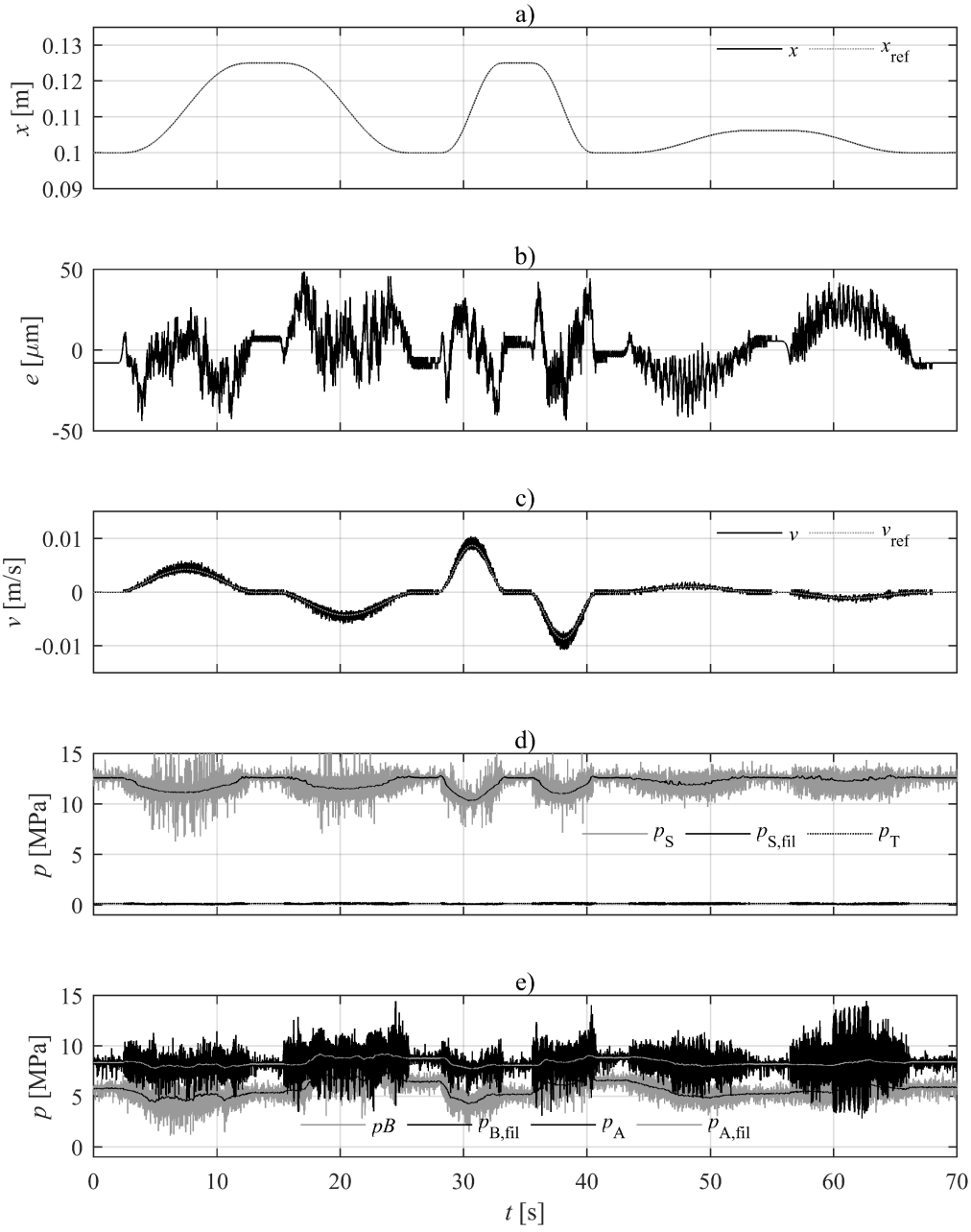

Figure 7.11: Tracking results with closed loop control

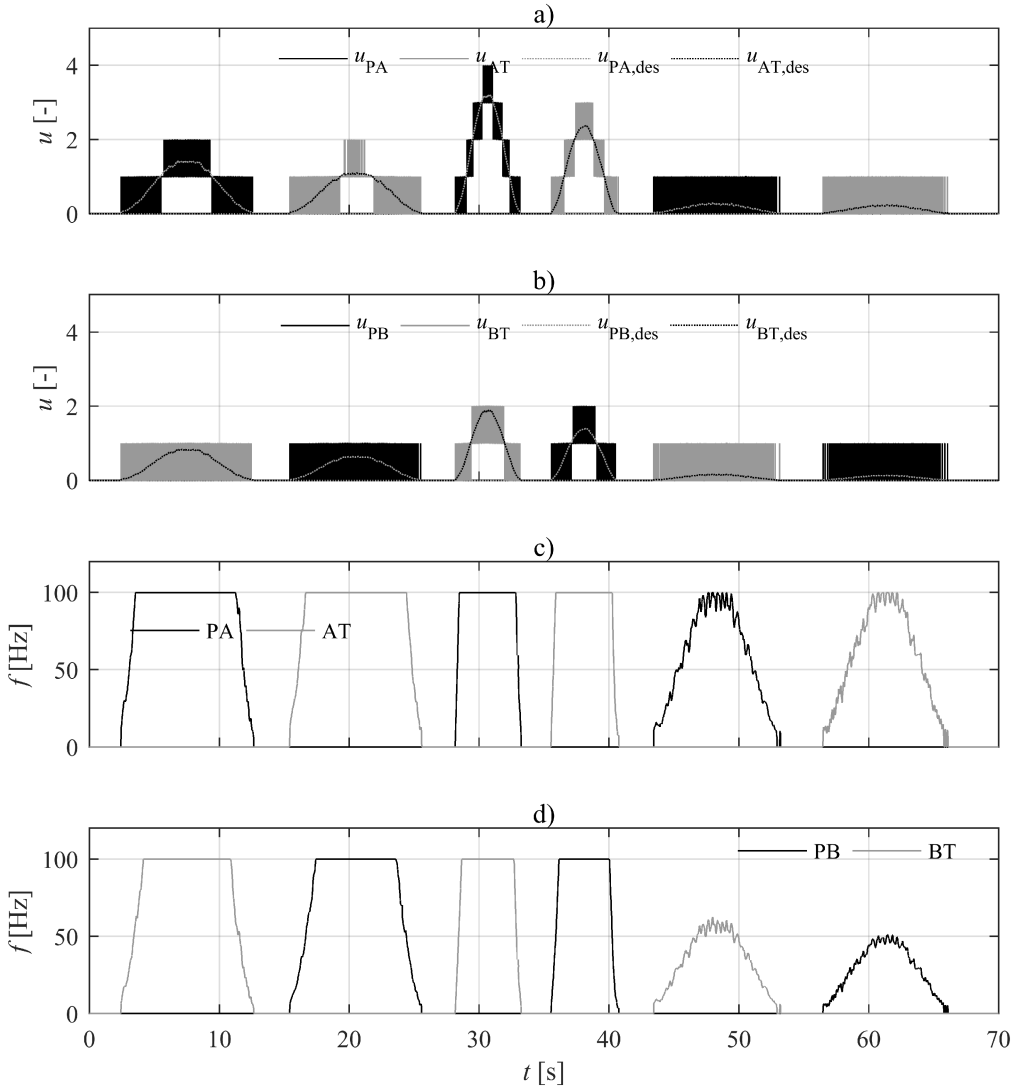

Figure 7.12: Controller internal signals during the trajectory

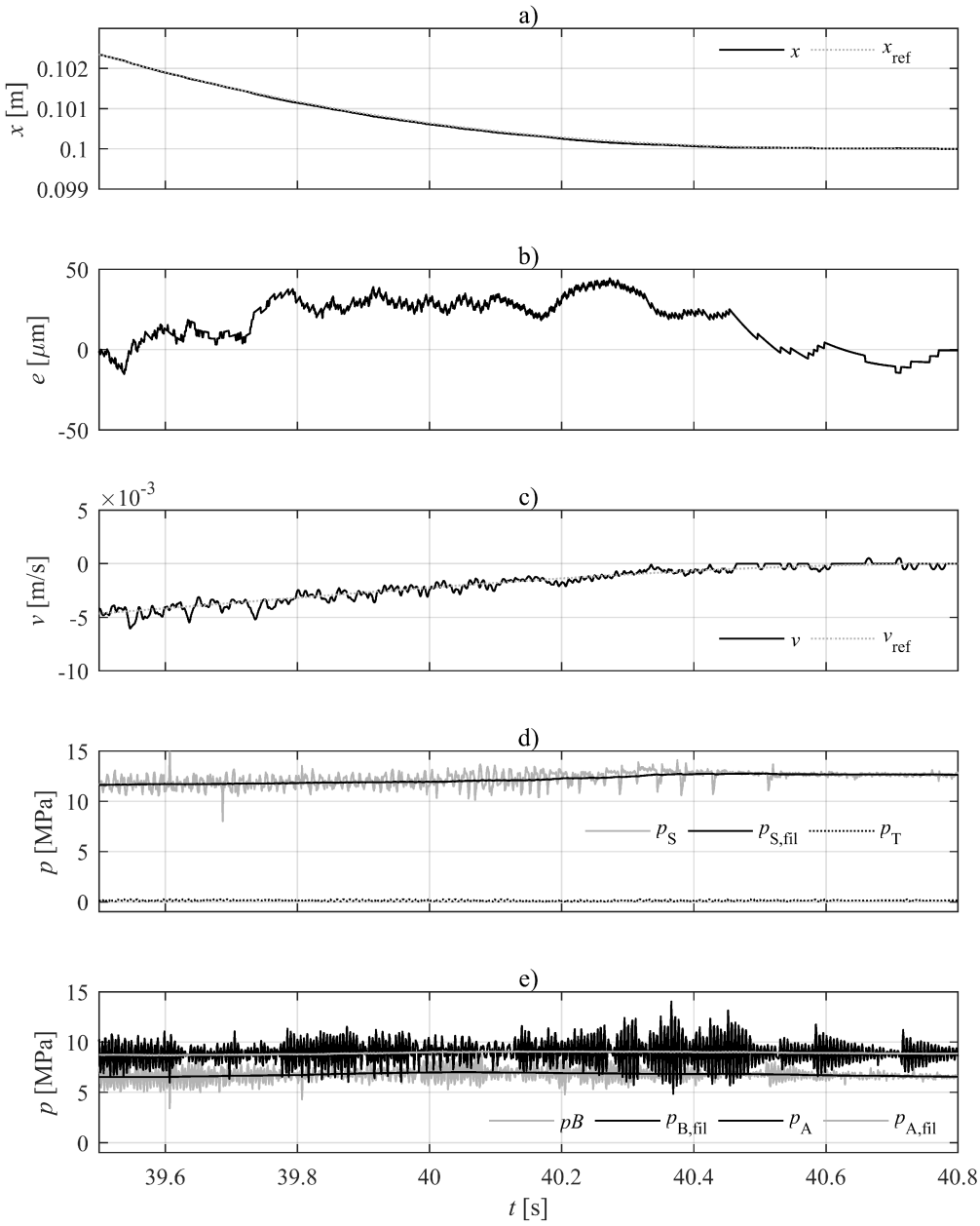

Figure 7.13: Zoomed tracking results with closed loop control

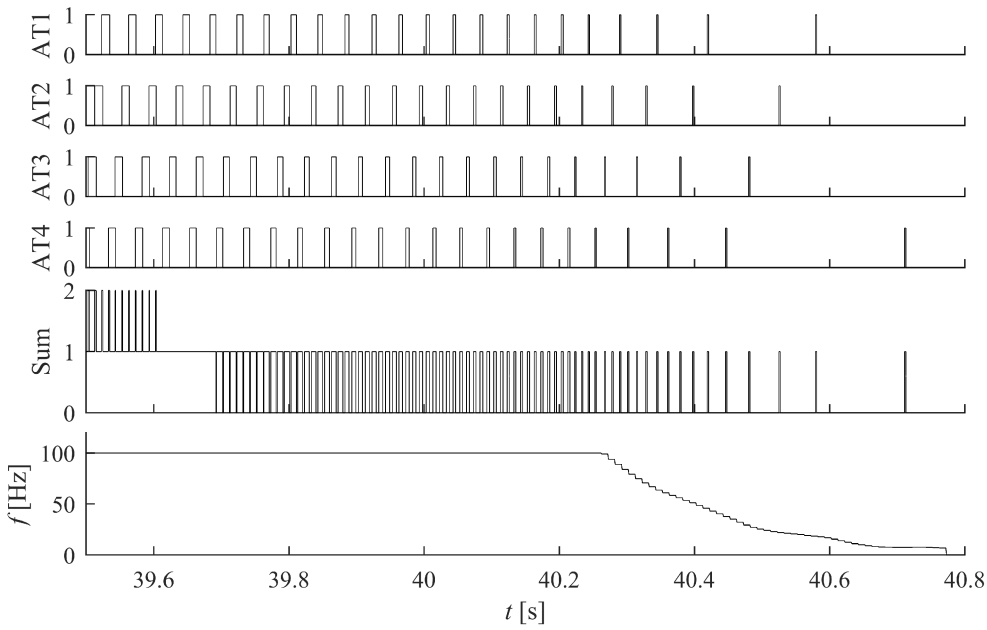

Figure 7.14: Zoomed controller signals of AT DFCU

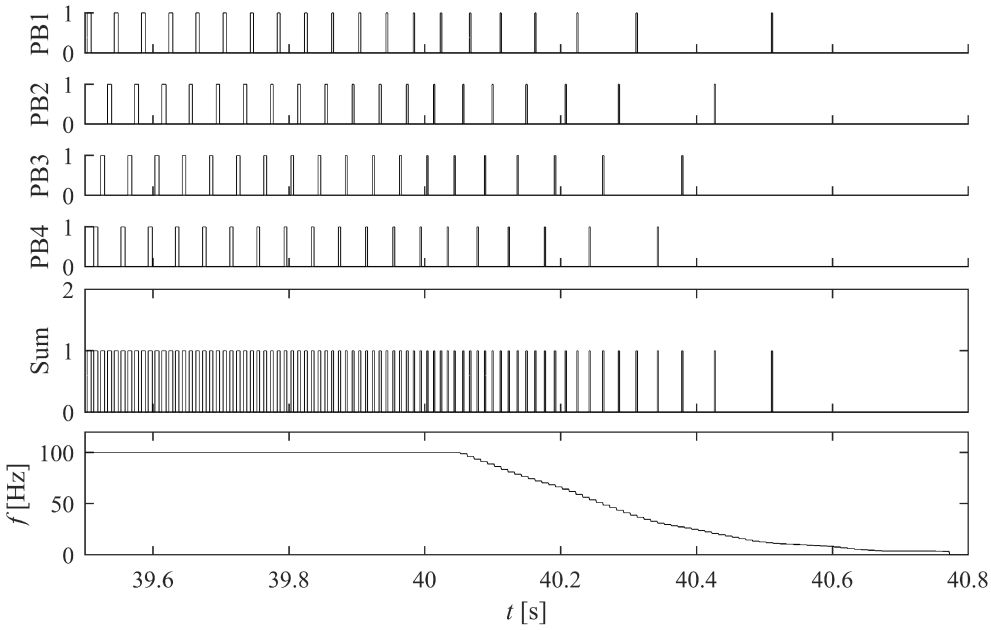

Figure 7.15: Zoomed controller signals of PB DFCU

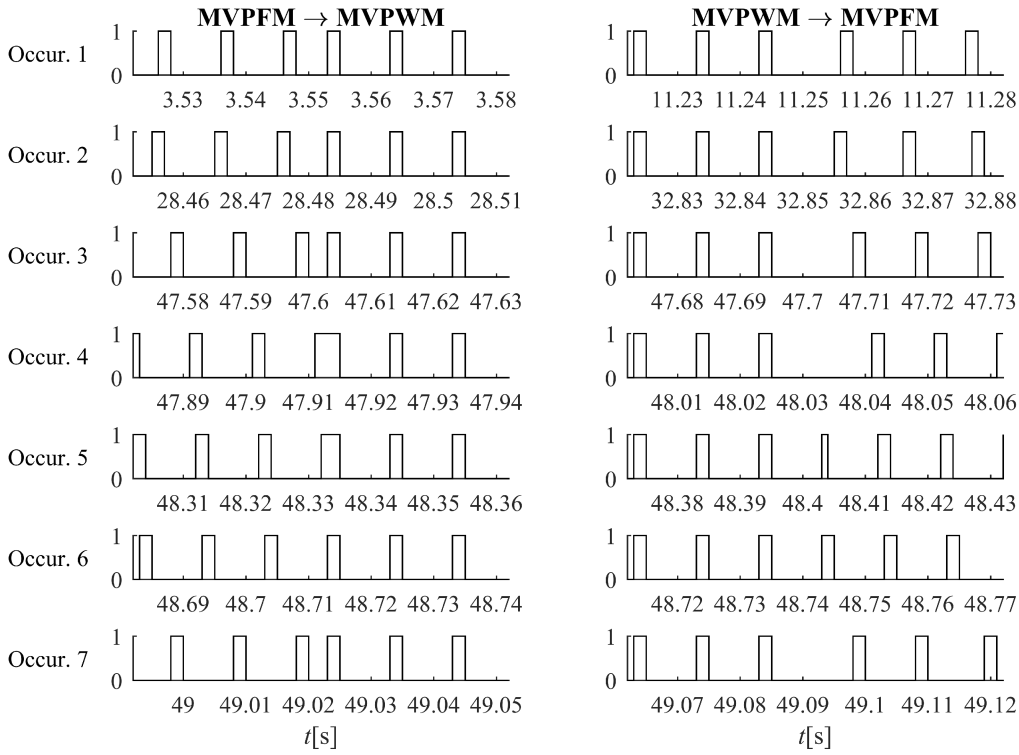

Figure 7.16: The synchronizing errors in the modulation method changes in PA DFCU

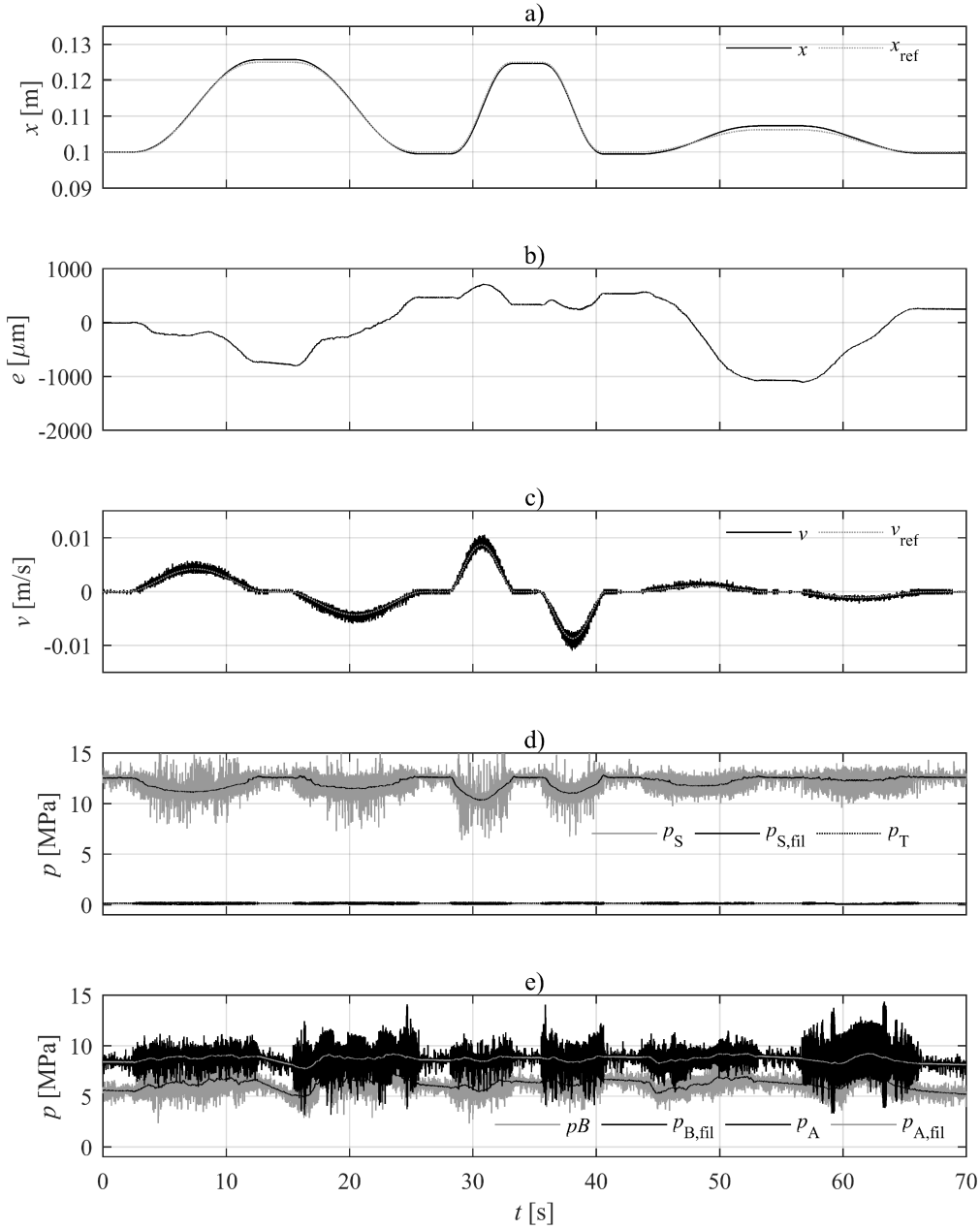

Figure 7.17: The tracking control results with openloop control

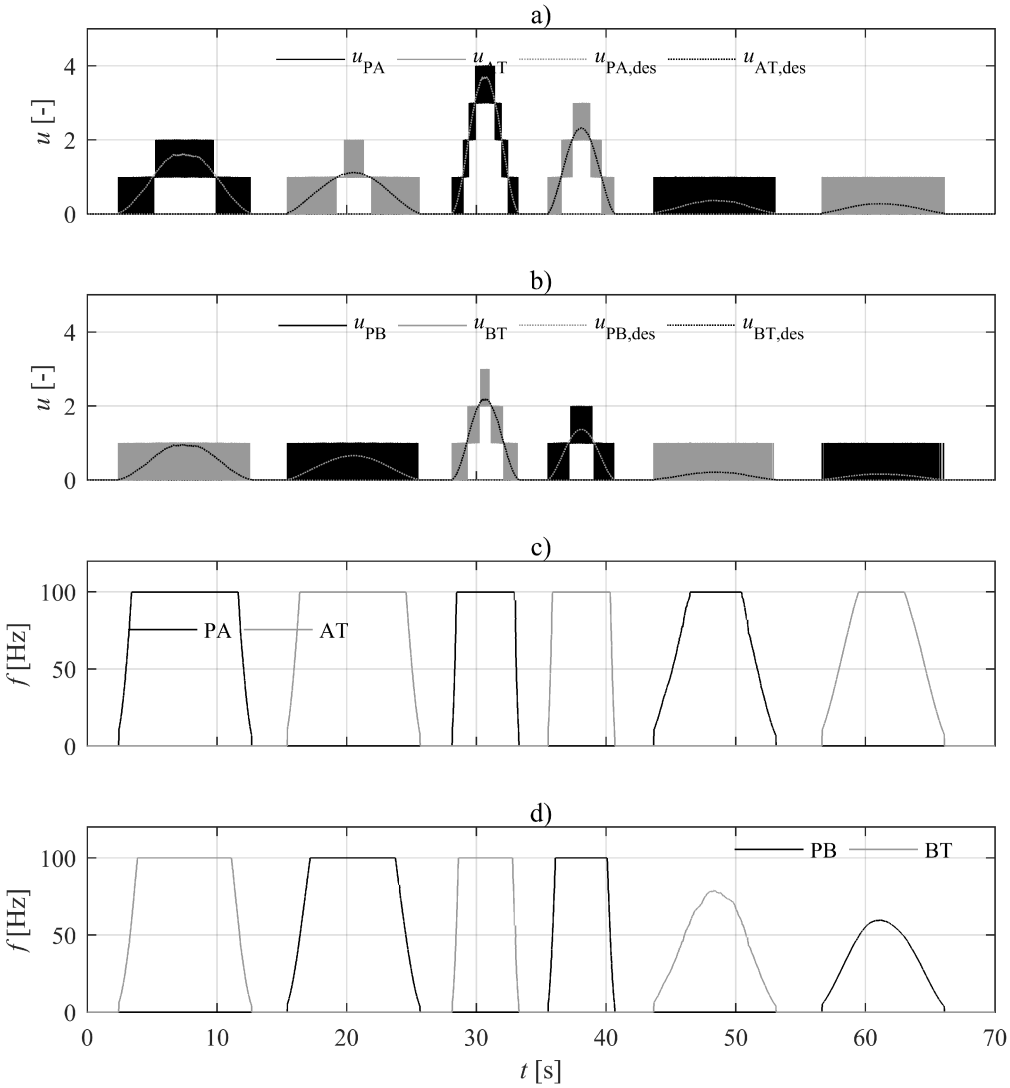

Figure 7.18: The controller inner signals during the trajectory with openloop control

8 Discussion

A study of prototype valves shows a water hydraulic miniature valve can be produced, whose properties are sufficient for equal coded DFCU. All three miniature valve prototypes support this statement. WHV1, the first prototype, exhibited that small, fast, and low-power solenoid valves can be produced using stainless steel. Moreover, this prototype showed that stainless steel parts do not automatically mean reduced flow density of the valve, despite less optimal magnetic properties of those alloys. WHV2 showed similar results, being even faster and lesser power consuming. Significance of these results are increased by the fact that the coil volume was significantly reduced, which was expected to increase the power consumption. In addition, the design of WHV2 resolved the durability issue faced by WHV1, showing much less wear in the seat contact area. In particular, the ceramic ball as the sealing element did not show any marks of wear. Also the seat part was much less worn after a million opening cycles. In the design of WHV3, industrial and commercial aspects were taken more into account, since the valve was the result of co-operation with an industrial partner. As a result, the mechanical design changed considerably, promoting mechanical reliability; unfortunately, this yielded increased size. However, the electric power consumption and response times remained on the same level, making it reasonable for the use in equal coded valve systems. The hydraulic part of the valve utilized the same ceramic ball concept as WHV2, and passed the durability test of 11 million opening cycles.

The final tracking control study was carried out with the valve system containing 16 WHV3 on/off valves in total. This is a relatively low number of valves in a digital hydraulic valve system and very low number in an equal coded valve system. Previously, sufficient resolution was estimated to need more than a hundred valves with that coding method. However, by evaluating the achieved tracking control result with the performance indices, the following numbers was obtained: $\rho_1 = 5$ ms ($e_{\max} = 50$ µm, $v_{\max} = 10$ mm/s) and $\rho_2 = 188$. These numbers reveal that the tracking performance of this system exceeds the results of previous studies. The second best results, presented in [37], achieved the same value for ρ_1, utilizing a valve system with same number of valves in total but increasing the resolution with binary coding; however, taking the natural angular frequency into account using the performance number ρ_2, the results of this study is about 2.5 times better.

The tracking control result is excellent, especially considering the simplicity of the motion controller, which was a filtered P-controller with velocity feed-forward controller. The adjustment of parameters was made straightforward based on the linear analysis and the measured hydraulic natural angular frequency. The model-based valve controller utilized the novel switching scheme and had only two valve flow models, which in turn were simple with only one parameter per model. Those parameters were measured with the test setup. In addition, four correction parameters for pulse width, one for each DFCU,

were adjusted based on the measurement with the test setup. Thus, the effort needed for tuning the controllers was minimal. The utilized controller also performed excellently in positioning, and thus, a separate controller for this task was not required.

In this study, the output resolution was increased with the circulating switching control. Although the switched flow rate was a quarter of the full flow rate, the results show relatively high velocity fluctuation and high pressure fluctuation. The highest fluctuation in pressures occurred at the situation where the modulation method was repeatedly changed between MVPWM and MVPFM. This indicates the need for hysteresis or synchronization in the mode switching. However, the pressure fluctuation at other regions were also high despite 17 times higher switching frequency compared to the hydraulic natural frequency of the system. This phenomenon might be amplified by the high inertia load and low capacitance. During MVPFM modulation, the switching frequency is lower; however, that does not show larger fluctuation neither in velocity or pressures, even though minimum frequency is close to the natural hydraulic frequency of the system.

The switching frequency of single valves in the tracking experiment was 25 Hz. This seemed to be sufficient frequency for WHV3, with no signs of overheating the coil. However, the durability of the valve is a question with long-term continuous usage. As the advantage of the developed switching method, the frequency can be decreased by adding more valves to the system, maintaining the effective output frequency. Thus, the developed method can also be used to make a compromise between low number of valves and durability. The controlling accuracy, however, does not seem to require a compromise with valve number, since four valves per DFCU seem to give adequate accuracy. On the contrary, the number of valves needs to be increased if the flow rate demand is higher.

The novel switching scheme can be adjusted to different applications with three parameters. T_{slow} defines the effective output frequency, which naturally needs to be selected according to the application. T_{fast} defines the time interval by which the pulse width or period length can be varied. Thus, it affects the effective output resolution. On the other hand, some calculation is done at that sampling interval, and thus, it cannot be too short. There might be also some other restricting factors as in this study, where T_{fast} was limited to one millisecond due to CAN bus, which could not transfer messages with a shorter time interval. However, there were no signs in the results indicating that the resolution is too small. The third parameter is the length of PFM pulse. This is best to be short, but the utilized valve should act in the normal mode.

The PWM response of WHV3 was not measured, and thus, the selection of the PFM pulse length was based on the response times. The velocity response of the final system indicates that WHV3 behaves differently with the WHV2, which according to its PWM response is well on the linear area after two milliseconds, i.e., the utilized pulse length. However, the velocity response of the final system shows the highest velocity error (less accurate model) at the beginning of the PWM modulation, indicating that the valve is not in the most linear area with the 2 ms pulse. The same can be seen in the tracking results: the largest position error occurs systematically at low speeds.

9 Conclusions

In this thesis, a water hydraulic servo system was developed. The system was selected to utilize the equal coded digital hydraulic approach. The main obstacles to applying this technology have been the high number of required valves and the difficulty of finding a suitable one for the purpose. The equal coding, by nature, results in a relatively low resolution if the system is used in a typical way, and therefore, a high number of valves are required to enable accurate motion control. Thus, the main research questions in the thesis are related to these obstacles, the first one asking whether it is possible to produce a water hydraulic valve suitable for the purpose, and the second one asking if the number of required valves could be reduced by intelligent switching control.

In order to answer these questions, in total, three versions of a water hydraulic miniature valve, and a circulating switching control algorithm were developed. The last valve was a prototype of a commercial valve, having design contribution also from the industrial side. The final servo system was built using that industrial prototype, and it utilized the developed control algorithm.

The developed valves show fast response, low electric power consumption, and small size, all of these being the requirements for a valve to be used in equal coded valve system. All the valve parts were made from corrosion resistant materials, and thus, they are suitable in water hydraulic systems. The results with the prototypes show that a water hydraulic miniature valve can be produced with good properties for the digital hydraulic usage. This gives the answer to the first research question. The final tracking control study showed excellent tracking accuracy with a valve system having only 4x4 equal size on/off valves. The total number of valves is much lower than that estimated to be required if switching control was not utilized. This, in turn, shows that intelligent switching control techniques are effective to reduce the required number of valves, and therefore gives the answer to the second research question.

However, a little concern remains about the long-term durability of the developed valve when the switching control is utilized. Although the developed method enables relatively low switching frequency to a single valve, long-term use easily cumulates very high number of switching cycles. Therefore, further development in the valve durability might be required.

Bibliography

[1] E. Urata, S. Miyakawa, and C. Yamasaina, "Hydrostatic support of spool for water hydraulic servovalves," in *The Fourth Scandinavian International Conference on Fluid Power*, vol. 2, Tampere, Finland, Sep. 1995, pp. 910–929.

[2] X. Wang, J. Zheng, S. Sun, and J. Chang, "Research on hydrostatic bearing technology applied in water hydraulic servo valve," in *Computer-Aided Industrial Design Conceptual Design, 2009. CAID CD 2009. IEEE 10th International Conference on*, Nov 2009, pp. 2140–2145.

[3] K. Koskinen, M. Vilenius, T. Virvalo, and E. Mäkinen, "Water as a pressure medium in position servo systems," in *The Fourth Scandinavian International Conference on Fluid Power*, vol. 2, Tampere, Finland, Sep. 1995, pp. 859–871.

[4] M. Linjama, K. T. Koskinen, and M. Vilenius, "Pseudo-proportional position control of water hydraulic cylinder using on/off valves," in *Proceedings of the JFPS International Symposium on Fluid Power*, vol. 2002, no. 5-1, 2002, pp. 155–160.

[5] A. Laamanen, M. Linjama, J. Tammisto, K. T. Koskinen, and M. Vilenius, "Velocity control of water hydraulic motor," in *Proceedings of the JFPS International Symposium on Fluid Power*, vol. 2002, no. 5-1, 2002, pp. 167–172.

[6] anon. (2016) Valmet technical paper series, digital hydraulics. [Online]. Available: http://www.valmet.com/globalassets/media/downloads/white-papers/process-improvements-and-parts/wpp_digihydraulics.pdf

[7] H. Fischer, A. Laamanen, A. Iso-Heiko, O. Schäfer, M. Karvonen, O. Karhu, K. Huhtala, V.-P. Pulkkinen, and A. Huttunen, "Digital hydraulics on rails – pilot project of improving reliability on railway rolling stock by utilizing digital valve system," in *Proceedings of the Fourteenth Scandinavian International Conference on Fluid Power, SICFP15*, Tampere, Finland, May 2015.

[8] M. Linjama and M. Vilenius, "Digital hydraulics - towards perfect valve technology," in *Proceedings of The Tenth Scandinavian International Conference on Fluid Power (SICFP'07)*, Tampere, Finland, May 2007.

[9] M. Linjama, "Fundamentals of digital microhydraulic," in *Proceedings of the 8th International Fluid Power Conference*, Dresden, Germany, Mar. 2012.

[10] M. Paloniitty, M. Linjama, and K. Huhtala, "Concept of digital microhydraulic valve system utilising lamination technology," in *Conference Proceedings, 9th International Fluid Power Conference, 24th - 26th March, 2014, Aachen, Germany, Modern Fluid Power - Challenges, Responsibilities, Markets, Vol. 1*, H. Murrenhoff, Ed., Aachen, Germany, Mar. 2014, pp. 303–313.

[11] M. Karvonen, M. Juhola, V. Ahola, L. Söderlund, and M. Linjama, "A miniature needle valve," in *Proceedings of The Third Workshop on Digital Fluid Power*. Tampere University of Technology Finland, 2010, pp. 61–78.

[12] V. Puumala, "Nopea neulaventtiili digitaalihydrauliikkaan [in Finnish]," Master's thesis, Tampere University of Technology, Tampere, Finland, 2012.

[13] M. Linjama, M. Paloniitty, L. Tiainen, and K. Huhtala, "Mechatronic design of digital hydraulic micro valve package," *Procedia Engineering*, vol. 106, pp. 97–107, 2015. [Online]. Available: http://www.sciencedirect.com/science/article/pii/S1877705815009388

[14] M. Paloniitty, M. Karvonen, M. Linjama, and T. Tiainen, "Laminated manifold for digital hydraulics - principles, challenges and benefits," in *Proceedings of The fifth workshop on digital fluid power DFP12*, Tampere, Finland, Oct. 2012.

[15] L. Tiainen, "Digitaalihydraulisen venttiilistön ohjauselektroniikan suunnittelu [in Finnish]," Master's thesis, Tampere University of Technology, Tampere, Finland, 2014.

[16] M. Linjama, M. Huova, O. Karhu, and K. Huhtala, "High-performance digital hydraulic tracking control of a mobile boom mockup," in *10th International Fluid Power Conference, Dresden 2016*, 2016.

[17] M. Paloniitty and M. Linjama, "High-linear digital hydraulic valve control by an equal coded valve system and novel switching schemes," *Proceedings of the Institution of Mechanical Engineers, Part I: Journal of Systems and Control Engineering*, 1 2018.

[18] M. Paloniitty and M. Linjama, "A miniature on/off valve concept for high performance water hydraulics," in *ASME/BATH 2017 Symposium on Fluid Power and Motion Control*. American Society of Mechanical Engineers, 2017.

[19] M. Paloniitty, M. Linjama, and K. Huhtala, "Durability study on high speed water hydraulic miniature on/off-valve," in *DFP16, Proceedings of the eighth workshop on digital fluid power, May 24-25, 2016, Tampere, Finland*, 5 2016, pp. 201–211.

[20] F. Majdič, J. Pezdirnik, and M. Kalin, "Experimental validation of the lifetime performance of a proportional 4/3 hydraulic valve operating in water," *Tribology International*, vol. 44, no. 12, pp. 2013–2021, 2011.

[21] Y. Yang, C. Semini, N. Tsagarakis, D. Caldwell, and Y. Zhu, "Water hydraulics - a novel design of spool-type valves for enhanced dynamic performance," in *Advanced Intelligent Mechatronics, 2008. AIM 2008. IEEE/ASME International Conference on*, July 2008, pp. 1308–1314.

[22] E. Urata, S. Miyakawa, C. Yamashina, and Y. Nakao, "Frequency response of a water hydraulic servovalve," in *Robotics and Automation, 1995. Proceedings., 1995 IEEE International Conference on*, vol. 3, May 1995, pp. 2212–2217 vol.3.

[23] F. Majdic, J. Pezdirnik, and M. Kalin, "Comparative tribological investigations of continuous control valves for water hydraulics," *SICFP*, vol. 7, pp. 21–23, 2007.

[24] T. Takahashi, C. Yamashina, and S. Miyakawa, "Development of water hydraulic proportional control valve," in *Proceedings of the JFPS International Symposium on Fluid Power*, vol. 1999, no. 4. The Japan Fluid Power System Society, 1999, pp. 549–554.

[25] W. Xinhua, Z. Jian, S. Shuwen, L. Wei, and C. Jiaqing, "Research on performance of slide-valve in water hydraulic servo-valve with hydrostatic bearing," in *Mechanic Automation and Control Engineering (MACE), 2010 International Conference on*, June 2010, pp. 3619–3622.

[26] H. Sairiala, M. Linjama, K. Koskinen, and M. Vilenius, "Low-cost proportional valve for low-pressure water hydraulics," in *Bath Workshop on Power Transmission and Motion Control*, 2001, pp. 135–145.

[27] K. T. Koskinen and M. J. Vilenius, "Steady state and dynamic characteristics of water hydraulic proportional ceramic spool valve," *International Journal of Fluid Power*, vol. 1, no. 1, pp. 5–15, 2000.

[28] E. Urata, S. Miyakawa, C. Yamashina, Y. Nakao, Y. Usami, and M. Shinoda, "Development of a water hydraulic servo valve," *JSME International Journal, Series B: Fluids and Thermal Engineering*, vol. 41, no. 2, pp. 286–293, 1998, cited By :21. [Online]. Available: www.scopus.com

[29] M. Hyvönen, K. Koskinen, J. Lepistö, and M. Vilenius, "Experiences of using servo valves with pure tap water," in *Proc. 5th Int. Conference on Fluid Power – SICFP*, vol. 2, 1997, pp. 21–32.

[30] T. Oomichi and A. Tanaka, "Development of water hydraulic servo control system considering water characteristics," *Nippon Kikai Gakkai Ronbunshu, C Hen/Transactions of the Japan Society of Mechanical Engineers, Part C*, vol. 62, no. 599, pp. 2612–2619, 1996, cited By :1. [Online]. Available: www.scopus.com

[31] T. Watanabe, T. Inayama, and O. Takeo, "Design concept of small flow rate servo valve for water hydraulic system," in *System Integration, 2009. SII 2009. IEEE/SICE International Symposium on*, Jan 2009, pp. 1–6.

[32] K. Suzuki, S. Akazawa, and Y. Nakao, "Development of cam-drive type proportional valve for water hydraulics," *International Journal of Automation Technology*, vol. 6, no. 4, pp. 450–456, 2012, cited By :1. [Online]. Available: www.scopus.com

[33] M. O. Linjama, K. T. Koskinen, J. O. Tammisto, and M. J. Vilenius, "Two-way solenoid valves in low-pressure water hydraulics," *American Society of Mechanical Engineers, The Fluid Power and Systems Technology Division (Publication) FPST*, vol. 7, pp. 55–60, 2000, cited By :6. [Online]. Available: www.scopus.com

[34] M. Linjama, J. Tammisto, K. Koskinen, and M. Vilenius, "On/off position control of low-pressure water hydraulic cylinder using low-cost valves," in *Proceedings. Sixth Triennal International Symposium on Fluid Control, Measurement and Visualization, FLUCOME*, 2000, pp. 13–17.

[35] M. Linjama, S. Oshima, K. T. Koskinen, and M. Vilenius, "High-precision on/off position control of low-pressure water hydraulic cylinder," in *Proceedings of the Seventh Scandinavian International Conference on Fluid Power*, May 2001.

[36] M. Linjama, K. T. Koskinen, and M. Vilenius, "Accurate trajectory tracking control of water hydraulic cylinder with non-ideal on/off valves," *International Journal of Fluid Power*, vol. 4, no. 1, pp. 7–16, 2003.

[37] M. Linjama and M. Vilenius, "Improved digital hydraulic tracking control of water hydraulic cylinder drive," *International Journal of Fluid Power*, vol. 6, no. 1, pp. 29–39, 2005.

[38] A. Laamanen, P. Anttonen, and M. Linjama, "Digital flow control unit for controlling amount of water used for binding dust," in *The Third Workshop on Digital Fluid Power*, Tampere, Finland, Oct. 2010, pp. 119–128.

[39] Z. M. Zhang and Y. J. Gong, "Design analysis of water hydraulic digital valve," in *Applied Mechanics and Materials*, vol. 101. Trans Tech Publ, 2012, pp. 148–153.

[40] Z. M. Zhang and Y. J. Gong, "Design and simulation on multi-digit numerical control valve in water hydraulics," in *Advanced Materials Research*, vol. 422. Trans Tech Publ, 2012, pp. 257–261.

[41] S. Park, A. Kitagawa, and M. Kawashima, "Water hydraulic high-speed solenoid valve part 1: development and static behaviour," *Proceedings of the Institution of Mechanical Engineers, Part I: Journal of Systems and Control Engineering*, vol. 218, no. 5, pp. 399–409, 2004.

[42] S. Park, "Development of a proportional poppet-type water hydraulic valve," *Proceedings of the Institution of Mechanical Engineers, Part C: Journal of Mechanical Engineering Science*, vol. 223, no. 9, pp. 2099–2107, 2009.

[43] S.-H. Park, "Design and performance characteristic analysis of servo valve-type water hydraulic poppet valve," *Journal of mechanical science and technology*, vol. 23, no. 9, pp. 2468–2478, 2009.

[44] B. Lühmann, "Digital gesteuerte hydraulikventile und ihre anwendung," Ph.D. dissertation, Braunschweig University of Technology, 1983.

[45] T. Muto, H. Yamada, and Y. Suematsu, "Pwm-digital control of hydraulic actuator utilizing 2-way solenoid valves," *Japan Hydraulics & Pneumatics*, vol. 19, no. 7, pp. 564–571, 1988.

[46] I. Schepers, D. Schmitz, D. Weiler, O. Cochoy, and U. Neumann, "A novel model for optimized development and application of switching valves in closed loop control," *International Journal of Fluid Power*, vol. 12, no. 3, pp. 31–40, 2011.

[47] T. Muto, H. Yamada, and Y. Suematsu, "Digital control of hydraulic actuator system operated by differential pulse width modulation," *JSME International Journal, Series III*, vol. 33, no. 4, pp. 641–648, 1990.

[48] R. B. van Varseveld and G. M. Bone, "Accurate position control of a pneumatic actuator using on/off solenoid valves," vol. 2, no. 3, pp. 195–204, 1997.

[49] G. Belforte, S. Mauro, and G. Mattiazzo, "A method for increasing the dynamic performance of pneumatic servosystems with digital valves," *Mechatronics*, vol. 14, no. 10, pp. 1105–1120, 2004.

[50] I. Schepers, D. Weiler, and J. Weber, "Comparison and evaluation of digital control methods for on/off valves," in *Proceedings of The fifth workshop on digital fluid power DFP12*, Tampere, Finland, Oct. 2012.

[51] C. Ferraresi, "A new pcm-pwm combined technique for pneumatic flow-requlation valves," in *Proceedings of the Joint Hungarian - British International Mechatronics Conference*, 1994.

[52] H. Kogler and R. Scheidl, "The hydraulic buck converter exploiting the load capacitance," in *Proc. 8th International Fluid Power Conference (8. IFK) Vol*, vol. 2, no. 3, 2012, pp. 297–309.

[53] M. Paloniitty, M. Linjama, and K. Huhtala, "Equal coded digital hydraulic valve system - improving tracking control with pulse frequency modulation," *Procedia Engineering*, vol. 106, pp. 83–91, 2015. [Online]. Available: //www.sciencedirect.com/science/article/pii/S1877705815009364

[54] E. Mäkinen and T. Virvalo, "On the motion control of a water hydraulic servo cylinder drive," in *The Seventh Scandinavian International Conference on Fluid Power*, 2001, pp. 109–123.

[55] S. Cho, M. Linjama, H. Sairiala, K. Koskinen, and M. Vilenius, "Sliding mode tracking control of a low-pressure water hydraulic cylinder under non-linear friction," *Proceedings of the Institution of Mechanical Engineers, Part I: Journal of Systems and Control Engineering*, vol. 216, no. 5, pp. 383–392, 2002.

[56] H. Sairiala, K. Koskinen, and M. Vilenius, "Trajectory tracking control of low-pressure water hydraulic cylinder drive with proportional valve," in *7th Triennial International Symposium on Fluid Control, Measurement and Visualization, Sorrento, Italy, August 25-28, 2003*, 2003.

[57] H. Sairiala, K. T. Koskinen, and M. Vilenius, "Control of water hydraulic manipulator with proportional valves," in *Power Transmission and Motion Control, PTMC 2005*, 2005, pp. 107–115. [Online]. Available: www.scopus.com

[58] T. Virvalo and J. Mattila, "Follow-up accuracy of water hydraulic swing," in *Proceedings of the Fifth International Symposium on Fluid Power Transmission and Control, ISFP 2007, June 6-8, 2007, Beidaihe, China*, 2007.

[59] M. Linjama, J. Seppälä, J. Mattila, and M. Vilenius, "Comparison of digital hydraulic and traditional servo system in demanding water hydraulic tracking control," *In: Johnston, DN & Plummer, AR (eds.). Fluid Power and Motion Control FPMC 2008, 10-12 September 2008, Bath, UK*, 2008.

[60] L. Zhai, T. Virvalo, and J. Mattila, "Modelling, simulation and control of a water hydraulic manipulator," in *In: Lu, Y., Wang, Q., Li, W. & Ju, B.(eds.) Proceedings of the Seventh International Conference on Fluid Power Transmission and Control, ICFP 2009, April 7-10, 2009, Hangzhou, China*, 2009.

[61] E. Makinen and T. Virvalo, "Improving the accuracy of the water hydraulic position servo by compensating servo-valve nonlinearities," in *Bath Workshop on Power Transmission and Motion Control (PTMC 2000), University of Bath, UK*, 2000, pp. 13–15.

[62] H. Sairiala, K. Koskinen, M. Vilenius, P. Jauhola, and J. Selkosmaa, "Control of a water hydraulic cylinder drive with new proportional valve," in *In: Koskinen, KT & Vilenius, M.(eds.) The Eight Scandinavian International Conference on Fluid Power, Proceedings of the Conference, May 7-9, 2003, Tampere, Finland, SICFP´ 03*, 2003.

[63] H. Wu, H. Handroos, P. Pessi, J. Kilkki, and L. Jones, "Development and control towards a parallel water hydraulic weld/cut robot for machining processes in iter vacuum vessel," *Fusion Engineering and Design*, vol. 75, pp. 625–631, 2005.

[64] K. Ito, T. Yamada, S. Ikeo, and K. Takahashi, "Application of simple adaptive control to water hydraulic servo cylinder system," *Chinese Journal of Mechanical Engineering*, vol. 25, no. 5, pp. 882–888, 2012.

[65] W.-H. Zhu and J.-C. Piedboeuf, "Adaptive output force tracking control of hydraulic cylinders with applications to robot manipulators," *Journal of dynamic systems, measurement, and control*, vol. 127, no. 2, pp. 206–217, 2005.

[66] L. Zhai, T. Virvalo, J. Mattila, and H. Saarinen, "Analysis and control of a water hydraulic manipulator for iter divertor remote maintenance," *International Journal of Fluid Power*, vol. 11, no. 1, pp. 47–59, 2010. [Online]. Available: http://dx.doi.org/10.1080/14399776.2010.10780997

[67] T. Lantela, J. Kajaste, J. Kostamo, and M. Pietola, "Pilot operated miniature valve with fast response and high flow capacity," *International Journal of Fluid Power*, vol. 15, no. 1, pp. 11–18, 2014.

[68] D. C. Jiles, *Introduction to Magnetism and Magnetic Materials*. CRC Press, 1998.

[69] A. Sedriks, "Corrosion resistance of stainless steels and nickel alloys," in *Corrosion: Fundamentals, Testing, and Protection, ASM Handbook*, vol. volume 13A. ASM International, 2003, pp. 697–702.

[70] P. Oxley, J. Goodell, and R. Molt, "Magnetic properties of stainless steels at room and cryogenic temperatures," *Journal of Magnetism and Magnetic Materials*, vol. 321, no. 14, pp. 2107–2114, 2009.

[71] D. A. DeAntonio, "Soft magnetic ferritic stainless steels," *Advanced Materials & Processes*, vol. 161, no. 10, pp. 29–32, 2003.

[72] S. Tavares, D. Fruchart, S. Miraglia, and D. Laborie, "Magnetic properties of an aisi 420 martensitic stainless steel," *Journal of alloys and compounds*, vol. 312, no. 1, pp. 307–314, 2000.

[73] J. R. Brauer, *Magnetic Actuators and Sensors*. Wiley-IEEE Press, 2013.

[74] I. Schepers, D. Weiler, and J. Weber, "Optimized pulse modulation: A novel idea of a digital control method for on/off valves," in *ASME 2011 Dynamic Systems and Control Conference and Bath/ASME Symposium on Fluid Power and Motion Control*. American Society of Mechanical Engineers, 2011, pp. 363–366.

[75] T. Lantela, J. Kostamo, J. Kajaste, and M. Pietola, "Analysis of the performance of fast acting miniature solenoid actuator for digital valves," in *Conference Proceedings, 9th International Fluid Power Conference, 24th - 26th March, 2014, Aachen, Germany, Modern Fluid Power - Challenges, Responsibilities, Markets, Vol. 1*, H. Murrenhoff, Ed. Aachen, Germany: Hp - Fördervereinigung Fluidtechnik E.v., Mar. 2014, pp. 278–291.

[76] S. Esqué, J. Mattila, H. Saarinen, M. Siuko, T. Virvalo, A. Muhammad, H. Mäkinen, S. Verho, A. Timperi, J. Järvenpää, J. Palmer, M. Irving, and M. Vilenius, "The use of virtual prototyping and simulation in iter maintenance device development," *Fusion Engineering and Design*, vol. 82, no. 15, pp. 2073 – 2080, 2007, proceedings of the 24th Symposium on Fusion Technology. [Online]. Available: http://www.sciencedirect.com/science/article/pii/S0920379607000841

[77] H. E. Merritt, *Hydraulic control systems*. New York: Wiley, 1967.

[78] M. Linjama, "The modeling and actuator space control of flexible hydraulic cranes," Ph.D. dissertation, Tampere University of Technology, 1998.

[79] R. C. Dorf and R. H. Bishop, *Modern control systems*. Pearson, 2005.

Appendix A: Joint kinematics

The piston position was measured indirectly using a boom angle sensor. The joint geometry of the boom is shown in Fig. 1. The boom position with unpressurized hydraulic system (tilted left) is regarded as the zero position for both the angle and piston. The piston position was calculated with the law of cosines as follows:

$$x = \sqrt{{L_1}^2 + {L_2}^2 - 2L_1L_2\cos(\beta)} - x_0, \tag{1}$$

where x_0 is the cylinder length at zero position, and L_1 L_2 are link lengths as presented in Fig. 1. Since the angle α is the measured angle, β is calculated as $\beta = \alpha + \beta_0$, where β_0 is the value of β at zero position. The resulting relationship between the angle and the piston position is quite linear as shown in Fig. 2

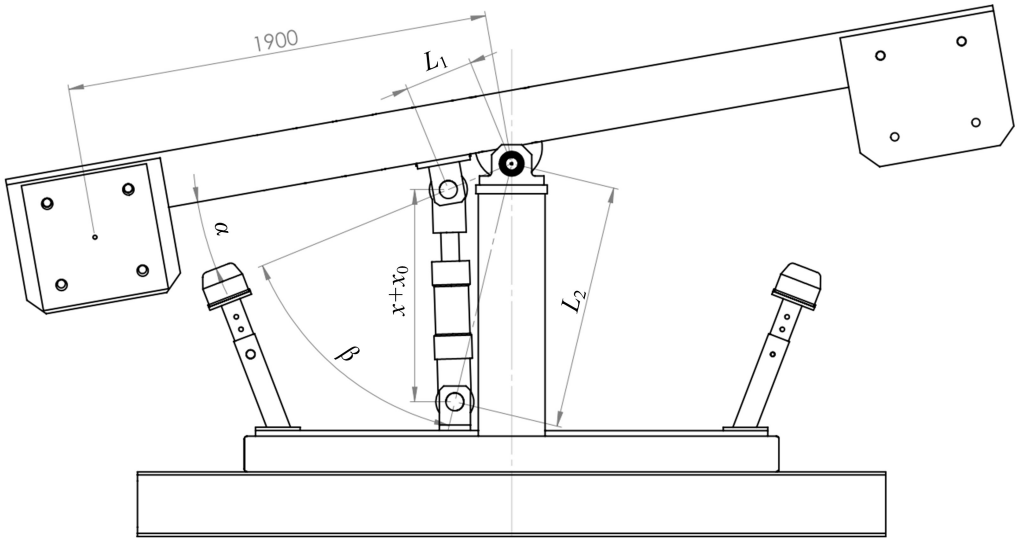

Figure 1: Joint geometry

Table 1: Dimensions of the boom joint

L_1	307 mm
L_2	1098.6 mm
β_0	41.9°
x_0	894 mm

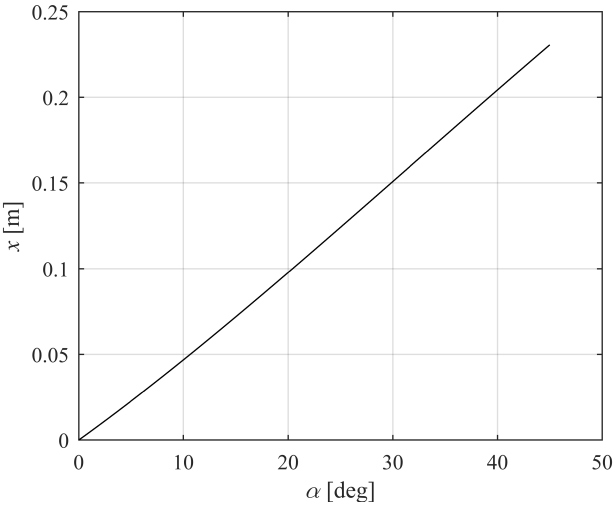

Figure 2: Cylinder piston position as a function of boom angle.

Appendix B: Bode diagram of pressure filter

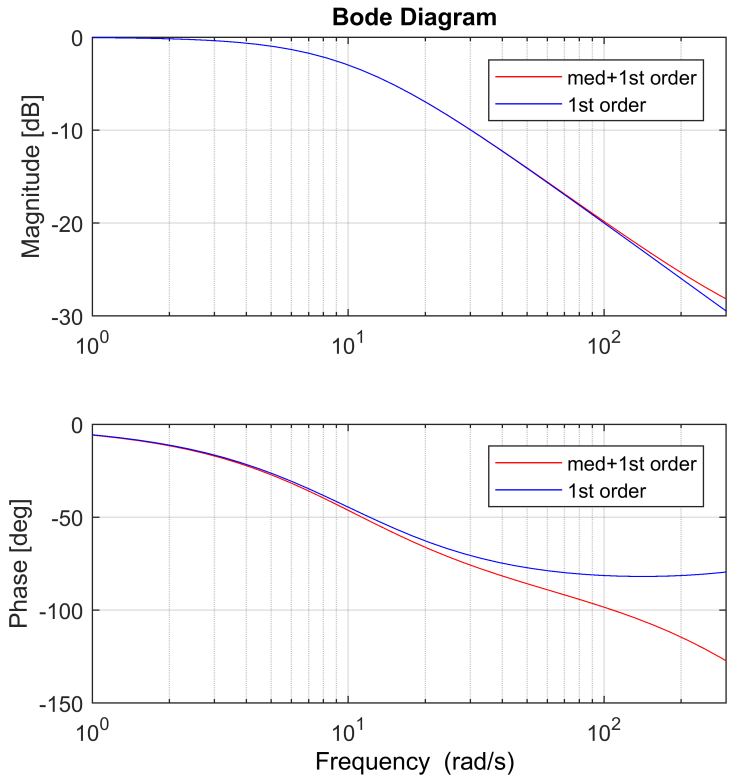

Figure 3: Simulated bode diagram of combined three sample median filter and first order low-pass filter. Bode diagram of pure 1st order filter was added for comparison.

Tampereen teknillinen yliopisto
PL 527
33101 Tampere

Tampere University of Technology
P.O.B. 527
FI-33101 Tampere, Finland

ISBN 978-952-15-4207-7
ISSN 1459-2045